Università degli Studi di Padova
Facoltà di Ingegneria

Corso di Laurea Triennale
in Ingegneria delle Telecomunicazioni

LO STANDARD LTE

Candidato:
Gianluca Caparra
560702

Relatore:
Nevio Benvenuto

A.A. 2009/10

INDEX:

DEFINITIONS

Acronyms

3GPP	third generation partnership project
BCH	broadcast channel
BTS	base transceiver station
CCE	control channel element
CFI	control format indicator
CN	core network
CP	cyclic prefix
CQI	channel quality indicator
CRC	cyclic redundancy check
DCI	downlink control information
DL-SCH	downlink shared transport channel
DwPTS	downlink pilot timeslot
eNB	evolved node b
EPS	evolved packet system
E-UTRA	evolved – UMTS terrestrial radio access
E-UTRAN	evolved – UMTS terrestrial radio access network
EVM	error vector magnitude
FDD	frequency division duplexing
GP	guard period
HARQ	hybrid automatic repeat request
HSPA	high speed packet access
LOS	line of sight
LSB	least significant bit
LTE	long term evolution
MBSFN	multi media broadcast over a single frequency network
MCH	multicast channel
MCS	modulation and coding scheme
MIMO	multiple input multiple output
MSB	most significant bit
NLOS	non line of sight
OFDMA	orthogonal frequency division multiple access
PAPR	peak to average power ratio
PBCH	physical broadcast channel
PCFICH	physical control format indicator channel
PCH	paging channel
PDCCH	physical downlink control channel
PDSCH	physical downlink shared channel
PHICH	physical hybrid arq indicator channel
PMCH	physical multicast channel
PMI	precoding matrix indicator
PRACH	physical random access channel
PRB	physical resource block
PUCCH	physical uplink control channel
PUSCH	physical uplink shared channel
RACH	random access channel
RA-RNTI	radio network temporary identifier
RB	resource block
RBG	resource block group
RI	rank indicator
RNTI	radio network temporary identifier
SAE	system architecture evolution

SC-FDMA	single carrier frequency division multiple access
SISO	single input single output
SNR	signal to noise ratio
SRS	sounding reference signal
TDD	time division duplexing
TTI	transmission time interval
UCI	uplink control information
UE	user equipment
UL-SCH	uplink shared transport channel
UMTS	universal mobile telecommunications system
UpPTS	uplink pilot timeslot
VRB	virtual resource block
W-CDMA	wideband code division multiple access

Symbols

(k,l)	resource element with frequency-domain index k and time-domain index l
$a_{k,l}^{(p)}$	value of resource element (k,l) [for antenna port p]
D	matrix for supporting cyclic delay diversity
D_{RA}	density of random access opportunities per radio frame
f_0	carrier frequency
f_{RA}	PRACH resource frequency index within the considered time-domain location
$M_{\mathrm{sc}}^{\mathrm{PUSCH}}$	scheduled bandwidth for uplink transmission, expressed as a number of subcarriers
$M_{\mathrm{RB}}^{\mathrm{PUSCH}}$	scheduled bandwidth for uplink transmission, expressed as a number of resource blocks
$M_{\mathrm{bit}}^{(q)}$	number of coded bits to transmit on a physical channel [for codeword q]
$M_{\mathrm{symb}}^{(q)}$	number of modulation symbols to transmit on a physical channel [for codeword q]
$M_{\mathrm{symb}}^{\mathrm{layer}}$	number of modulation symbols to transmit per layer for a physical channel
$M_{\mathrm{symb}}^{\mathrm{ap}}$	number of modulation symbols to transmit per antenna port for a physical channel
N	a constant equal to 2048 for $\Delta f = 15\,\mathrm{kHz}$ and 4096 for $\Delta f = 7.5\,\mathrm{kHz}$
$N_{\mathrm{CP},l}$	downlink cyclic prefix length for OFDM symbol l in a slot
N_{CS}	cyclic shift value used for random access preamble generation
$N_{\mathrm{RB}}^{\mathrm{HO}}$	offset used for PUSCH frequency hopping, expressed in number of resource blocks (set by higher layers)
$N_{\mathrm{ID}}^{\mathrm{cell}}$	physical layer cell identity
$N_{\mathrm{ID}}^{\mathrm{MBSFN}}$	MBSFN area identity
$N_{\mathrm{RB}}^{\mathrm{DL}}$	downlink bandwidth configuration, expressed in multiples of $N_{\mathrm{sc}}^{\mathrm{RB}}$
$N_{\mathrm{RB}}^{\mathrm{min,DL}}$	smallest downlink bandwidth configuration, expressed in multiples of $N_{\mathrm{sc}}^{\mathrm{RB}}$
$N_{\mathrm{RB}}^{\mathrm{max,DL}}$	largest downlink bandwidth configuration, expressed in multiples of $N_{\mathrm{sc}}^{\mathrm{RB}}$
$N_{\mathrm{RB}}^{\mathrm{UL}}$	uplink bandwidth configuration, expressed in multiples of $N_{\mathrm{sc}}^{\mathrm{RB}}$
$N_{\mathrm{RB}}^{\mathrm{min,UL}}$	smallest uplink bandwidth configuration, expressed in multiples of $N_{\mathrm{sc}}^{\mathrm{RB}}$
$N_{\mathrm{RB}}^{\mathrm{max,UL}}$	largest uplink bandwidth configuration, expressed in multiples of $N_{\mathrm{sc}}^{\mathrm{RB}}$
$N_{\mathrm{RS}}^{\mathrm{PUCCH}}$	number of reference symbols per slot for PUCCH
$N_{\mathrm{symb}}^{\mathrm{DL}}$	number of OFDM symbols in a downlink slot
$N_{\mathrm{symb}}^{\mathrm{UL}}$	number of SC-FDMA symbols in an uplink slot
$N_{\mathrm{sc}}^{\mathrm{RB}}$	resource block size in the frequency domain, expressed as a number of subcarriers
N_{SP}	number of downlink to uplink switch points within the radio frame

N_{SRS}	number of SC-FDMA symbols used for SRS transmission in a subframe (0 or 1)
N_{TA}	timing offset between uplink and downlink radio frames at the UE, expressed in units of T_{s}
$N_{\mathrm{TA\ offset}}$	fixed timing advance offset, expressed in units of T_{s}
n_{PDCCH}	number of PDCCHs present in a subframe
n_{PRB}	physical resource block number
$n_{\mathrm{PRB}}^{\mathrm{RA}}$	first physical resource block occupied by PRACH resource considered
$n_{\mathrm{PRB\,offset}}^{\mathrm{RA}}$	first physical resource block available for PRACH
n_{VRB}	virtual resource block number
n_{RNTI}	radio network temporary identifier
n_{f}	system frame number
n_{s}	slot number within a radio frame
P	number of cell-specific antenna ports
p	antenna port number
q	codeword number
r_{RA}	index for PRACH versions with same preamble format and PRACH density
Q_m	modulation order: 2 for QPSK, 4 for 16QAM and 6 for 64QAM transmissions
$s_l^{(p)}(t)$	time-continuous baseband signal for antenna port p and OFDM symbol l in a slot
T_{f}	radio frame duration
T_{s}	basic time unit
T_{slot}	slot duration
Δf	subcarrier spacing
Δf_{RA}	subcarrier spacing for the random access preamble
υ	number of transmission layers

Chapter 1

INTRODUCTION

Third-generation UMTS, based on wideband code-division multiple access (W-CDMA), has been deployed all over the world. The original UMTS has been updated several times, first introducing the HSDPA and after the HSUPA, to ensure that this system remains competitive in the future. In November 2004 the third generation partnership project (3GPP) began a project to define the Long-Term Evolution (LTE) of UMTS cellular technology. Figure 1-1 show the UMTS timeline.

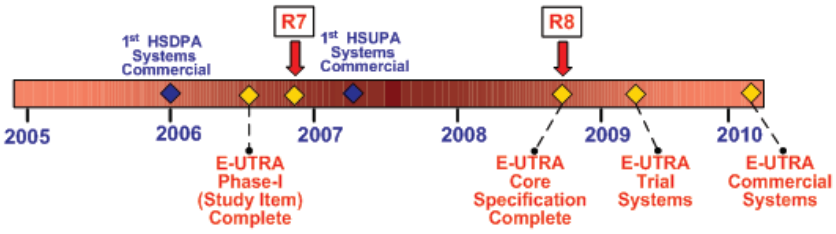

Figure 1-1: LTE standards timeline.

The specifications related to this effort are formally known as the evolved UMTS terrestrial radio access (E-UTRA) and evolved UMTS terrestrial radio access network (E-UTRAN), but are more commonly referred to by the project name LTE. The first version of LTE is documented in Release 8 of the 3GPP specifications.

A parallel 3GPP project called System Architecture Evolution (SAE) is defining a new all-IP, packet-only core network (CN) known as the evolved packet core (EPC). The combination of the EPC and the evolved RAN (E-UTRA plus E-UTRAN) is the evolved packet system (EPS). Depending on the context, any of the terms LTE, E-UTRA, E-UTRAN, SAE, EPC and EPS may get used to describe some system's parts or the entire system.

LTE aims to achieve the following:

- Increased downlink and uplink peak data rates, as shown in Table 1-1. Note that the downlink is specified for single input single output (SISO) and multiple input multiple output (MIMO) antenna configurations at a fixed 64QAM modulation format, whereas the uplink is specified only for SISO but at different modulation format. These figures represent the physical limitation of the frequency division duplex (FDD) air interface in ideal radio conditions with allowance for signaling overheads. Lower rates are specified for specific UE categories, and performance requirements under non-ideal radio conditions have also been developed.
- Scalable channel bandwidths of 1.4, 3, 5, 10, 15, and 20 MHz in both the uplink and the downlink.

- Spectral efficiency improvements over High Speed Packet Access (HSPA) of three to four times in the downlink and two to three times in the uplink.
- High coverage, cell sizes of 5 – 100 km with slight degradation after 30 km.
- Sub-5 ms latency for small IP packets.
- Performance optimized for low mobile speeds from 0 to 15 km/h, supported with high performance from 15 to 120 km/h; functional support from 120 to 350 km/h, under consideration for 350 to 500 km/h
- Co-existence with legacy standards while evolving toward an all-IP network.

FDD downlink (64QAM)	Antenna configuration		
	SISO	2x2 MIMO	4x4 MIMO
Peak data rate Mbps	100	172.8	326.4

FDD uplink (single antenna)	Modulation depth		
	QPSK	16QAM	64QAM
Peak data rate Mbps	50	57.6	86.4

Table 1-1: LTE (FDD) downlink and uplink peak data rates.

The key features of LTE are:

- Multiple access scheme:
  - ✓ DL: OFDMA with Cyclic Prefix
  - ✓ UL: Single Carrier FDMA (SC-FDMA) with Cyclic Prefix
- Adaptive modulation and coding
- Advanced MIMO spatial multiplexing techniques
  - ✓ (2 or 4)x(2 or 4) downlink and uplink supported
  - ✓ Multi-user MIMO also supported
- Support for both FDD and TDD
- H-ARQ, mobility support, rate control, security

Table 1-2 show a comparison of LTE and UMTS Release 6 standard.

Requirement	Current Release (Rel-6 HSxPA)	LTE E-UTRA
Peak data rate	14 Mbps DL / 5.76 Mbps UL	100 Mbps DL / 50 Mbps UL
Spectral Efficiency	0.6 – 0.8 DL / 0.35 UL (bps/Hz/sector)	3-4x DL / 2-3x UL improvement
5% packet call throughput	64 Kbps DL / 5 Kbps UL	3-4x DL / 2-3x UL improvement
Averaged user throughput	900 Kbps DL / 150 Kbps UL	3-4x DL / 2-3x UL improvement
Latency	50 ms	5 ms
Call setup time	2 sec	50 ms
Broadcast data rate	384 Kbps	6-8x improvement
Mobility	Up to 250 km/h	Up to 350 km/h
Multi-antenna support	No	Yes
Bandwidth	5 MHz	Scalable (up to 20 MHz)

Table 1-2: LTE vs. UMTS comparison.

The specifications for the LTE E-UTRA and E-UTRAN are contained in the 36 series of 3GPP specification documents, divided into the following categories:

- TS 36.1xx: radio specifications and evolved Node B (eNB) conformance testing
- TS 36.2xx: physical layer specifications
- TS 36.3xx: layer 2 and 3 air interface signaling specifications
- TS 36.4xx: network signaling specifications
- TS 36.5xx: user equipment conformance testing
- TS 36.8xx and TS 36.9xx: technical reports containing background information

The downlink transmission scheme for E-UTRA FDD and TDD modes is based on conventional OFDM (Orthogonal Frequency Division Multiple Access). In an OFDM system, the available spectrum is divided into multiple carriers, called subcarriers. Each of these subcarriers is independently modulated by a low rate data stream.

OFDM has several benefits including its robustness against multipath fading and its efficient receiver architecture, but have also some disadvantage.

OFDM advantages:

- Wide channels are more resistant to fading and OFDM equalizers are much simpler to implement than CDMA
- Almost completely resistant to multi-path due to very long symbols
- Ideally suited to MIMO due to easy matching of transmit signals to the uncorrelated RF channels

OFDM disadvantages:

- Sensitive to frequency errors and phase noise due to close subcarrier spacing
- Sensitive to Doppler shift which creates interference between subcarriers
- Pure OFDM creates high Peak-to-Average Power Ratio (PAPR) which is why SC-FDMA is used on UL
- More complex than CDMA for handling inter-cell interference at cell edge

In the time domain, a guard interval may be added to each symbol to combat inter-OFDM-symbol-interference due to channel delay spread. In E-UTRA, the guard interval is a cyclic prefix which is inserted prior to each OFDM symbol.

During the study item phase of LTE, alternatives for the optimum uplink transmission scheme were investigated. While OFDMA is seen optimum to fulfill the LTE requirements in downlink, OFDMA properties are less favorable for the uplink. This is mainly due to weaker PAPR properties of an OFDMA signal, resulting in worse uplink coverage. Thus, the LTE uplink transmission scheme for FDD and TDD mode is based on SC-FDMA (Single Carrier Frequency Division Multiple Access) with cyclic prefix.

SC-FDMA is a hybrid transmission scheme combining the low PAPR of single carrier schemes with the frequency allocation flexibility and multipath protection provided by OFDMA.
The low PAPR was one of the main reasons for selecting SCFDMA as LTE uplink access scheme because the PAPR characteristics are important for cost-effective design of UE power amplifiers.
Still, SC-FDMA signal processing has some similarities with OFDMA signal processing, so parametrization of downlink and uplink can be harmonized.
LTE supports both intra- and inter-subframe frequency hopping. It is configured per cell by higher layers whether both intra- and inter-subframe hopping or only inter-subframe hopping is supported. In intra-subframe hopping (inter-slot hopping), the UE hops to another frequency allocation from one slot to another within one subframe. In inter-subframe hopping, the frequency resource allocation changes from one subframe to another. Also, the UE is being told whether to use type 1 or type 2 frequency hopping, and receives the index of the first resource block of the uplink allocation.

- Type 1 hopping refers to the use of an explicit offset in the 2nd slot resource allocation.
- Type 2 hopping refers to the use of a pre-defined hopping pattern. The bandwidth available for physical uplink shared channel (PUSCH) is sub-divided into sub-bands (e.g. 4 sub-bands with 5 resource blocks each in the 5 MHz case), and the hopping is performed between sub-bands (from one slot or subframe to another, depending on whether intra- or inter-subframe are configured,respectively). Additionally, mirroring can be applied according to a mirroring function, which means that the resource block allocation starts from the other direction of the sub-band where they are located in. Note that in case of type 2 hopping, the resource allocation for the UE cannot be larger than the sub-band configured.

LTE MIMO Concepts

Multiple Input Multiple Output (MIMO) systems form an essential part of LTE in order to achieve the ambitious requirements for throughput and spectral efficiency. MIMO refers to the use of multiple antennas at transmitter and receiver side. For a 2x2 configuration for MIMO two transmit antennas at the base station and two receive antennas at the terminal side is used. Different gains can be achieved depending on the MIMO mode that is used.
In the following, a general description of spatial multiplexing and transmit diversity is provided. Afterwards, LTE-specific MIMO features are highlighted.

Spatial Multiplexing

Spatial multiplexing allows to transmit different streams of data simultaneously on the same resource block(s) by exploiting the spatial dimension of the radio channel. These data streams can belong to onesingle user (single user MIMO / SU-MIMO) or to different users (multi user MIMO /

MU-MIMO). While SU-MIMO increases the data rate of one user, MU-MIMO allows to increase the overall capacity. Spatial multiplexing is only possible if the mobile radio channel allows it.

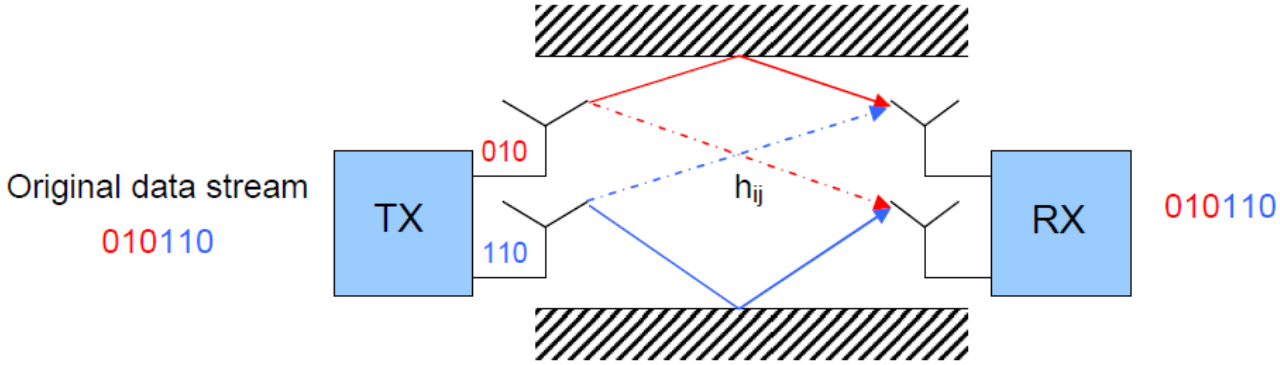

Figure 1-2: Spatial multiplexing.

Figure 1-2 shows a simplified illustration of spatial multiplexing. In this example, each transmit antenna transmits a different data stream. This is the basic case for spatial multiplexing. Each receive antenna may receive the data streams from all transmit antennas.

The number of data streams that can be transmitted in parallel over the MIMO channel is given by min {Nt, Nr} where Nt is the number of transmit antennas and Nr is the number of receive antennas.

The transmission quality degrades significantly in case the two antennas are not sufficiently de-correlated, for example in an environment with little scattering or when antennas are too closely spaced. Note that Figure 1-2 only shows an example. In practical MIMO implementations, the data streams are often weighted and added, so that each antenna actually transmits a combination of the streams.

Transmit Diversity

Instead of increasing data rate or capacity, MIMO can be used to exploit diversity and increase the robustness of data transmission. Transmit diversity schemes are already known from WCDMA release 99 and will also be part of LTE. Each transmit antenna transmits essentially the same stream of data, so the receiver gets replicas of the same signal. This increases the signal to noise ratio at the receiver side and thus the robustness of data transmission especially in fading scenarios. Typically an additional antenna-specific coding is applied to the signals before transmission to increase the diversity effect. Often, space-time coding is used.

Switching between the two MIMO modes transmit diversity and spatial multiplexing is possible depending on channel conditions.

Cyclic Delay Diversity (CDD)

Cyclic delay diversity is an additional type of diversity which can be used in conjunction with spatial multiplexing in LTE. An antenna-specific delay is applied to the signals transmitted from each antenna port. This effectively introduces artificial multipath to the signal as seen by the receiver. By doing so, the frequency diversity of the radio channel is increased. As a special method of delay diversity, cyclic delay diversity applies a cyclic shift to the signals transmitted from each antenna port.

Downlink MIMO modes in LTE

Different downlink MIMO modes are envisaged in LTE which can be adjusted according to channel condition, traffic requirements, and UE capability. The following transmission modes are possible in LTE:

- Single-Antenna transmission, no MIMO
- Transmit diversity
- Open-loop spatial multiplexing, no UE feedback required
- Closed-loop spatial multiplexing, UE feedback required
- Multi-user MIMO (more than one UE is assigned to the same resource block)
- Closed-loop precoding for rank=1 (i.e. no spatial multiplexing, but precoding is used)
- Beamforming

Precoding on transmitter side is used to support spatial multiplexing. This is achieved by multiplying the signal with a precoding matrix **W** before transmission. The optimum precoding matrix **W** is selected from a predefined "codebook" which is known at eNodeB and UE side. The optimum pre-coding matrix is the one which offers maximum capacity.

The UE estimates the radio channel and selects the optimum precoding matrix. This feedback is provided to the eNodeB. Depending on the available bandwidth, this information is made available per resource block or group of resource blocks, since the optimum precoding matrix may vary between resource blocks. The network may configure a subset of the codebook that the UE is able to select from. In case of UEs with high velocity, the quality of the feedback may deteriorate. Thus, an open loop spatial multiplexing mode is also supported which is based on predefined settings for spatial multiplexing and precoding. In case of four antenna ports, different precoders are assigned cyclically to the resource elements.

The eNB will select the optimum MIMO mode and precoding configuration. The information is conveyed to the UE as part of the downlink control information (DCI) on PDCCH. In case of transmit diversity mode, only one code word can be transmitted. Each antenna transmits the same information stream, but with different coding.

LTE employs Space Frequency Block Coding (SFBC) as transmit diversity scheme. A special precoding matrix is applied at transmitter side in the precoding stage. At a certain point in time, the antenna ports transmit the same data symbols, but with different coding and on different subcarriers.

Reporting of UE feedback

In order for MIMO schemes to work properly, each UE has to report information about the mobile radio channel to the base station. A lot of different reporting modes and formats are available which are selected according to MIMO mode of operation and network choice.

The reporting may consist of the following elements:

- CQI (channel quality indicator) is an indication of the downlink mobile radio channel quality as experienced by this UE. Essentially, the UE is proposing to the eNodeB an optimum modulation scheme and coding rate to use for a given radio link quality, so that the resulting transport block error rate would not exceed 10%. 16 combinations of modulation scheme and coding rate are specified as possible CQI values. The UE may report different types of CQI. A so-called "wideband CQI" refers to the complete system bandwidth. Alternatively, the UE may evaluate a "sub-band CQI" value per sub-band of a certain number of resource blocks which is configured by higher layers. The full set of sub-bands would cover the entire system bandwidth. In case of spatial multiplexing, a CQI per code word needs to be reported.
- PMI (precoding matrix indicator) is an indication of the optimum precoding matrix to be used in the base station for a given radio condition. The network configures the number of resource blocks that are represented by a PMI report. Thus to cover the full bandwidth, multiple PMI reports may be needed. PMI reports are needed for closed loop spatial multiplexing, multi-user MIMO and closed-loop rank 1 precoding MIMO modes.
- RI (rank indication) is the number of useful transmission layers when spatial multiplexing is used. In case of transmit diversity, rank is equal to 1. The reporting may be periodic or aperiodic and is configured by the radio network. Aperiodic reporting is triggered by a CQI request contained in the uplink scheduling grant. The UE would sent the report on PUSCH. In case of periodic reporting, PUCCH is used in case no PUSCH is available.

Uplink MIMO

Uplink MIMO schemes for LTE will differ from downlink MIMO schemes to take into account terminal complexity issues. For the uplink, MU-MIMO can be used. Multiple user terminals may transmit simultaneously on the same resource block. This is also referred to as spatial division multiple access (SDMA). The scheme requires only one transmit antenna at UE side which is a big

advantage. The UEs sharing the same resource block have to apply mutually orthogonal pilot patterns.

To exploit the benefit of two or more transmit antennas but still keep the UE cost low, transmit antenna selection can be used. In this case, the UE has two transmit antennas but only one transmit chain and amplifier. A switch will then choose the antenna that provides the best channel to the eNB.

This decision is made according to feedback provided by the eNB. The CRC parity bits of the DCI format 0 are scrambled with an antenna selection mask indicating UE antenna.

User Equipment category

It was decided to divide the terminals according to their potential, Table 1-3 explain these categories.

Note that the UE category for the downlink and for the uplink must be the same.

UE category	Max downlink data rate (Mbps)	Number of DL transmit data stream	Max uplink data rate (Mbps)	Support for uplink 64QAM
1	10	1	5	No
2	50	2	25	Not yet decided
3	100	2	50	Not yet decided
4	150	Not yet decided	50	Not yet decided
5	300	4	75	Yes

Table 1-3: UE categories.

Operating band and channel bandwidth

E-UTRA is designed to operate in the operating bands defined in Table 1-5, Table 1-6 specify the channel bandwidth for every operating band.

Table 1-4 show the transmission bandwidth configuration at the various channel bandwidth.

Channel bandwidth $BW_{Channel}$ [MHz]	**1.4**	**3**	**5**	**10**	**15**	**20**
Transmission bandwidth configuration N_{RB}	6	15	25	50	75	100
Number of occupied subcarriers	72	180	300	600	900	1200
IDFT (TX) / DFT (RX) size	128	256	512	1024	1536	2048
Sample rate [MHz]	1.92	3.84	7.68	15.36	23.04	30.72
Samples per slot	960	1920	3840	7680	11520	15360

Table 1-4: Transmission bandwidth configuration N_{RB} in E-UTRA channel bandwidths.

E-UTRA Operating Band	**Uplink (UL) operating band BS receive UE transmit**	**Downlink (DL) operating band BS transmit UE receive**	**Duplex Mode**
	F_{UL_low} – F_{UL_high}	**F_{DL_low} – F_{DL_high}**	
1	1920 MHz – 1980 MHz	2110 MHz – 2170 MHz	FDD
2	1850 MHz – 1910 MHz	1930 MHz – 1990 MHz	FDD
3	1710 MHz – 1785 MHz	1805 MHz – 1880 MHz	FDD
4	1710 MHz – 1755 MHz	2110 MHz – 2155 MHz	FDD
5	824 MHz – 849 MHz	869 MHz – 894MHz	FDD
6[1]	830 MHz – 840 MHz	875 MHz – 885 MHz	FDD
7	2500 MHz – 2570 MHz	2620 MHz – 2690 MHz	FDD
8	880 MHz – 915 MHz	925 MHz – 960 MHz	FDD
9	1749.9 MHz – 1784.9 MHz	1844.9 MHz – 1879.9 MHz	FDD
10	1710 MHz – 1770 MHz	2110 MHz – 2170 MHz	FDD
11	1427.9 MHz – 1447.9 MHz	1475.9 MHz – 1495.9 MHz	FDD
12	698 MHz – 716 MHz	728 MHz – 746 MHz	FDD
13	777 MHz – 787 MHz	746 MHz – 756 MHz	FDD
14	788 MHz – 798 MHz	758 MHz – 768 MHz	FDD
15	Reserved	Reserved	FDD
16	Reserved	Reserved	FDD
17	704 MHz – 716 MHz	734 MHz – 746 MHz	FDD
18	815 MHz – 830 MHz	860 MHz – 875 MHz	FDD
19	830 MHz – 845 MHz	875 MHz – 890 MHz	FDD
20	832 MHz – 862 MHz	791 MHz – 821 MHz	FDD
21	1447.9 MHz – 1462.9 MHz	1495.9 MHz – 1510.9 MHz	FDD
...			
33	1900 MHz – 1920 MHz	1900 MHz – 1920 MHz	TDD
34	2010 MHz – 2025 MHz	2010 MHz – 2025 MHz	TDD
35	1850 MHz – 1910 MHz	1850 MHz – 1910 MHz	TDD
36	1930 MHz – 1990 MHz	1930 MHz – 1990 MHz	TDD
37	1910 MHz – 1930 MHz	1910 MHz – 1930 MHz	TDD
38	2570 MHz – 2620 MHz	2570 MHz – 2620 MHz	TDD
39	1880 MHz – 1920 MHz	1880 MHz – 1920 MHz	TDD
40	2300 MHz – 2400 MHz	2300 MHz – 2400 MHz	TDD
Note 1: Band 6 is not applicable			

Table 1-5: E-UTRA operating bands.

E-UTRA band / channel bandwidth						
E-UTRA Band	**1.4 MHz**	**3 MHz**	**5 MHz**	**10 MHz**	**15 MHz**	**20 MHz**
1			Yes	Yes	Yes	Yes
2	Yes	Yes	Yes	Yes	Yes[1]	Yes[1]
3	Yes	Yes	Yes	Yes	Yes[1]	Yes[1]
4	Yes	Yes	Yes	Yes	Yes	Yes
5	Yes	Yes	Yes	Yes[1]		
6			Yes	Yes[1]		
7			Yes	Yes	Yes	Yes[1]
8	Yes	Yes	Yes	Yes[1]		
9			Yes	Yes	Yes[1]	Yes[1]
10			Yes	Yes	Yes	Yes
11			Yes	Yes[1]		
12	Yes	Yes	Yes[1]	Yes[1]		
13			Yes[1]	Yes[1]		
14			Yes[1]	Yes[1]		
...						
17			Yes[1]	Yes[1]		
18			Yes	Yes[1]	Yes[1]	
19			Yes	Yes[1]	Yes[1]	
20			Yes	Yes[1]	Yes[1]	Yes[1]
21			Yes	Yes[1]	Yes[1]	
...						
33			Yes	Yes	Yes	Yes
34			Yes	Yes	Yes	
35	Yes	Yes	Yes	Yes	Yes	Yes
36	Yes	Yes	Yes	Yes	Yes	Yes
37			Yes	Yes	Yes	Yes
38			Yes	Yes	Yes	Yes
39			Yes	Yes	Yes	Yes
40			Yes	Yes	Yes	Yes
NOTE 1: bandwidth for which a relaxation of the specified UE receiver sensitivity requirement (Clause 7.3) is allowed.						

Table 1-6: E-UTRA channel bandwidth.

Channel spacing

The spacing between carriers will depend on the deployment scenario, the size of the frequency block available and the channel bandwidths. The nominal channel spacing between two adjacent E-UTRA carriers is defined as following:

$$\text{Nominal Channel spacing} = (BW_{Channel(1)} + BW_{Channel(2)})/2$$

where $BW_{Channel(1)}$ and $BW_{Channel(2)}$ are the channel bandwidths of the two respective E-UTRA carriers. The channel spacing can be adjusted to optimize performance in a particular deployment scenario.

Channel raster

The channel raster is 100 kHz for all bands, which means that the carrier centre frequency must be an integer multiple of 100 kHz.

Carrier frequency and EARFCN

The carrier frequency in the uplink and downlink is designated by the E-UTRA Absolute Radio Frequency Channel Number (EARFCN) in the range 0 - 65535.

The relation between EARFCN and the carrier frequency in MHz for the downlink is given by the following equation, where F_{DL_low} and $N_{Offs\text{-}DL}$ are given in Table 1-7 and N_{DL} is the downlink EARFCN.

$$F_{DL} = F_{DL\_low} + 0.1(N_{DL} - N_{Offs\text{-}DL})$$

The relation between EARFCN and the carrier frequency in MHz for the uplink is given by the following equation where F_{UL_low} and $N_{Offs\text{-}UL}$ are given in Table 1-7 and N_{UL} is the uplink EARFCN.

$$F_{UL} = F_{UL\_low} + 0.1(N_{UL} - N_{Offs\text{-}UL})$$

E-UTRA Operating Band	Downlink			Uplink		
	F_{DL_low} [MHz]	$N_{Offs\text{-}DL}$	Range of N_{DL}	F_{UL_low} [MHz]	$N_{Offs\text{-}UL}$	Range of N_{UL}
1	2110	0	0 – 599	1920	18000	18000 – 18599
2	1930	600	600 - 1199	1850	18600	18600 – 19199
3	1805	1200	1200 – 1949	1710	19200	19200 – 19949
4	2110	1950	1950 – 2399	1710	19950	19950 – 20399
5	869	2400	2400 – 2649	824	20400	20400 – 20649
6	875	2650	2650 – 2749	830	20650	20650 – 20749
7	2620	2750	2750 – 3449	2500	20750	20750 – 21449
8	925	3450	3450 – 3799	880	21450	21450 – 21799
9	1844.9	3800	3800 – 4149	1749.9	21800	21800 – 22149
10	2110	4150	4150 – 4749	1710	22150	22150 – 22749
11	1475.9	4750	4750 – 4949	1427.9	22750	22750 – 22949
12	728	5000	5000 – 5179	698	23000	23000 – 23179
13	746	5180	5180 – 5279	777	23180	23180 – 23279
14	758	5280	5280 – 5379	788	23280	23280 – 23379
…						
17	734	5730	5730 – 5849	704	23730	23730 – 23849
18	860	5850	5850 – 5999	815	23850	23850 – 23999
19	875	6000	6000 – 6149	830	24000	24000 – 24149
20	791	6150	6150 - 6449	832	24150	24150 - 24449
21	1495.9	6450	6450 – 6599	1447.9	24450	24450 – 24599
…						
33	1900	36000	36000 – 36199	1900	36000	36000 – 36199
34	2010	36200	36200 – 36349	2010	36200	36200 – 36349
35	1850	36350	36350 – 36949	1850	36350	36350 – 36949
36	1930	36950	36950 – 37549	1930	36950	36950 – 37549
37	1910	37550	37550 – 37749	1910	37550	37550 – 37749
38	2570	37750	37750 – 38249	2570	37750	37750 – 38249
39	1880	38250	38250 – 38649	1880	38250	38250 – 38649
40	2300	38650	38650 – 39649	2300	38650	38650 – 39649

NOTE: The channel numbers that designate carrier frequencies so close to the operating band edges that the carrier extends beyond the operating band edge shall not be used. This implies that the first 7, 15, 25, 50, 75 and 100 channel numbers at the lower operating band edge and the last 6, 14, 24, 49, 74 and 99 channel numbers at the upper operating band edge shall not be used for channel bandwidths of 1.4, 3, 5, 10, 15 and 20 MHz respectively.

Table 1-7: E-UTRA channel numbers.

Chapter 2

FRAME

Downlink and uplink transmissions are organized into radio frames with T_f = 10 ms duration [1]. Two radio frame structures are supported:

- Type 1 applicable to FDD
- Type 2 applicable to TDD

2.1 Frame structure type 1

The frame structure type 1 is applicable to both full duplex and half duplex FDD. Each radio frame is $T_f = 307200 \cdot T_s = 10\,\text{ms}$ long and consists of 20 slots of length $T_{slot} = 15360 \cdot T_s = 0.5\,\text{ms}$, numbered from 0 to 19. A subframe is defined as two consecutive slots where subframe i consists of slots $2i$ and $2i+1$.

For FDD, 10 subframes are available for downlink transmission and 10 subframes are available for uplink transmissions in each 10 ms interval. Uplink and downlink transmissions are separated in the frequency domain. In half-duplex FDD operation, the UE cannot transmit and receive at the same time while there are no such restrictions in full-duplex FDD.

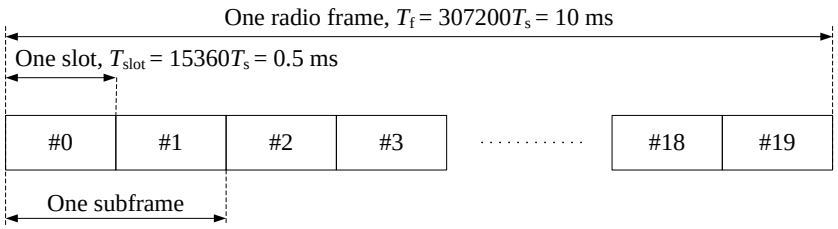

Figure 2.1: Frame structure type 1.

2.2 Frame structure type 2

The frame structure type 2 as shown in Figure 2.2 is applicable to TDD. Each radio frame of length $T_f = 307200 \cdot T_s = 10\,\text{ms}$ consists of two half-frames of length $153600 \cdot T_s = 5\,\text{ms}$ each. Each half-frame consists of five subframes of length $30720 \cdot T_s = 1\,\text{ms}$. The supported uplink-downlink configurations are listed in Table 2.2-1 where, for each subframe in a radio frame, “D” denotes the subframe is reserved for downlink transmissions, “U” denotes the subframe is reserved for uplink transmissions and “S” denotes a special subframe with the three fields DwPTS, GP and UpPTS. The length and the of DwPTS and UpPTS is given by Table 2.2-2 subject to the total length of DwPTS, GP and UpPTS being equal to $30720 \cdot T_s = 1\,\text{ms}$. Each subframe i is defined as two slots, $2i$ and $2i+1$ of length $T_{slot} = 15360 \cdot T_s = 0.5\,\text{ms}$ in each subframe.

The duration of the GP depends on the signal propagation time from the BS to the MS and back as well as on the time the MS requires to switch from receiving to sending. The duration of the GP is configured by the network based on the cell size.

Because the overall length of the special subframe remains constant and the GP length varies based on cell size, the lengths of the DwPTS and UpPTS also have to be adjusted. Nine different special subframe configurations are provided for LTE TDD.

While the GP separates between the UL and the DL, the other special fields are used for data transmission. The DwPTS field carries synchronization and user data as well as the downlink control channel for transmitting scheduling and control information. The UpPTS field is used for transmitting the physical random access channel (PRACH) and the sounding reference signal (SRS).

One of the advantages of using LTE TDD is that it is possible to dynamically change the uplink and downlink balance and characteristics to meet the load conditions.

Uplink-downlink configurations with both 5 ms and 10 ms downlink-to-uplink switch-point periodicity are supported.

In case of 5 ms downlink-to-uplink switch-point periodicity, the special subframe exists in both half-frames, else in case of 10 ms downlink-to-uplink switch-point periodicity, the special subframe exists in the first half-frame only.

Subframes 0 and 5 and DwPTS are always reserved for downlink transmission. UpPTS and the subframe immediately following the special subframe are always reserved for uplink transmission.

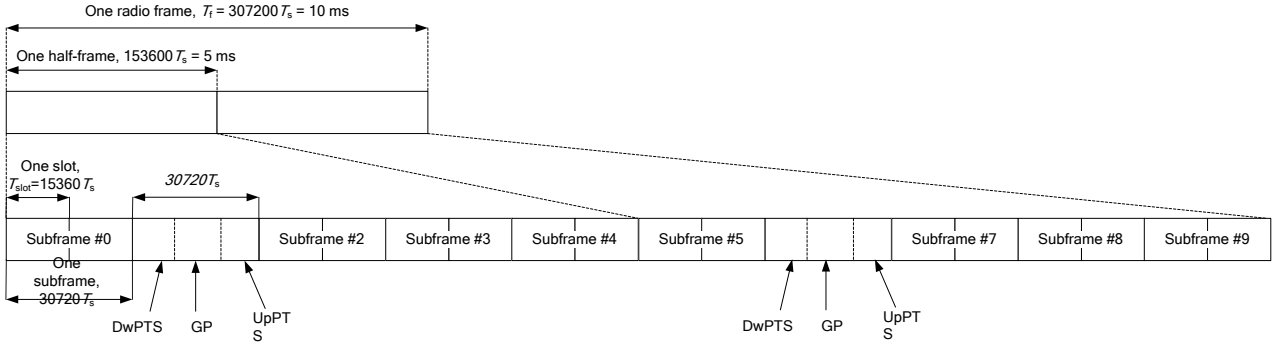

Figure 2.2: Frame structure type 2 (for 5 ms switch-point periodicity).

Uplink-downlink configuration	Downlink-to-Uplink Switch-point periodicity	Subframe number									
		0	1	2	3	4	5	6	7	8	9
0	5 ms	D	S	U	U	U	D	S	U	U	U
1	5 ms	D	S	U	U	D	D	S	U	U	D
2	5 ms	D	S	U	D	D	D	S	U	D	D
3	10 ms	D	S	U	U	U	D	D	D	D	D
4	10 ms	D	S	U	U	D	D	D	D	D	D
5	10 ms	D	S	U	D	D	D	D	D	D	D
6	5 ms	D	S	U	U	U	D	S	U	U	D

Table 2.2-1: Uplink-downlink configurations.

Special subframe configuration	Normal cyclic prefix in downlink			Extended cyclic prefix in downlink		
	DwPTS	UpPTS		DwPTS	UpPTS	
		Normal cyclic prefix in uplink	Extended cyclic prefix in uplink		Normal cyclic prefix in uplink	Extended cyclic prefix in uplink
0	$6592 \cdot T_s$	$2192 \cdot T_s$	$2560 \cdot T_s$	$7680 \cdot T_s$	$2192 \cdot T_s$	$2560 \cdot T_s$
1	$19760 \cdot T_s$			$20480 \cdot T_s$		
2	$21952 \cdot T_s$			$23040 \cdot T_s$		
3	$24144 \cdot T_s$			$25600 \cdot T_s$		
4	$26336 \cdot T_s$			$7680 \cdot T_s$	$4384 \cdot T_s$	$5120 \cdot T_s$
5	$6592 \cdot T_s$	$4384 \cdot T_s$	$5120 \cdot T_s$	$20480 \cdot T_s$		
6	$19760 \cdot T_s$			$23040 \cdot T_s$		
7	$21952 \cdot T_s$			-	-	-
8	$24144 \cdot T_s$			-	-	-

Table 2.2-2: Configuration of special subframe (lengths of DwPTS/GP/UpPTS).

Chapter 3

DOWNLOAD

3.1 Slot structure e resource elements

3.1.1 Resource grid

The transmitted signal in each slot is described by a resource grid of $N_{\mathrm{RB}}^{\mathrm{DL}} N_{\mathrm{sc}}^{\mathrm{RB}}$ subcarriers and $N_{\mathrm{symb}}^{\mathrm{DL}}$ OFDM symbols. The resource grid structure is illustrated in Figure 3.1.1. The quantity $N_{\mathrm{RB}}^{\mathrm{DL}}$ depends on the downlink transmission bandwidth configured in the cell and shall fulfill

$$N_{\mathrm{RB}}^{\min,\mathrm{DL}} \le N_{\mathrm{RB}}^{\mathrm{DL}} \le N_{\mathrm{RB}}^{\max,\mathrm{DL}}$$

where $N_{\mathrm{RB}}^{\min,\mathrm{DL}} = 6$ and $N_{\mathrm{RB}}^{\max,\mathrm{DL}} = 110$ are the smallest and largest downlink bandwidths, respectively, supported by the current version of this specification [1].

The number of OFDM symbols in a slot depends on the cyclic prefix length and subcarrier spacing configured and is given in Table 3.1.1.

In case of multi-antenna transmission, there is one resource grid defined per antenna port. An antenna port is defined by its associated reference signal. The set of antenna ports supported depends on the reference signal configuration in the cell:

- Cell-specific reference signals, associated with non-Multi-media Broadcast over a Single Frequency Network (MBSFN) transmission, support a configuration of one, two, or four antenna ports and the antenna port number p shall fulfil $p = 0$, $p \in \{0,1\}$, and $p \in \{0,1,2,3\}$, respectively.
- MBSFN reference signals, associated with MBSFN transmission, are transmitted on antenna port $p = 4$.
- UE-specific reference signals are transmitted on antenna port(s) $p = 5$, $p = 7$, $p = 8$, or $p \in \{7,8\}$.
- Positioning reference signals are transmitted on antenna port $p = 6$.

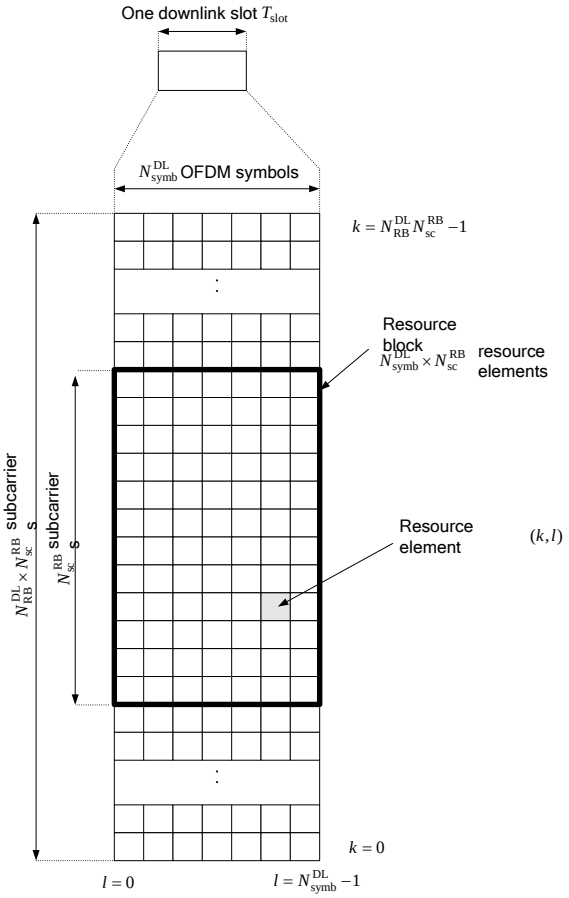

Figure 3.1.1: Downlink resource grid.

Configuration		N_{sc}^{RB}	N_{symb}^{DL}
Normal cyclic prefix	$\Delta f = 15$ kHz	12	7
Extended cyclic prefix	$\Delta f = 15$ kHz		6
	$\Delta f = 7.5$ kHz	24	3

Table 3.1.1: Physical resource blocks parameters.

3.1.2 Resource elements

Each element in the resource grid for antenna port p is called a resource element and is uniquely identified by the index pair (k,l) in a slot where $k = 0,\ldots,N_{RB}^{DL} N_{sc}^{RB} - 1$ and $l = 0,\ldots,N_{symb}^{DL} - 1$ are the indices in the frequency and time domains, respectively. Resource element (k,l) on antenna port p corresponds to the complex value $a_{k,l}^{(p)}$.

3.1.3 Resource blocks

Resource blocks are used to describe the mapping of certain physical channels to resource elements. Physical and virtual resource blocks are defined.

3.1.3.1 Physical resource block

A physical resource block is defined as $N_{\text{symb}}^{\text{DL}}$ consecutive OFDM symbols in the time domain and $N_{\text{sc}}^{\text{RB}}$ consecutive subcarriers in the frequency domain, where $N_{\text{symb}}^{\text{DL}}$ and $N_{\text{sc}}^{\text{RB}}$ are given by Table 3.1.1.

A physical resource block thus consists of $N_{\text{symb}}^{\text{DL}} \times N_{\text{sc}}^{\text{RB}}$ resource elements, corresponding to one slot in the time domain and 180 kHz in the frequency domain.

Physical resource blocks are numbered from 0 to $N_{\text{RB}}^{\text{DL}} - 1$ in the frequency domain. The relation between the physical resource block number n_{PRB} in the frequency domain and resource elements (k, l) in a slot is given by

$$n_{\text{PRB}} = \left\lfloor \frac{k}{N_{\text{sc}}^{\text{RB}}} \right\rfloor$$

3.1.3.2 Virtual resource block

A virtual resource block is of the same size as a physical resource block. Two types of virtual resource blocks are defined:

- Virtual resource blocks of localized type
- Virtual resource blocks of distributed type

For each type of virtual resource blocks, a pair of virtual resource blocks over two slots in a subframe is assigned together by a single virtual resource block number, n_{VRB}.

Virtual resource blocks of localized type

Virtual resource blocks of localized type are mapped directly to physical resource blocks such that virtual resource block n_{VRB} corresponds to physical resource block $n_{\text{PRB}} = n_{\text{VRB}}$. Virtual resource blocks are numbered from 0 to $N_{\text{VRB}}^{\text{DL}} - 1$, where $N_{\text{VRB}}^{\text{DL}} = N_{\text{RB}}^{\text{DL}}$.

Virtual resource blocks of distributed type

Virtual resource blocks of distributed type are so mapped to physical resource blocks:

the parameter N_{gap} is given by Table 3.1.3.2, for $6 \le N_{\text{RB}}^{\text{DL}} \le 49$, only one gap value $N_{\text{gap},1}$ is defined and $N_{\text{gap}} = N_{\text{gap},1}$. For $50 \le N_{\text{RB}}^{\text{DL}} \le 110$, two gap values $N_{\text{gap},1}$ and $N_{\text{gap},2}$ are defined. Whether $N_{\text{gap}} = N_{\text{gap},1}$ or $N_{\text{gap}} = N_{\text{gap},2}$ is signaled as part of the downlink scheduling assignment.

Virtual resource blocks of distributed type are numbered from 0 to $N_{\text{VRB}}^{\text{DL}} - 1$, where $N_{\text{VRB}}^{\text{DL}} = N_{\text{VRB,gap1}}^{\text{DL}} = 2 \cdot \min(N_{\text{gap}}, N_{\text{RB}}^{\text{DL}} - N_{\text{gap}})$ for $N_{\text{gap}} = N_{\text{gap},1}$ and $N_{\text{VRB}}^{\text{DL}} = N_{\text{VRB,gap2}}^{\text{DL}} = \lfloor N_{\text{RB}}^{\text{DL}} / 2N_{\text{gap}} \rfloor \cdot 2N_{\text{gap}}$ for $N_{\text{gap}} = N_{\text{gap},2}$.

Consecutive $\tilde{N}_{\mathrm{VRB}}^{\mathrm{DL}}$ VRB numbers compose a unit of VRB number interleaving, where $\tilde{N}_{\mathrm{VRB}}^{\mathrm{DL}} = N_{\mathrm{VRB}}^{\mathrm{DL}}$ for $N_{\mathrm{gap}} = N_{\mathrm{gap},1}$ and $\tilde{N}_{\mathrm{VRB}}^{\mathrm{DL}} = 2N_{\mathrm{gap}}$ for $N_{\mathrm{gap}} = N_{\mathrm{gap},2}$.

Interleaving of VRB numbers of each interleaving unit is performed with 4 columns and N_{row} rows, where $N_{\mathrm{row}} = \left\lceil \tilde{N}_{\mathrm{VRB}}^{\mathrm{DL}} / (4P) \right\rceil \cdot P$, and P is RBG size.

VRB numbers are written row by row in the rectangular matrix, and read out column by column. N_{null} nulls are inserted in the last $N_{\mathrm{null}}/2$ rows of the 2nd and 4th column, where $N_{\mathrm{null}} = 4N_{\mathrm{row}} - \tilde{N}_{\mathrm{VRB}}^{\mathrm{DL}}$. Nulls are ignored when reading out.

System BW ($N_{\mathrm{RB}}^{\mathrm{DL}}$)	**Gap (N_{gap})**	
	1st Gap ($N_{\mathrm{gap},1}$)	**2nd Gap ($N_{\mathrm{gap},2}$)**
6-10	$\left\lceil N_{\mathrm{RB}}^{\mathrm{DL}} / 2 \right\rceil$	N/A
11	4	N/A
12-19	8	N/A
20-26	12	N/A
27-44	18	N/A
45-49	27	N/A
50-63	27	9
64-79	32	16
80-110	48	16

Table 3.1.3.2: RB gap values.

3.1.4 Resource element groups

Resource-element groups are used for defining the mapping of control channels to resource elements.

A resource-element group is represented by the index pair (k', l') of the resource element with the lowest index k in the group with all resource elements in the group having the same value of l. The set of resource elements (k, l) in a resource-element group depends on the number of cell-specific reference signals configured as described below with $k_0 = n_{\mathrm{PRB}} \cdot N_{\mathrm{sc}}^{\mathrm{RB}}$, $0 \le n_{\mathrm{PRB}} < N_{\mathrm{RB}}^{\mathrm{DL}}$.

- In the first OFDM symbol of the first slot in a subframe the two resource-element groups in physical resource block n_{PRB} consist of resource elements $(k, l = 0)$ with $k = k_0 + 0, k_0 + 1, \ldots, k_0 + 5$ and $k = k_0 + 6, k_0 + 7, \ldots, k_0 + 11$, respectively.
- In the second OFDM symbol of the first slot in a subframe in case of one or two cell-specific reference signals configured, the three resource-element groups in physical resource block n_{PRB} consist of resource elements $(k, l = 1)$ with $k = k_0 + 0, k_0 + 1, \ldots, k_0 + 3$, $k = k_0 + 4, k_0 + 5, \ldots, k_0 + 7$ and $k = k_0 + 8, k_0 + 9, \ldots, k_0 + 11$, respectively.
- In the second OFDM symbol of the first slot in a subframe in case of four cell-specific reference signals configured, the two resource-element groups in physical resource block

n_{PRB} consist of resource elements $(k, l = 1)$ with $k = k_0 + 0, k_0 + 1, \ldots, k_0 + 5$ and $k = k_0 + 6, k_0 + 7, \ldots, k_0 + 11$, respectively.

- In the third OFDM symbol of the first slot in a subframe, the three resource-element groups in physical resource block n_{PRB} consist of resource elements $(k, l = 2)$ with $k = k_0 + 0, k_0 + 1, \ldots, k_0 + 3$, $k = k_0 + 4, k_0 + 5, \ldots, k_0 + 7$ and $k = k_0 + 8, k_0 + 9, \ldots, k_0 + 11$, respectively
- In the fourth OFDM symbol of the first slot in a subframe in case of normal cyclic prefix, the three resource-element groups in physical resource block n_{PRB} consist of resource elements $(k, l = 3)$ with $k = k_0 + 0, k_0 + 1, \ldots, k_0 + 3$, $k = k_0 + 4, k_0 + 5, \ldots, k_0 + 7$ and $k = k_0 + 8, k_0 + 9, \ldots, k_0 + 11$, respectively.
- In the fourth OFDM symbol of the first slot in a subframe in case of extended cyclic prefix, the two resource-element groups in physical resource block n_{PRB} consist of resource elements $(k, l = 3)$ with $k = k_0 + 0, k_0 + 1, \ldots, k_0 + 5$ and $k = k_0 + 6, k_0 + 7, \ldots, k_0 + 11$, respectively.

3.1.5 Guard period

For half-duplex FDD operation, a guard period is created by the UE by not receiving the last part of a downlink subframe immediately preceding an uplink subframe from the same UE.
For frame structure type 2 (TDD), the GP field in Figure 3.2-1 serves as a guard period.

3.2 Downlink physical channel

The following physical channel are defined:

- Physical Broadcast Channel (PBCH): carries system information for UEs requiring to access the network, this includes for example the system bandwidth.
- Physical Control Format Indicator Channel (PCFICH): is transmitted in the first OFDM symbol of the subframe or of the DwPTS field and reports how many OFDM symbols (1, 2, 3 or 4) carry PDCCH data in that subframe.
- Physical Downlink Control Channel (PDCCH): contains the downlink control information (DCI), whereby the DCI formats differ somewhat for LTE TDD and LTE FDD. The PDCCH is transmitted at the start of every subframe and informs the mobile station where the PDSCH data intended for it is located in the downlink and which resources it may use for transmitting in the uplink.
- Physical Downlink Shared Channel (PDSCH): used only to transmit user data. The data rate can be increased by using the MIMO method of spatial multiplexing, in which multiple data streams are transmitted simultaneously via a multiple antenna system. The mobile station returns an acknowledgement (ACK) in the uplink. If errors occur during the transmission, a request is sent to repeat the transmission (NACK). In contrast to LTE FDD, LTE TDD can

send a single ACK/NACK response for multiple PDSCH transmissions (for multiple subframes).

- Physical Hybrid ARQ Indicator Channel (PHICH): carries the ACK/NACK responses for transmitted uplink packets.
- Physical Multicast Channel (PMCH): carries system information for multicast purposes.

3.2.1 Mapping to transport channel and channel coding

Table 3.2.1-1 and Table 3.2.1-2 respectively specifies the mapping of the downlink transport channels and of the downlink control channel information to their corresponding physical channels and their channel coding scheme.

TrCH	Physical Channel	Coding scheme	Coding rate
DL-SCH	PDSCH	Turbo coding	1/3
MCH	PMCH		
PCH	PDSCH		
BCH	PBCH	Tail biting convolutional coding	1/3

Table 3.2.1-1

Control information	Physical Channel	Coding scheme	Coding rate
CFI	PCFICH	Block code	1/16
HI	PHICH	Repetition code	1/3
DCI	PDCCH	Tail biting convolutional coding	1/3

Table 3.2.1-2

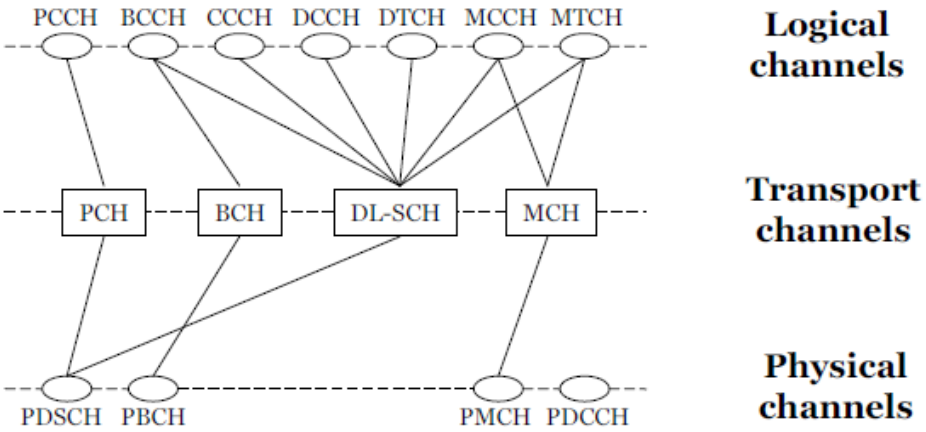

Figure 3.2.1

3.2.2 Modulation

Table 3.2.1-1 and Table 3.2.1-2 respectively specifies the modulation schemes used on each defined physical download channel.

Physical channel	Modulation schemes
PDSCH	QPSK, 16QAM, 64QAM
PMCH	QPSK, 16QAM, 64QAM
PBCH	QPSK
PCFICH	QPSK
PDCCH	QPSK
PHICH	BPSK

Table 3.2.2: Modulation schemes.

3.2.3 General description of physical channel

This section describes a general structure, applicable to more than one physical channel.

The baseband signal representing a downlink physical channel is defined in terms of the following steps:

- Scrambling of coded bits in each of the codewords to be transmitted on a physical channel.
- Modulation of scrambled bits to generate complex-valued modulation symbols.
- Mapping of the complex-valued modulation symbols onto one or several transmission layers.
- Precoding of the complex-valued modulation symbols on each layer for transmission on the antenna ports.
- Mapping of complex-valued modulation symbols for each antenna port to resource elements.
- Generation of complex-valued time-domain OFDM signal for each antenna port.

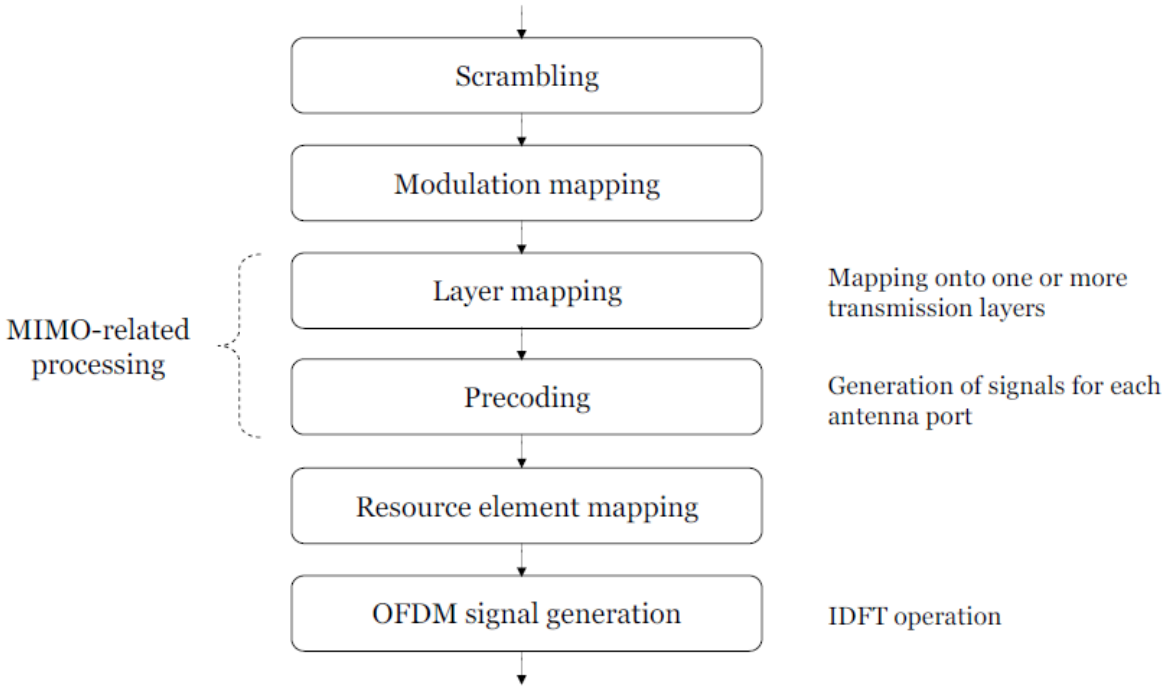

Figure 3.2.2: Overview of physical channel processing.

3.2.3.1 Scrambling

For each codeword q, the block of bits $b^{(q)}(0),\ldots,b^{(q)}(M_{\text{bit}}^{(q)}-1)$, where $M_{\text{bit}}^{(q)}$ is the number of bits in codeword q transmitted on the physical channel in one subframe, shall be scrambled prior to modulation, resulting in a block of scrambled bits $\tilde{b}^{(q)}(0),\ldots,\tilde{b}^{(q)}(M_{\text{bit}}^{(q)}-1)$ according to

$$\tilde{b}^{(q)}(i)=\left(b^{(q)}(i)+c^{(q)}(i)\right)\bmod 2$$

where the scrambling sequence $c^{(q)}(i)$ is given by section A.2. The scrambling sequence generator shall be initialised at the start of each subframe, where the initialisation value of c_{init} depends on the transport channel type according to

$$c_{\text{init}}=\begin{cases} n_{\text{RNTI}}\cdot 2^{14}+q\cdot 2^{13}+\lfloor n_s/2\rfloor\cdot 2^9+N_{\text{ID}}^{\text{cell}} & \text{for PDSCH} \\ \lfloor n_s/2\rfloor\cdot 2^9+N_{\text{ID}}^{\text{MBSFN}} & \text{for PMCH} \end{cases}$$

where n_{RNTI} corresponds to the RNTI associated with the PDSCH transmission.

Up to two codewords can be transmitted in one subframe, i.e., $q\in\{0,1\}$. In the case of single codeword transmission, q is equal to zero.

3.2.3.2 Layer mapping

The complex-valued modulation symbols for each of the codewords to be transmitted are mapped onto one or several layers. Complex-valued modulation symbols $d^{(q)}(0),\ldots,d^{(q)}(M_{\text{symb}}^{(q)}-1)$ for codeword q shall be mapped onto the layers $x(i)=\left[x^{(0)}(i)\ \ \ldots\ \ x^{(\upsilon-1)}(i)\right]^T$, $i=0,1,\ldots,M_{\text{symb}}^{\text{layer}}-1$ where υ is the number of layers and $M_{\text{symb}}^{\text{layer}}$ is the number of modulation symbols per layer.

3.2.3.3 Precoding

The precoder takes as input a block of vectors $x(i)=\left[x^{(0)}(i)\ \ \ldots\ \ x^{(\upsilon-1)}(i)\right]^T$, $i=0,1,\ldots,M_{\text{symb}}^{\text{layer}}-1$ from the layer mapping and generates a block of vectors $y(i)=\left[\ldots\ \ y^{(p)}(i)\ \ \ldots\right]^T$, $i=0,1,\ldots,M_{\text{symb}}^{\text{ap}}-1$ to be mapped onto resources on each of the antenna ports, where $y^{(p)}(i)$ represents the signal for antenna port p.

3.2.3.4 Mapping to resource elements

For each of the antenna ports used for transmission of the physical channel, the block of complex-valued symbols $y^{(p)}(0),\ldots,y^{(p)}(M_{\text{symb}}^{\text{ap}}-1)$ shall be mapped in sequence starting with $y^{(p)}(0)$ to resource elements (k,l) which meet all of the following criteria:

- they are in the physical resource blocks corresponding to the virtual resource blocks assigned for transmission

- they are not used for transmission of PBCH, synchronization signals, cell-specific reference signals, MBSFN reference signals or UE-specific reference signals
- they are not in an OFDM symbol used for PDCCH

The mapping to resource elements (k,l) on antenna port p not reserved for other purposes shall be in increasing order of first the index k over the assigned physical resource blocks and then the index l, starting with the first slot in a subframe.

3.2.4 Physical Downlink shared channel (PDSCH)

The physical downlink shared channel shall be processed and mapped to resource elements as described in section 3.2.3 with the following exceptions:

- In resource blocks in which UE-specific reference signals are not transmitted, the PDSCH shall be transmitted on the same set of antenna ports as the PBCH, which is one of $\{0\}$, $\{0,1\}$, or $\{0,1,2,3\}$
- In resource blocks in which UE-specific reference signals are transmitted, the PDSCH shall be transmitted on antenna port(s) $\{5\}$, $\{7\}$, $\{8\}$, or $\{7,8\}$

3.2.5 Physical Multicast Channel (PMCH)

The physical multicast channel shall be processed and mapped to resource elements as described in section 3.2.3 with the following exceptions:

- Layer mapping and precoding shall be done assuming a single antenna port and the transmission shall use antenna port 4.
- In the subframes where PMCH is transmitted on a carrier supporting a mix of PDSCH and PMCH transmissions, up to two of the first OFDM symbols of a subframe can be reserved for non-MBSFN transmission and shall not be used for PMCH transmission. In a cell with 4 cell-specific antenna ports, the first two OFDM symbols of a subframe are reserved for non-MBSFN transmission in the subframes in which the PMCH is transmitted. The non-MBSFN symbols shall use the same cyclic prefix as used for subframe 0. On a carrier supporting a mix of PDSCH and PMCH transmission, PMCH shall not be transmitted in subframes 0, 4, 5 and 9 for frame structure type 1 and not in subframes 0, 1, 5, 6 for frame structure type 2.

3.2.6 Physical broadcast channel (PBCH)

3.2.6.1 Scrambling

The block of bits $b(0),\ldots,b(M_{\text{bit}}-1)$, where M_{bit}, the number of bits transmitted on the physical broadcast channel, equals 1920 for normal cyclic prefix and 1728 for extended cyclic prefix, shall be scrambled with a cell-specific sequence prior to modulation, resulting in a block of scrambled bits $\tilde{b}(0),\ldots,\tilde{b}(M_{\text{bit}}-1)$ according to

$$\tilde{b}(i) = \left(b(i) + c(i)\right) \bmod 2$$

The scrambling sequence shall be initialised with $c_{\text{init}} = N_{\text{ID}}^{\text{cell}}$ in each radio frame fulfilling $n_{\text{f}} \bmod 4 = 0$.

3.2.6.2 Layer mapping and precoding

The block of modulation symbols $d(0),\ldots,d(M_{\text{symb}}-1)$ shall be mapped to layers according to one of sections 3.2.3.2 with $M_{\text{symb}}^{(0)} = M_{\text{symb}}$ and precoded according to one of sections 3.2.3.3.

3.2.6.3 Mapping to resource elements

The block of complex-valued symbols $y^{(p)}(0),\ldots,y^{(p)}(M_{\text{symb}}-1)$ for each antenna port is transmitted during 4 consecutive radio frames starting in each radio frame fulfilling $n_{\text{f}} \bmod 4 = 0$ and shall be mapped in sequence starting with $y(0)$ to resource elements (k,l). The mapping to resource elements (k,l) not reserved for transmission of reference signals shall be in increasing order of first the index k, then the index l in slot 1 in subframe 0 and finally the radio frame number.

The resource-element indices are given by

$$k = \frac{N_{\text{RB}}^{\text{DL}} N_{\text{sc}}^{\text{RB}}}{2} - 36 + k', \qquad k' = 0,1,\ldots,71$$
$$l = 0,1,\ldots,3$$

where resource elements reserved for reference signals shall be excluded. The mapping operation shall assume cell-specific reference signals for antenna ports 0-3 being present irrespective of the actual configuration. The UE shall assume that the resource elements assumed to be reserved for reference signals in the mapping operation above but not used for transmission of reference signal are not available for PDSCH transmission. The UE shall not make any other assumptions about these resource elements.

3.2.7 Physical control format indicator channel (PCFICH)

The physical control format indicator channel carries information about the number of OFDM symbols used for transmission of PDCCHs in a subframe. The set of OFDM symbols possible to use for PDCCH in a subframe is given by Table 3.2.7.

The PCFICH shall be transmitted when the number of OFDM symbols for PDCCH is greater than zero.

Subframe	**Number of OFDM symbols for PDCCH when** $N_{RB}^{DL} > 10$	**Number of OFDM symbols for PDCCH when** $N_{RB}^{DL} \leq 10$
Subframe 1 and 6 for frame structure type 2	1, 2	2
MBSFN subframes on a carrier supporting both PMCH and PDSCH for 1 or 2 cell-specificc antenna ports	1, 2	2
MBSFN subframes on a carrier supporting both PMCH and PDSCH for 4 cell-specific antenna ports	2	2
MBSFN subframes on a carrier not supporting PDSCH	0	0
Non-MBSFN subframes (except subframe 6 for frame structure type 2) configured with positioning reference signals	1, 2, 3	2, 3
All other cases	1, 2, 3	2, 3, 4

Table 3.2.7: Number of OFDM symbols used for PDCCH.

3.2.7.1 Scrambling

The block of bits $b(0),\ldots,b(31)$ transmitted in one subframe shall be scrambled with a cell-specific sequence prior to modulation, resulting in a block of scrambled bits $\tilde{b}(0),\ldots,\tilde{b}(31)$ according to

$$\tilde{b}(i) = \left(b(i) + c(i)\right) \bmod 2$$

The scrambling sequence generator shall be initialised with $c_{init} = \left(\lfloor n_s/2 \rfloor + 1\right) \cdot \left(2N_{ID}^{cell} + 1\right) \cdot 2^9 + N_{ID}^{cell}$ at the start of each subframe.

3.2.7.2 Layer mapping and precoding

The block of modulation symbols $d(0),\ldots,d(15)$ shall be mapped to layers according to one of sections 3.2.3.2 with $M_{symb}^{(0)} = 16$ and precoded according to one of Sections 3.2.3.3

The PCFICH shall be transmitted on the same set of antenna ports as the PBCH.

3.2.7.3 Mapping to resource elements

The mapping to resource elements is defined in terms of quadruplets of complex-valued symbols. Let $z^{(p)}(i) = \left\langle y^{(p)}(4i), y^{(p)}(4i+1), y^{(p)}(4i+2), y^{(p)}(4i+3) \right\rangle$ denote symbol quadruplet i for antenna port p. For each of the antenna ports, symbol quadruplets shall be mapped in increasing order of i to the four resource-element groups in the first OFDM symbol in a downlink subframe with the representative resource-element given by

$z^{(p)}(0)$ is mapped to the resource - element group represented by $k = \bar{k}$

$z^{(p)}(1)$ is mapped to the resource - element group represented by $k = \bar{k} + \left\lfloor N_{\mathrm{RB}}^{\mathrm{DL}}/2 \right\rfloor \cdot N_{\mathrm{sc}}^{\mathrm{RB}}/2$

$z^{(p)}(2)$ is mapped to the resource - element group represented by $k = \bar{k} + \left\lfloor 2N_{\mathrm{RB}}^{\mathrm{DL}}/2 \right\rfloor \cdot N_{\mathrm{sc}}^{\mathrm{RB}}/2$

$z^{(p)}(3)$ is mapped to the resource - element group represented by $k = \bar{k} + \left\lfloor 3N_{\mathrm{RB}}^{\mathrm{DL}}/2 \right\rfloor \cdot N_{\mathrm{sc}}^{\mathrm{RB}}/2$

where the additions are modulo $N_{\mathrm{RB}}^{\mathrm{DL}} N_{\mathrm{sc}}^{\mathrm{RB}}$,

$$\bar{k} = \left(N_{\mathrm{sc}}^{\mathrm{RB}}/2\right) \cdot \left(N_{\mathrm{ID}}^{\mathrm{cell}} \bmod 2N_{\mathrm{RB}}^{\mathrm{DL}}\right)$$

and $N_{\mathrm{ID}}^{\mathrm{cell}}$ is the physical-layer cell identity as given by section 3.3.1.

3.2.8 Physical downlink control channel (PDCCH)

The physical downlink control channel carries scheduling assignments and other control information. A physical control channel is transmitted on an aggregation of one or several consecutive control channel elements (CCEs), where a control channel element corresponds to 9 resource element groups. The number of resource-element groups not assigned to PCFICH or PHICH is N_{REG}. The CCEs available in the system are numbered from 0 and $N_{CCE} - 1$, where $N_{CCE} = \lfloor N_{REG}/9 \rfloor$.

The PDCCH supports multiple formats as listed in Table 3.2.8.

A PDCCH consisting of n consecutive CCEs may only start on a CCE fulfilling $i \bmod n = 0$, where i is the CCE number.

Multiple PDCCHs can be transmitted in a subframe.

PDCCH format	Number of CCEs	Number of resource-element groups	Number of PDCCH bits
0	1	9	72
1	2	18	144
2	4	36	288
3	8	72	576

Table 3.2.8: Supported PDCCH formats.

3.2.9 Physical hybrid ARQ indicator channel (PHICH)

The PHICH carries the hybrid-ARQ ACK/NACK. Multiple PHICHs mapped to the same set of resource elements constitute a PHICH group, where PHICHs within the same PHICH group are separated through different orthogonal sequences. A PHICH resource is identified by the index pair $\left(n_{\mathrm{PHICH}}^{\mathrm{group}}, n_{\mathrm{PHICH}}^{\mathrm{seq}}\right)$, where $n_{\mathrm{PHICH}}^{\mathrm{group}}$ is the PHICH group number and $n_{\mathrm{PHICH}}^{\mathrm{seq}}$ is the orthogonal sequence index within the group.

For frame structure type 1, the number of PHICH groups $N_{\mathrm{PHICH}}^{\mathrm{group}}$ is constant in all subframes and given by

$$N_{\text{PHICH}}^{\text{group}} = \begin{cases} \lceil N_{\text{g}} \left(N_{\text{RB}}^{\text{DL}} / 8 \right) \rceil & \text{for normal cyclic prefix} \\ 2 \cdot \lceil N_{\text{g}} \left(N_{\text{RB}}^{\text{DL}} / 8 \right) \rceil & \text{for extended cyclic prefix} \end{cases}$$

where $N_{\text{g}} \in \{1/6, 1/2, 1, 2\}$ is provided by higher layers. The index $n_{\text{PHICH}}^{\text{group}}$ ranges from 0 to $N_{\text{PHICH}}^{\text{group}} - 1$.

For frame structure type 2, the number of PHICH groups may vary between downlink subframes and is given by $m_i \cdot N_{\text{PHICH}}^{\text{group}}$ where m_i is given by Table 3.2.9-1 and $N_{\text{PHICH}}^{\text{group}}$ by the expression above. The index $n_{\text{PHICH}}^{\text{group}}$ in a downlink subframe with non-zero PHICH resources ranges from 0 to $m_i \cdot N_{\text{PHICH}}^{\text{group}} - 1$.

The PHICH duration is configurable by higher layers according to Table 3.2.9-2.

Uplink-downlink configuration	**Subframe number** i									
	0	**1**	**2**	**3**	**4**	**5**	**6**	**7**	**8**	**9**
0	2	1	-	-	-	2	1	-	-	-
1	0	1	-	-	1	0	1	-	-	1
2	0	0	-	1	0	0	0	-	1	0
3	1	0	-	-	-	0	0	0	1	1
4	0	0	-	-	0	0	0	0	1	1
5	0	0	-	0	0	0	0	0	1	0
6	1	1	-	-	-	1	1	-	-	1

Table 3.2.9-1: The factor m_i for frame structure type 2.

PHICH duration	**Non-MBSFN subframes**		**MBSFN subframes**
	Subframes 1 and 6 in case of frame structure type 2	**All other cases**	**On a carrier supporting both PDSCH and PMCH**
Normal	1	1	1
Extended	2	3	2

Table 3.2.9-2: PHICH duration.

3.3 Reference signal

Four types of downlink reference signals are defined:

- Cell-specific reference signals, associated with non-MBSFN transmission
- MBSFN reference signals, associated with MBSFN transmission
- UE-specific reference signals
- Positioning reference signals

There is one reference signal transmitted per downlink antenna port.

3.3.1 Cell-specific reference signals

Cell-specific reference signals shall be transmitted in all downlink subframes in a cell supporting non-MBSFN transmission. In case the subframe is used for transmission with MBSFN, only the first two OFDM symbols in a subframe can be used for transmission of cell-specific reference symbols.

Cell-specific reference signals are transmitted on one or several of antenna ports 0 to 3.

Cell-specific reference signals are defined for $\Delta f = 15\,\text{kHz}$ only.

3.3.1.1 Sequence generation

The reference-signal sequence $r_{l,n_s}(m)$ is defined by

$$r_{l,n_s}(m) = \frac{1}{\sqrt{2}}(1-2\cdot c(2m)) + j\frac{1}{\sqrt{2}}(1-2\cdot c(2m+1)), \quad m = 0,1,\ldots,2N_{\mathrm{RB}}^{\max,\mathrm{DL}} - 1$$

where n_s is the slot number within a radio frame and l is the OFDM symbol number within the slot. The pseudo-random sequence generator shall be initialised with $c_{\mathrm{init}} = 2^{10}\cdot(7\cdot(n_s+1)+l+1)\cdot(2\cdot N_{ID}^{cell}+1)+2\cdot N_{ID}^{cell}+N_{CP}$ at the start of each OFDM symbol where

$$N_{CP} = \begin{cases} 1 & \text{for normal CP} \\ 0 & \text{for extended CP} \end{cases}$$

3.3.1.2 Mapping to resource elements

Figures 3.3.1.2-1 and 3.3.1.2-2 illustrate the resource elements used for reference signal transmission respectively for normal and extended cyclic prefix.

The notation R_p is used to denote a resource element used for reference signal transmission on antenna port p.

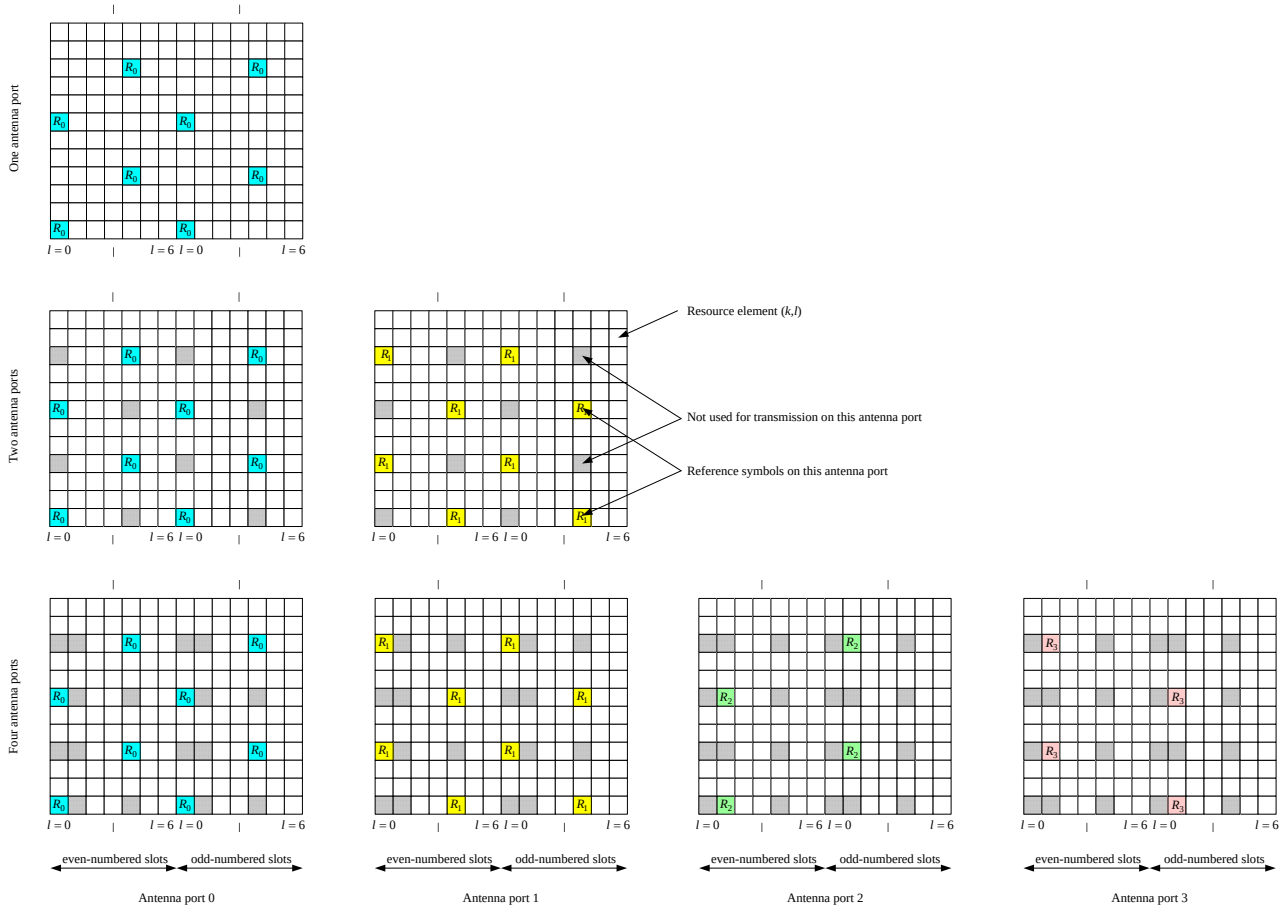

Figure 3.3.1.2-1. Mapping of downlink reference signals for normal cyclic prefix.

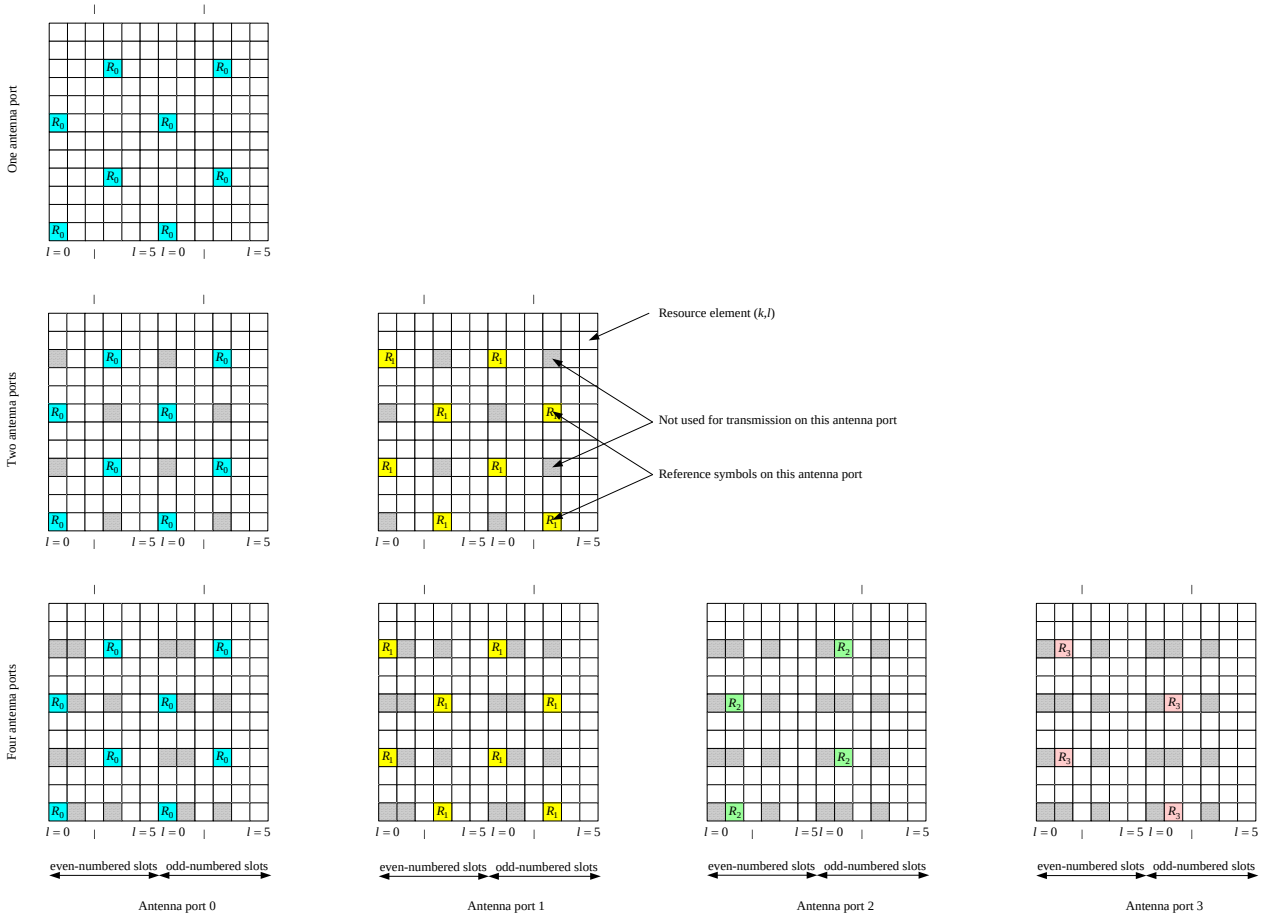

Figure 3.3.1.2-2. Mapping of downlink reference signals for extended cyclic prefix.

3.3.2 MBSFN reference signals

MBSFN reference signals shall only be transmitted in subframes allocated for MBSFN transmissions. MBSFN reference signals are transmitted on antenna port 4.

MBSFN reference signals are defined for extended cyclic prefix only.

3.3.2.1 Sequence generation

The MBSFN reference-signal sequence $r_{l,n_s}(m)$ is defined by

$$r_{l,n_s}(m) = \frac{1}{\sqrt{2}}\left(1-2\cdot c(2m)\right) + j\frac{1}{\sqrt{2}}\left(1-2\cdot c(2m+1)\right), \quad m = 0,1,\ldots,6N_{\mathrm{RB}}^{\max,\mathrm{DL}}-1$$

where n_s is the slot number within a radio frame and l is the OFDM symbol number within the slot. The pseudo-random sequence generator shall be initialised with

$$c_{\mathrm{init}} = 2^9\cdot\left(7\cdot(n_s+1)+l+1\right)\cdot\left(2\cdot N_{\mathrm{ID}}^{\mathrm{MBSFN}}+1\right)+N_{\mathrm{ID}}^{\mathrm{MBSFN}}$$

at the start of each OFDM symbol.

3.3.2.2 Mapping to resource elements

Figure 3.3.2.2-1 illustrates the resource elements used for MBSFN reference signal transmission in case of $\Delta f = 15\,\mathrm{kHz}$.

In case of $\Delta f = 7.5\,\text{kHz}$ for a MBSFN-dedicated cell, the MBSFN reference signal shall be mapped to resource elements according to Figure 3.3.2.2-2. The notation R_p is used to denote a resource element used for reference signal transmission on antenna port p.

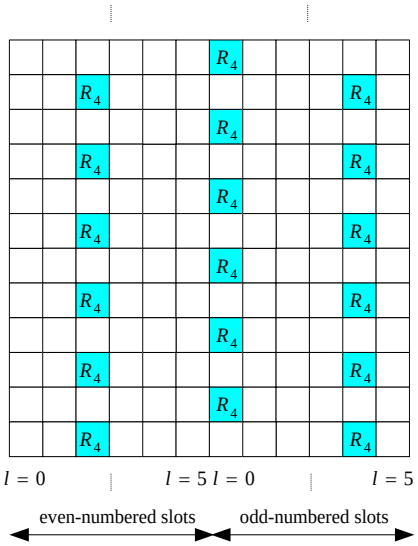

Figure 3.3.2.2-1: Mapping of MBSFN reference signals for $\Delta f = 15\,\text{kHz}$.

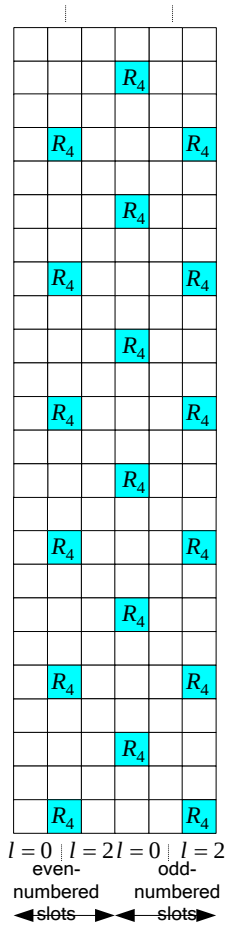

Figure 3.3.2.2-2: Mapping of MBSFN reference signals for $\Delta f = 7.5\,\text{kHz}$.

3.3.3 UE-specific reference signals

UE-specific reference signals are supported for single-antenna-port transmission of PDSCH and are transmitted on antenna port 5, 7, or 8. UE-specific reference signals are also supported for spatial multiplexing on antenna ports 7 and 8. UE-specific reference signals are transmitted only on the resource blocks upon which the corresponding PDSCH is mapped. The UE-specific reference signal is not transmitted in resource elements (k,l) in which one of the physical channels or physical signals other than UE-specific reference signal are transmitted using resource elements with the same index pair (k,l) regardless of their antenna port p.

3.3.3.1 Sequence generation

For antenna port 5, the UE-specific reference-signal sequence $r_{n_s}(m)$ is defined by

$$r_{n_s}(m) = \frac{1}{\sqrt{2}}\left(1-2\cdot c(2m)\right) + j\frac{1}{\sqrt{2}}\left(1-2\cdot c(2m+1)\right), \qquad m = 0,1,\ldots,12N_{\mathrm{RB}}^{\mathrm{PDSCH}}-1$$

where $N_{\mathrm{RB}}^{\mathrm{PDSCH}}$ denotes the bandwidth in resource blocks of the corresponding PDSCH transmission. The pseudo-random sequence generator shall be initialised with $c_{\mathrm{init}} = \left(\lfloor n_s/2 \rfloor + 1\right)\cdot\left(2N_{\mathrm{ID}}^{\mathrm{cell}}+1\right)\cdot 2^{16} + n_{\mathrm{RNTI}}$ at the start of each subframe.

For antenna ports 7 and 8, the reference-signal sequence $r(m)$ is defined by

$$r(m) = \frac{1}{\sqrt{2}}\left(1-2\cdot c(2m)\right) + j\frac{1}{\sqrt{2}}\left(1-2\cdot c(2m+1)\right), \qquad m = 0,1,\ldots,12N_{\mathrm{RB}}^{\max,\mathrm{DL}}-1.$$

The pseudo-random sequence generator shall be initialised with $c_{\mathrm{init}} = \left(\lfloor n_s/2 \rfloor + 1\right)\cdot\left(2N_{\mathrm{ID}}^{\mathrm{cell}}+1\right)\cdot 2^{16} + n_{\mathrm{SCID}}$ at the start of each subframe, where n_{SCID} is given by the scrambling identity field according to Table 3.3.3.1 in the most recent DCI format 2B associated with the PDSCH transmission. If there is no DCI format 2B associated with the PDSCH transmission, the UE shall assume that n_{SCID} is zero.

Scrambling identity field in DCI format 2B [3]	n_{SCID}
0	0
1	1

Table 3.3.3.1: Mapping of scrambling identity field in DCI format 2B to n_{SCID} values.

3.3.3.2 Mapping to resource elements

Figure 3.3.3.2-1 and Figure 3.3.3.2-2 illustrates respectively the resource elements used for UE-specific reference signals for normal cyclic prefix and extended cyclic prefix for antenna port 5.

Figure 3.3.3.2-3 illustrates the resource elements used for UE-specific reference signals for normal cyclic prefix for antenna ports 7 and 8.

The notation R_p is used to denote a resource element used for reference signal transmission on antenna port p.

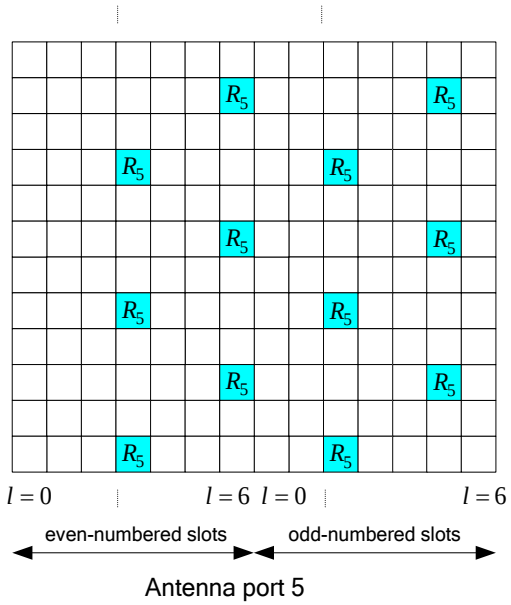

Figure 3.3.3.2-1: Mapping of UE-specific reference signals, antenna port 5 for normal cyclic prefix

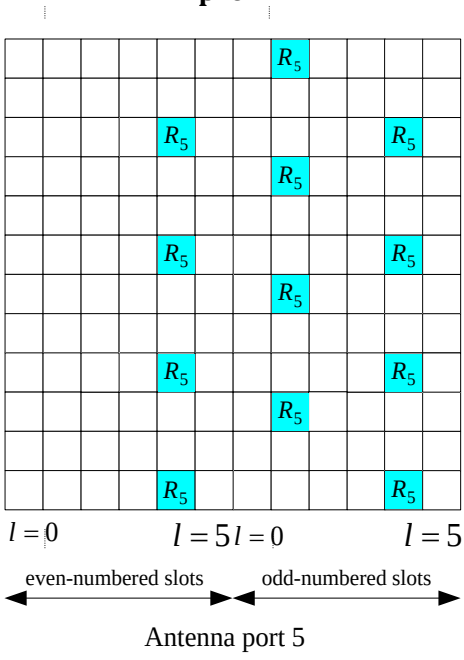

Figure 3.3.3.2-2: Mapping of UE-specific reference signals, antenna port 5 for extended cyclic prefix

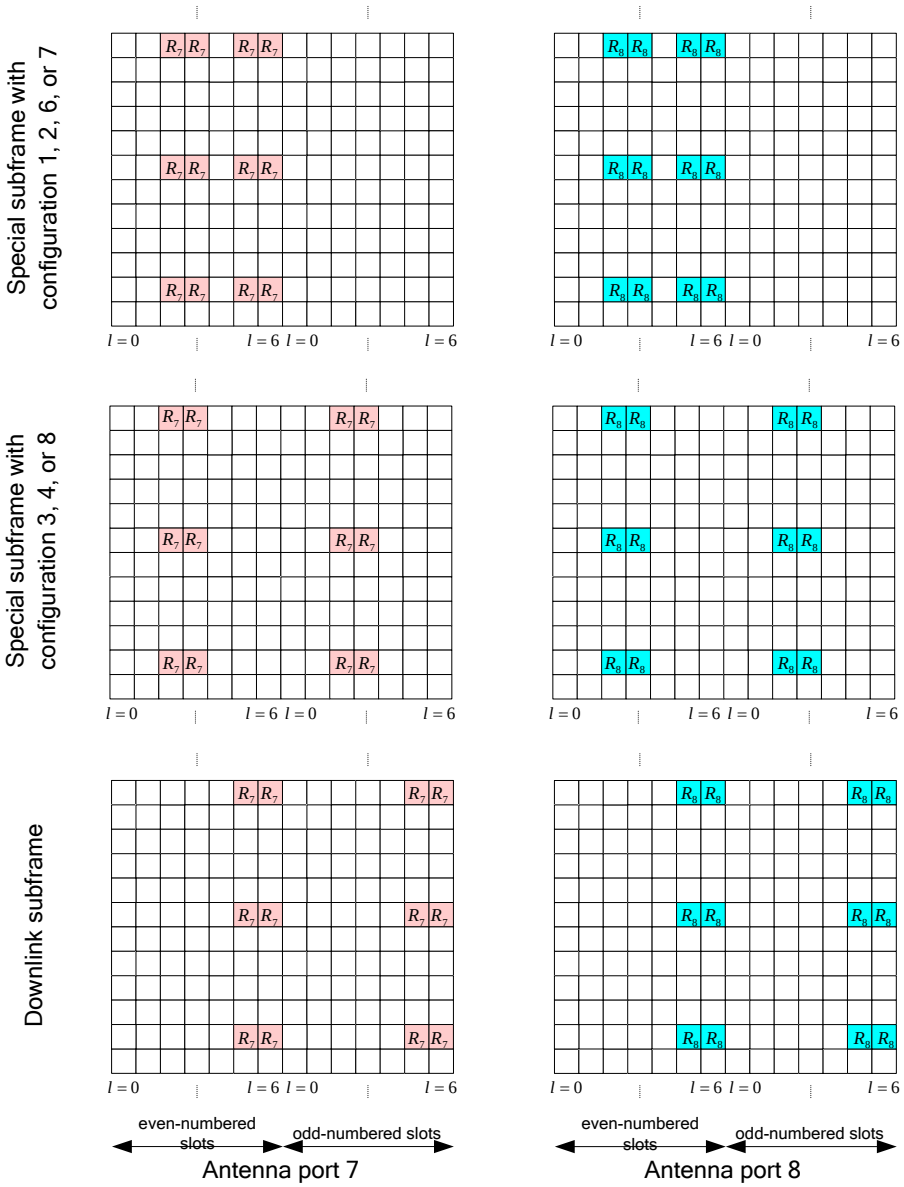

Figure 3.3.3.2-3: Mapping of UE-specific reference signals, antenna ports 7 and 8 for normal cyclic prefix.

3.3.4 Positioning reference signals

Positioning reference signals shall only be transmitted in resource blocks in downlink subframes configured for positioning reference signals transmission. If both normal and MBSFN subframes are configured as positioning subframes within a cell, the OFDM symbols in a MBSFN subframe configured for positioning reference signals transmission shall use the same cyclic prefix as used for subframe #0. If only MBSFN subframes are configured as positioning subframes within a cell, the OFDM symbols configured for positioning reference signals in these subframes shall use extended cyclic prefix length. Positioning reference signals are transmitted on antenna port 6.

The positioning reference signals shall not be mapped to resource elements (k,l) allocated to PBCH, PSS or SSS regardless of their antenna port p.

Positioning reference signals are defined for $\Delta f = 15\,\text{kHz}$ only.

3.3.4.1 Sequence generation

The reference-signal sequence $r_{l,n_s}(m)$ is defined by

$$r_{l,n_s}(m) = \frac{1}{\sqrt{2}}(1-2\cdot c(2m)) + j\frac{1}{\sqrt{2}}(1-2\cdot c(2m+1)), \quad m = 0,1,\ldots,2N_{\mathrm{RB}}^{\max,\mathrm{DL}} - 1$$

where n_s is the slot number within a radio frame, l is the OFDM symbol number within the slot. The pseudo random sequence generator shall be initialized with

$$c_{\mathrm{init}} = 2^{10}\cdot(7\cdot(n_s+1)+l+1)\cdot(2\cdot N_{\mathrm{ID}}^{\mathrm{cell}}+1)+2\cdot N_{\mathrm{ID}}^{\mathrm{cell}}+N_{\mathrm{CP}}$$

at the start of each OFDM symbol where

$$N_{\mathrm{CP}} = \begin{cases} 1 & \text{for normal CP} \\ 0 & \text{for extended CP} \end{cases}$$

3.3.4.2 Mapping to resource elements

Figure 3.3.4.2-1 and 3.3.4.2-2 illustrates respectively the resource elements used for positioning reference signals with normal and extended cyclic prefix.

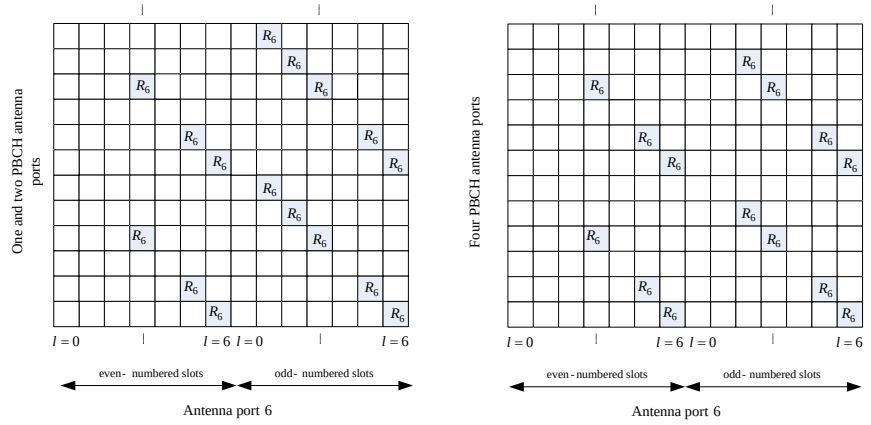

Figure 3.3.4.2-1: Mapping of positioning reference signals with normal cyclic prefix.

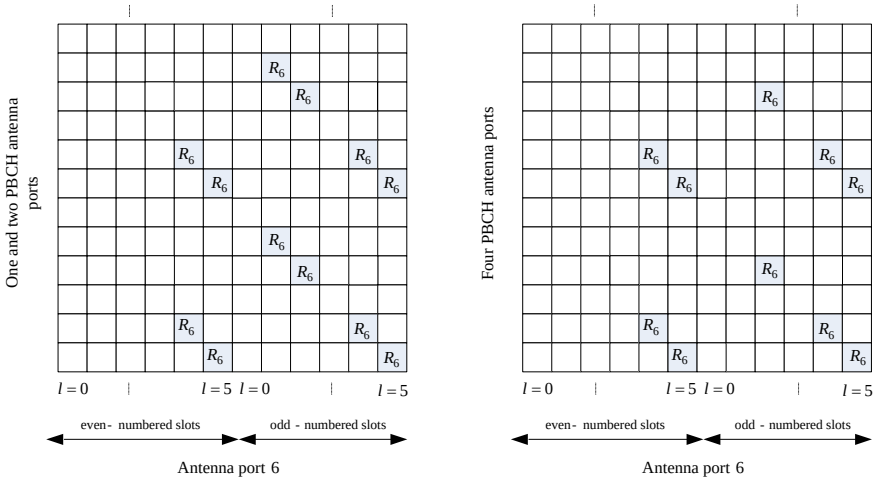

Figure 3.3.4.2-2: Mapping of positioning reference signals with extended cyclic prefix.

3.4 Synchronization signal

3.4.1 Physical-layer cell identities

There are 504 unique physical-layer cell identities. The physical-layer cell identities are grouped into 168 unique physical-layer cell-identity groups, each group containing three unique identities. The grouping is such that each physical-layer cell identity is part of one and only one physical-layer cell-identity group. A physical-layer cell identity $N_{\mathrm{ID}}^{\mathrm{cell}} = 3N_{\mathrm{ID}}^{(1)} + N_{\mathrm{ID}}^{(2)}$ is thus uniquely defined by a number $N_{\mathrm{ID}}^{(1)}$ in the range of 0 to 167, representing the physical-layer cell-identity group, and a number $N_{\mathrm{ID}}^{(2)}$ in the range of 0 to 2, representing the physical-layer identity within the physical-layer cell-identity group.

3.4.2 Primary synchronization signal

3.4.2.1 Sequence generation

The sequence $d(n)$ used for the primary synchronization signal is generated from a frequency-domain Zadoff-Chu sequence according to

$$d_u(n) = \begin{cases} e^{-j\frac{\pi u n(n+1)}{63}} & n = 0,1,\ldots,30 \\ e^{-j\frac{\pi u(n+1)(n+2)}{63}} & n = 31,32,\ldots,61 \end{cases}$$

where the Zadoff-Chu root sequence index u is given by Table 3.4.2.1.

$N_{\mathrm{ID}}^{(2)}$	**Root index** u
0	25
1	29
2	34

Table 3.4.2.1: Root indices for the primary synchronization signal.

3.4.2.2 Mapping to resource elements

The mapping of the sequence to resource elements depends on the frame structure. The UE shall not assume that the primary synchronization signal is transmitted on the same antenna port as any of the downlink reference signals. The UE shall not assume that any transmission instance of the primary synchronization signal is transmitted on the same antenna port, or ports, used for any other transmission instance of the primary synchronization signal.

The sequence $d(n)$ shall be mapped to the resource elements according to

$$a_{k,l} = d(n), \qquad n = 0,\ldots,61$$
$$k = n - 31 + \frac{N_{\mathrm{RB}}^{\mathrm{DL}} N_{\mathrm{sc}}^{\mathrm{RB}}}{2}$$

For frame structure type 1, the primary synchronization signal shall be mapped to the last OFDM symbol in slots 0 and 10.

For frame structure type 2, the primary synchronization signal shall be mapped to the third OFDM symbol in subframes 1 and 6. Resource elements (k,l) in the OFDM symbols used for transmission of the primary synchronization signal where

$$k = n - 31 + \frac{N_{\mathrm{RB}}^{\mathrm{DL}} N_{\mathrm{sc}}^{\mathrm{RB}}}{2}$$
$$n = -5,-4,\ldots,-1,62,63,\ldots 66$$

are reserved and not used for transmission of the primary synchronization signal.

3.4.3 Secondary synchronization signal

3.4.3.1 Sequence generation

The sequence $d(0),\ldots,d(61)$ used for the second synchronization signal is an interleaved concatenation of two length-31 binary sequences. The concatenated sequence is scrambled with a scrambling sequence given by the primary synchronization signal.

The combination of two length-31 sequences defining the secondary synchronization signal differs between subframe 0 and subframe 5 according to

$$d(2n) = \begin{cases} s_0^{(m_0)}(n)c_0(n) & \text{in subframe 0} \\ s_1^{(m_1)}(n)c_0(n) & \text{in subframe 5} \end{cases}$$
$$d(2n+1) = \begin{cases} s_1^{(m_1)}(n)c_1(n)z_1^{(m_0)}(n) & \text{in subframe 0} \\ s_0^{(m_0)}(n)c_1(n)z_1^{(m_1)}(n) & \text{in subframe 5} \end{cases}$$

where $0 \le n \le 30$. The indices m_0 and m_1 are derived from the physical-layer cell-identity group $N_{\mathrm{ID}}^{(1)}$ according to

$$m_0 = m' \bmod 31$$
$$m_1 = \left(m_0 + \lfloor m'/31 \rfloor + 1\right) \bmod 31$$
$$m' = N_{\mathrm{ID}}^{(1)} + q(q+1)/2, \quad q = \left\lfloor \frac{N_{\mathrm{ID}}^{(1)} + q'(q'+1)/2}{30} \right\rfloor, \quad q' = \lfloor N_{\mathrm{ID}}^{(1)}/30 \rfloor$$

where the output of the above expression is listed in Table 3.4.3.1.

The two sequences $s_0^{(m_0)}(n)$ and $s_1^{(m_1)}(n)$ are defined as two different cyclic shifts of the m-sequence $\tilde{s}(n)$ according to

$$s_0^{(m_0)}(n) = \tilde{s}\left((n+m_0) \bmod 31\right)$$
$$s_1^{(m_1)}(n) = \tilde{s}\left((n+m_1) \bmod 31\right)$$

where $\tilde{s}(i) = 1 - 2x(i)$, $0 \le i \le 30$, is defined by

$$x(\bar{i}+5) = \left(x(\bar{i}+2) + x(\bar{i})\right) \bmod 2, \qquad 0 \le \bar{i} \le 25$$

with initial conditions $x(0) = 0, \quad x(1) = 0, \quad x(2) = 0, \quad x(3) = 0, \quad x(4) = 1.$

The two scrambling sequences $c_0(n)$ and $c_1(n)$ depend on the primary synchronization signal and are defined by two different cyclic shifts of the m-sequence $\tilde{c}(n)$ according to

$$c_0(n) = \tilde{c}((n + N_{\mathrm{ID}}^{(2)}) \bmod 31)$$
$$c_1(n) = \tilde{c}((n + N_{\mathrm{ID}}^{(2)} + 3) \bmod 31)$$

where $N_{\mathrm{ID}}^{(2)} \in \{0,1,2\}$ is the physical-layer identity within the physical-layer cell identity group $N_{\mathrm{ID}}^{(1)}$ and $\tilde{c}(i) = 1 - 2x(i)$, $0 \le i \le 30$, is defined by

$$x(\bar{i} + 5) = \left(x(\bar{i} + 3) + x(\bar{i})\right) \bmod 2, \qquad 0 \le \bar{i} \le 25$$

with initial conditions $x(0) = 0, \quad x(1) = 0, \quad x(2) = 0, \quad x(3) = 0, \quad x(4) = 1.$

The scrambling sequences $z_1^{(m_0)}(n)$ and $z_1^{(m_1)}(n)$ are defined by a cyclic shift of the m-sequence $\tilde{z}(n)$ according to

$$z_1^{(m_0)}(n) = \tilde{z}((n + (m_0 \bmod 8)) \bmod 31)$$

$$z_1^{(m_1)}(n) = \tilde{z}((n + (m_1 \bmod 8)) \bmod 31)$$

where m_0 and m_1 are obtained from Table 3.4.3.1 and $\tilde{z}(i) = 1 - 2x(i)$, $0 \le i \le 30$, is defined by

$$x(\bar{i} + 5) = \left(x(\bar{i} + 4) + x(\bar{i} + 2) + x(\bar{i} + 1) + x(\bar{i})\right) \bmod 2, \qquad 0 \le \bar{i} \le 25$$

with initial conditions $x(0) = 0, \quad x(1) = 0, \quad x(2) = 0, \quad x(3) = 0, \quad x(4) = 1.$

$N_{\mathrm{ID}}^{(1)}$	m_0	m_1	$N_{\mathrm{ID}}^{(1)}$	m_0	m_1	$N_{\mathrm{ID}}^{(1)}$	m_0	m_1	$N_{\mathrm{ID}}^{(1)}$	m_0	m_1	$N_{\mathrm{ID}}^{(1)}$	m_0	m_1
0	0	1	34	4	6	68	9	12	102	15	19	136	22	27
1	1	2	35	5	7	69	10	13	103	16	20	137	23	28
2	2	3	36	6	8	70	11	14	104	17	21	138	24	29
3	3	4	37	7	9	71	12	15	105	18	22	139	25	30
4	4	5	38	8	10	72	13	16	106	19	23	140	0	6
5	5	6	39	9	11	73	14	17	107	20	24	141	1	7
6	6	7	40	10	12	74	15	18	108	21	25	142	2	8
7	7	8	41	11	13	75	16	19	109	22	26	143	3	9
8	8	9	42	12	14	76	17	20	110	23	27	144	4	10
9	9	10	43	13	15	77	18	21	111	24	28	145	5	11
10	10	11	44	14	16	78	19	22	112	25	29	146	6	12
11	11	12	45	15	17	79	20	23	113	26	30	147	7	13
12	12	13	46	16	18	80	21	24	114	0	5	148	8	14
13	13	14	47	17	19	81	22	25	115	1	6	149	9	15
14	14	15	48	18	20	82	23	26	116	2	7	150	10	16
15	15	16	49	19	21	83	24	27	117	3	8	151	11	17
16	16	17	50	20	22	84	25	28	118	4	9	152	12	18
17	17	18	51	21	23	85	26	29	119	5	10	153	13	19
18	18	19	52	22	24	86	27	30	120	6	11	154	14	20
19	19	20	53	23	25	87	0	4	121	7	12	155	15	21
20	20	21	54	24	26	88	1	5	122	8	13	156	16	22
21	21	22	55	25	27	89	2	6	123	9	14	157	17	23
22	22	23	56	26	28	90	3	7	124	10	15	158	18	24
23	23	24	57	27	29	91	4	8	125	11	16	159	19	25
24	24	25	58	28	30	92	5	9	126	12	17	160	20	26
25	25	26	59	0	3	93	6	10	127	13	18	161	21	27
26	26	27	60	1	4	94	7	11	128	14	19	162	22	28
27	27	28	61	2	5	95	8	12	129	15	20	163	23	29
28	28	29	62	3	6	96	9	13	130	16	21	164	24	30
29	29	30	63	4	7	97	10	14	131	17	22	165	0	7
30	0	2	64	5	8	98	11	15	132	18	23	166	1	8
31	1	3	65	6	9	99	12	16	133	19	24	167	2	9
32	2	4	66	7	10	100	13	17	134	20	25	-	-	-
33	3	5	67	8	11	101	14	18	135	21	26	-	-	-

Table 3.4.3.1: Mapping between physical-layer cell-identity group and the indices m_0 and m_1

3.4.3.2 Mapping to resource elements

The mapping of the sequence to resource elements depends on the frame structure. In a subframe for frame structure type 1 and in a half-frame for frame structure type 2, the same antenna port as for the primary synchronization signal shall be used for the secondary synchronization signal.

3.5 OFDM baseband signal generation

The time-continuous signal $s_l^{(p)}(t)$ on antenna port p in OFDM symbol l in a downlink slot is defined by

$$s_l^{(p)}(t) = \sum_{k=-\lfloor N_{\mathrm{RB}}^{\mathrm{DL}} N_{\mathrm{sc}}^{\mathrm{RB}}/2 \rfloor}^{-1} a_{k^{(-)},l}^{(p)} \cdot e^{j2\pi k \Delta f \left(t - N_{\mathrm{CP},l} T_{\mathrm{s}}\right)} + \sum_{k=1}^{\lceil N_{\mathrm{RB}}^{\mathrm{DL}} N_{\mathrm{sc}}^{\mathrm{RB}}/2 \rceil} a_{k^{(+)},l}^{(p)} \cdot e^{j2\pi k \Delta f \left(t - N_{\mathrm{CP},l} T_{\mathrm{s}}\right)}$$

for $0 \le t < (N_{\mathrm{CP},l} + N) \times T_{\mathrm{s}}$ where $k^{(-)} = k + \lfloor N_{\mathrm{RB}}^{\mathrm{DL}} N_{\mathrm{sc}}^{\mathrm{RB}}/2 \rfloor$ and $k^{(+)} = k + \lfloor N_{\mathrm{RB}}^{\mathrm{DL}} N_{\mathrm{sc}}^{\mathrm{RB}}/2 \rfloor - 1$. The variable N equals 2048 for $\Delta f = 15\,\mathrm{kHz}$ subcarrier spacing and 4096 for $\Delta f = 7.5\,\mathrm{kHz}$ subcarrier spacing.

The OFDM symbols in a slot shall be transmitted in increasing order of l, starting with $l = 0$, where OFDM symbol $l > 0$ starts at time $\sum_{l'=0}^{l-1} (N_{\mathrm{CP},l'} + N) T_{\mathrm{s}}$ within the slot. In case the first OFDM symbol(s) in a slot use normal cyclic prefix and the remaining OFDM symbols use extended cyclic prefix, the starting position the OFDM symbols with extended cyclic prefix shall be identical to those in a slot where all OFDM symbols use extended cyclic prefix. Thus there will be a part of the time slot between the two cyclic prefix regions where the transmitted signal is not specified.

Table 3.5 lists the value of $N_{\mathrm{CP},l}$ that shall be used. Note that different OFDM symbols within a slot in some cases have different cyclic prefix lengths.

Configuration		Cyclic prefix length $N_{\mathrm{CP},l}$
Normal cyclic prefix	$\Delta f = 15\,\mathrm{kHz}$	160 for $l = 0$ 144 for $l = 1,2,\ldots,6$
Extended cyclic prefix	$\Delta f = 15\,\mathrm{kHz}$	512 for $l = 0,1,\ldots,5$
	$\Delta f = 7.5\,\mathrm{kHz}$	1024 for $l = 0,1,2$

Table 3.5: OFDM parameters.

Chapter 4

UPLOAD

4.1 Slot structure and physical resources

4.1.1 Resource grid

The transmitted signal in each slot is described by a resource grid of $N_{RB}^{UL} N_{sc}^{RB}$ subcarriers and N_{symb}^{UL} SC-FDMA symbols. The resource grid is illustrated in Figure 4.1.1. The quantity N_{RB}^{UL} depends on the uplink transmission bandwidth configured in the cell and shall fulfill

$$N_{RB}^{min,UL} \leq N_{RB}^{UL} \leq N_{RB}^{max,UL}$$

where $N_{RB}^{min,UL} = 6$ and $N_{RB}^{max,UL} = 110$ are the smallest and largest uplink bandwidths, respectively, supported by the current version of specification [1].

The number of SC-FDMA symbols in a slot depends on the cyclic prefix length configured by the higher layer parameter *UL-CyclicPrefixLength* and is given in Table 4.1.1.

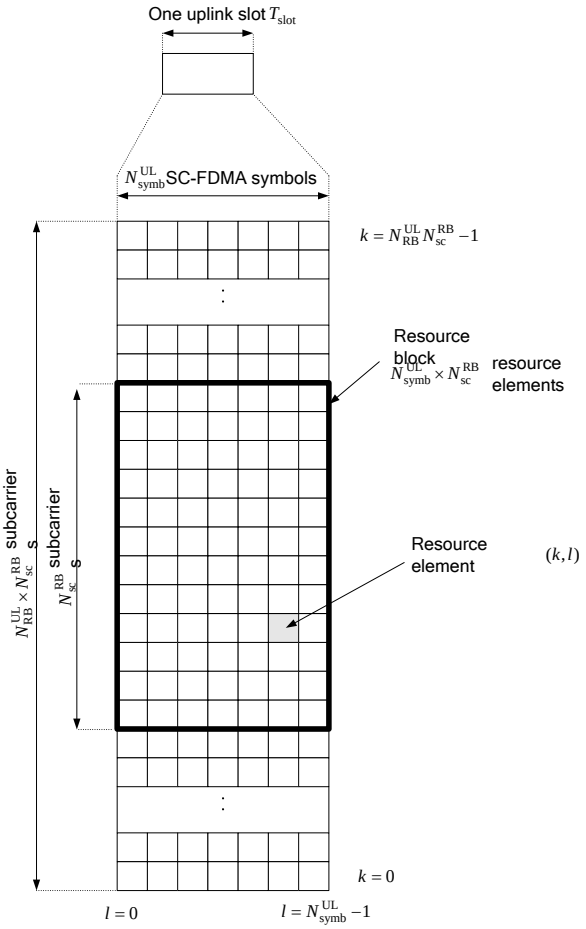

Figure 4.1.1: Uplink resource grid.

4.1.2 Resource elements

Each element in the resource grid is called a resource element and is uniquely defined by the index pair (k,l) in a slot where $k = 0,\ldots,N_{\mathrm{RB}}^{\mathrm{UL}}N_{\mathrm{sc}}^{\mathrm{RB}}-1$ and $l = 0,\ldots,N_{\mathrm{symb}}^{\mathrm{UL}}-1$ are the indices in the frequency and time domains, respectively. Resource element (k,l) corresponds to the complex value $a_{k,l}$. Quantities $a_{k,l}$ corresponding to resource elements not used for transmission of a physical channel or a physical signal in a slot shall be set to zero.

4.1.3 Resource blocks

A physical resource block is defined as $N_{\mathrm{symb}}^{\mathrm{UL}}$ consecutive SC-FDMA symbols in the time domain and $N_{\mathrm{sc}}^{\mathrm{RB}}$ consecutive subcarriers in the frequency domain, where $N_{\mathrm{symb}}^{\mathrm{UL}}$ and $N_{\mathrm{sc}}^{\mathrm{RB}}$ are given by Table 4.1.3. A physical resource block in the uplink thus consists of $N_{\mathrm{symb}}^{\mathrm{UL}} \times N_{\mathrm{sc}}^{\mathrm{RB}}$ resource elements, corresponding to one slot in the time domain and 180 kHz in the frequency domain.

Configuration	$N_{\mathrm{sc}}^{\mathrm{RB}}$	$N_{\mathrm{symb}}^{\mathrm{UL}}$
Normal cyclic prefix	12	7
Extended cyclic prefix	12	6

Table 4.1.3: Resource block parameters.

4.2 Uplink physical cannel

4.2.1 General description

For the uplink physical channels are defined as follows:

- Physical Uplink Shared Channel (PUSCH): This channel is the uplink counterpart of PDSCH, transmits the user data from the mobile station to the base station. The uplink control information such as channel quality, scheduling requests and ACK/NACK responses for downlink packets, are also transmitted via this channel. Like for PDSCH, a bundled ACK/NACK response can be sent for multiple PUSCH transmissions from the base station in LTE TDD mode.
- Physical Uplink Control Channel (PUCCH): If a mobile station does not have any packets to be transmitted on the PUSCH, the control information is sent via the PUCCH.
- Physical Random Access Channel (PRACH): This uplink physical channel is used for random access functions.

4.2.2 Mapping to transport channel and channel coding

Tables 4.2.2-1 and 4.2.2-2 respectively specifies the mapping of the uplink transport channels and of the uplink control channel information to their corresponding physical channels and the usage of channel coding scheme and the coding rate.

Transport Channel	Physical Channel	Coding scheme	Coding rate
UL-SCH	PUSCH	Turbo coding	1/3
RACH	PRACH		

Table 4.2.2-1

Control information	Physical Channel	Coding scheme	Coding rate
UCI	PUCCH, PUSCH	Block code	variable
		Tail biting convolutional coding	1/3

Table 4.2.2-2

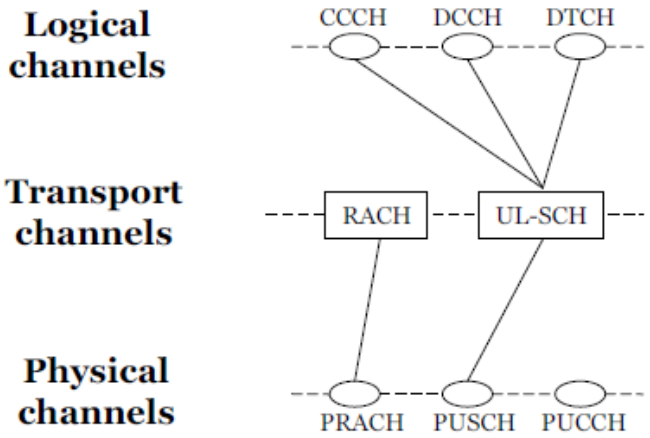

Figure 4.2.2

4.2.3 Physical uplink shared channel (PUSCH)

4.2.3.1 Baseband signal generation

The baseband signal representing the physical uplink shared channel is defined in terms of the following steps:

- scrambling
- modulation of scrambled bits to generate complex-valued symbols
- transform precoding to generate complex-valued symbols
- mapping of complex-valued symbols to resource elements
- generation of complex-valued time-domain SC-FDMA signal for each antenna port

The steps are showed in Figure 4.2.3.1.

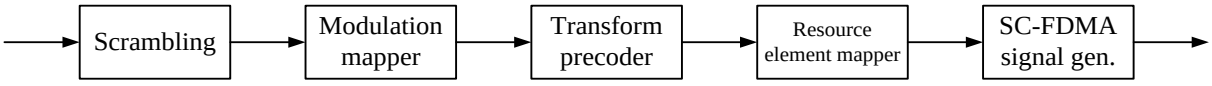

Figure 4.2.3.1

4.2.3.2 Modulation

The modulation schemes admitted for PUSCH are QPSK,16QAM and 64QAM.

4.2.3.3 Mapping to physical resource

The mapping to resource elements (k,l) corresponding to the physical resource blocks assigned for transmission and not used for transmission of reference signals and not reserved for possible SRS transmission shall be in increasing order of first the index k, then the index l, starting with the first slot in the subframe.

4.2.4 Physical uplink control channel (PUCCH)

4.2.4.1 Formats and modulation

The physical uplink control channel supports multiple formats as shown in Table 4.2.4.1-1.
Formats 2a and 2b are supported for normal cyclic prefix only.

PUCCH format	Modulation scheme	Number of bits per subframe, M_{bit}
1a	BPSK	1
1b	QPSK	2
2	QPSK	20
2a	QPSK+BPSK	21
2b	QPSK+QPSK	22

Table 4.2.4.1-1: Supported PUCCH formats and modulation schemes.

For PUCCH format 1, information is carried by the presence/absence of transmission of PUCCH from the UE.
For PUCCH formats 1a and 1b, one or two explicit bits are transmitted, respectively. The block of bits $b(0),\ldots,b(M_{\text{bit}}-1)$ shall be modulated as described in Table 4.2.4.1-2, resulting in a complex-valued symbol $d(0)$. The modulation schemes for the different PUCCH formats are given by Table 4.2.4.1-1.
The complex-valued symbol $d(0)$ shall be multiplied with a cyclically shifted length $N_{\text{seq}}^{\text{PUCCH}}=12$.

PUCCH format	$b(0),\ldots,b(M_{\text{bit}}-1)$	$d(0)$
1a	0	1
	1	-1
1b	00	1
	01	$-j$
	10	j
	11	-1

Table 4.2.4.1-2: Modulation symbol $d(0)$ for PUCCH formats 1a and 1b.

For PUCCH formats 2a and 2b, supported for normal cyclic prefix only, the bit(s) $b(20),\ldots,b(M_{\text{bit}}-1)$ shall be modulated as described in Table 4.2.4.1-3 resulting in a single modulation symbol $d(10)$.

PUCCH format	$b(20),\ldots,b(M_{\text{bit}}-1)$	$d(10)$
2a	0	1
	1	−1
2b	00	1
	01	$-j$
	10	j
	11	−1

Table 4.2.4.1-3: Modulation symbol $d(10)$ for PUCCH formats 2a and 2b.

4.2.4.2 Mapping to physical resource

PUCCH uses one resource block in each of the two slots in a subframe. Within the physical resource block used for transmission, the mapping of $z(i)$ to resource elements (k,l) not used for transmission of reference signals shall be in increasing order of first k, then l and finally the slot number, starting with the first slot in the subframe.

The PUCCH is never transmitted simultaneously with the PUSCH from the same UE and for frame structure type 2, the PUCCH is not transmitted in the UpPTS field.

4.2.5 Physical random access channel (PRACH)

The random access is used for various purpose for example: initial access, handover, following radio link failure.

There are 2 type of random access procedure: contention based and non-contention based.

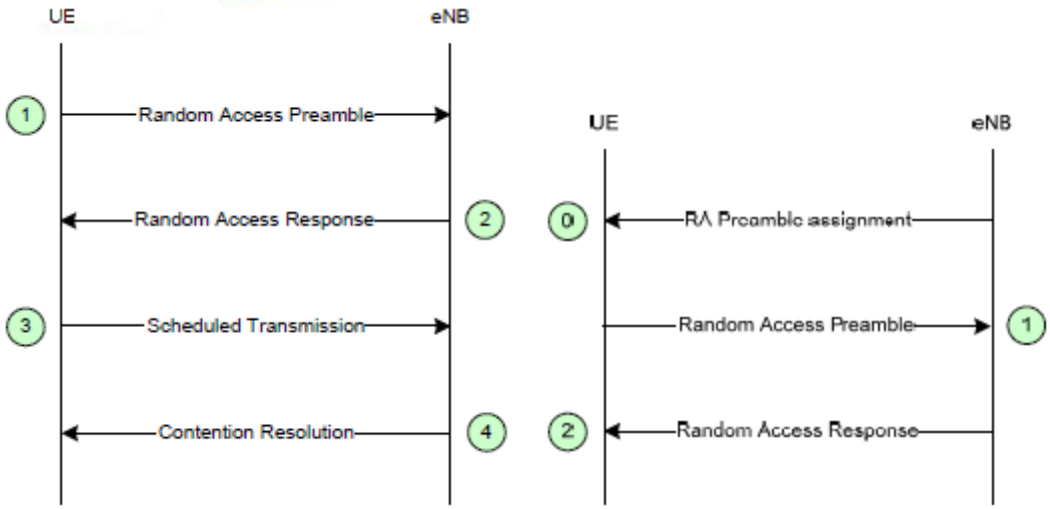

Figure 4.2.5: respectively contention and non-contention based random access procedure.

4.2.5.1 Time and frequency structure

The physical layer random access preamble, illustrated in Figure 4.2.5.1, consists of a cyclic prefix of length T_{CP} and a sequence part of length T_{SEQ}. The parameter values are listed in Table 4.2.5.1-1 and depend on the frame structure and the random access configuration.

Higher layers control the preamble format.

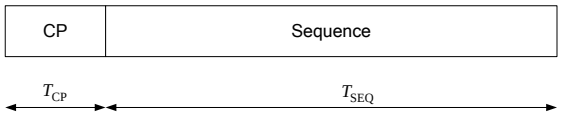

Figure 4.2.5.1: Random access preamble format.

Preamble format	T_{CP}	T_{SEQ}
0	$3168 \cdot T_s$	$24576 \cdot T_s$
1	$21024 \cdot T_s$	$24576 \cdot T_s$
2	$6240 \cdot T_s$	$2 \cdot 24576 \cdot T_s$
3	$21024 \cdot T_s$	$2 \cdot 24576 \cdot T_s$
4*	$448 \cdot T_s$	$4096 \cdot T_s$
* Frame structure type 2 and special subframe configurations with UpPTS lengths $4384 \cdot T_s$ and $5120 \cdot T_s$ only		

Table 4.2.5.1-1: Random access preamble parameters.

The transmission of a random access preamble, if triggered by the MAC layer, is restricted to certain time and frequency resources. These resources are enumerated in increasing order of the subframe number within the radio frame and the physical resource blocks in the frequency domain such that index 0 correspond to the lowest numbered physical resource block and subframe within the radio frame. PRACH resources within the radio frame are indicated by a PRACH Resource Index. For frame structure type 1 with preamble format 0-3, there is at most one random access resource per subframe. Table 4.2.5.1-2 lists the preamble formats according to Table 4.2.5.1-1 and the subframes in which random access preamble transmission is allowed for a given configuration in frame structure type 1. The start of the random access preamble shall be aligned with the start of the corresponding uplink subframe at the UE.

The first physical resource block n_{PRB}^{RA} allocated to the PRACH opportunity considered for preamble formats 0, 1, 2 and 3 is defined as $n_{PRB}^{RA} = n_{PRBoffset}^{RA}$, where the parameter *prach-FrequencyOffset,* $n_{PRBoffset}^{RA}$ is expressed as a physical resource block number configured by higher layers and fulfilling $0 \le n_{PRBoffset}^{RA} \le N_{RB}^{UL} - 6$.

The parameter *prach-ConfigurationIndex* is given by higher layers.

PRACH Configuration Index	Preamble Format	System frame number	Subframe number	PRACH Configuration Index	Preamble Format	System frame number	Subframe number
0	0	Even	1	32	2	Even	1
1	0	Even	4	33	2	Even	4
2	0	Even	7	34	2	Even	7
3	0	Any	1	35	2	Any	1
4	0	Any	4	36	2	Any	4
5	0	Any	7	37	2	Any	7
6	0	Any	1, 6	38	2	Any	1, 6
7	0	Any	2 ,7	39	2	Any	2 ,7
8	0	Any	3, 8	40	2	Any	3, 8
9	0	Any	1, 4, 7	41	2	Any	1, 4, 7
10	0	Any	2, 5, 8	42	2	Any	2, 5, 8
11	0	Any	3, 6, 9	43	2	Any	3, 6, 9
12	0	Any	0, 2, 4, 6, 8	44	2	Any	0, 2, 4, 6, 8
13	0	Any	1, 3, 5, 7, 9	45	2	Any	1, 3, 5, 7, 9
14	0	Any	0, 1, 2, 3, 4, 5, 6, 7, 8, 9	46	N/A	N/A	N/A
15	0	Even	9	47	2	Even	9
16	1	Even	1	48	3	Even	1
17	1	Even	4	49	3	Even	4
18	1	Even	7	50	3	Even	7
19	1	Any	1	51	3	Any	1
20	1	Any	4	52	3	Any	4
21	1	Any	7	53	3	Any	7
22	1	Any	1, 6	54	3	Any	1, 6
23	1	Any	2 ,7	55	3	Any	2 ,7
24	1	Any	3, 8	56	3	Any	3, 8
25	1	Any	1, 4, 7	57	3	Any	1, 4, 7
26	1	Any	2, 5, 8	58	3	Any	2, 5, 8
27	1	Any	3, 6, 9	59	3	Any	3, 6, 9
28	1	Any	0, 2, 4, 6, 8	60	N/A	N/A	N/A
29	1	Any	1, 3, 5, 7, 9	61	N/A	N/A	N/A
30	N/A	N/A	N/A	62	N/A	N/A	N/A
31	1	Even	9	63	3	Even	9

Table 4.2.5.1-2: Frame structure type 1 random access configuration for preamble formats 0-3.

For frame structure type 2 with preamble formats 0-4, there might be multiple random access resources in an UL subframe (or UpPTS for preamble format 4) depending on the UL/DL configuration [see table 2.2-2]. Table 4.2.5.1-3 lists PRACH configurations allowed for frame structure type 2 where the configuration index corresponds to a certain combination of preamble format, PRACH density value of random access opportunity, D_{RA} and version index, r_{RA}.

The start of the random access preamble formats 0-3 shall be aligned with the start of the corresponding uplink subframe at the UE assuming $N_{\mathrm{TA}} = 0$ and the random access preamble format 4 shall start $4832 \cdot T_{\mathrm{s}}$ before the end of the UpPTS at the UE.

PRACH configuration Index	Preamble Format	Density Per 10 ms D_{RA}	Version r_{RA}	PRACH configuration Index	Preamble Format	Density Per 10 ms D_{RA}	Version r_{RA}
0	0	0.5	0	32	2	0.5	2
1	0	0.5	1	33	2	1	0
2	0	0.5	2	34	2	1	1
3	0	1	0	35	2	2	0
4	0	1	1	36	2	3	0
5	0	1	2	37	2	4	0
6	0	2	0	38	2	5	0
7	0	2	1	39	2	6	0
8	0	2	2	40	3	0.5	0
9	0	3	0	41	3	0.5	1
10	0	3	1	42	3	0.5	2
11	0	3	2	43	3	1	0
12	0	4	0	44	3	1	1
13	0	4	1	45	3	2	0
14	0	4	2	46	3	3	0
15	0	5	0	47	3	4	0
16	0	5	1	48	4	0.5	0
17	0	5	2	49	4	0.5	1
18	0	6	0	50	4	0.5	2
19	0	6	1	51	4	1	0
20	1	0.5	0	52	4	1	1
21	1	0.5	1	53	4	2	0
22	1	0.5	2	54	4	3	0
23	1	1	0	55	4	4	0
24	1	1	1	56	4	5	0
25	1	2	0	57	4	6	0
26	1	3	0	58	N/A	N/A	N/A
27	1	4	0	59	N/A	N/A	N/A
28	1	5	0	60	N/A	N/A	N/A
29	1	6	0	61	N/A	N/A	N/A
30	2	0.5	0	62	N/A	N/A	N/A
31	2	0.5	1	63	N/A	N/A	N/A

Table 4.2.5.1-3: Frame structure type 2 random access configurations for preamble formats 0-4.

4.2.5.2 Preamble sequence generation

The random access preambles are generated from Zadoff-Chu sequences with zero correlation zone, generated from one or several root Zadoff-Chu sequences. The network configures the set of preamble sequences the UE is allowed to use.

There are 64 preambles available in each cell. The set of 64 preamble sequences in a cell is found by including first, in the order of increasing cyclic shift, all the available cyclic shifts of a root Zadoff-Chu sequence with the logical index RACH_ROOT_SEQUENCE, where RACH_ROOT_SEQUENCE is broadcasted as part of the System Information.

The u^{th} root Zadoff-Chu sequence is defined by

$$x_u(n) = e^{-j\frac{\pi u n(n+1)}{N_{ZC}}}, \quad 0 \le n \le N_{ZC} - 1$$

where the length N_{ZC} of the Zadoff-Chu sequence is given by Table 4.2.5.2-1.

Preamble format	N_{ZC}
0 – 3	839
4	139

Table 4.2.5.2-1: Random access preamble sequence length.

From the u^{th} root Zadoff-Chu sequence, random access preambles with zero correlation zones of length $N_{CS}-1$ are defined by cyclic shifts according to

$$x_{u,v}(n) = x_u((n+C_v) \bmod N_{ZC})$$

where the cyclic shift is given by

$$C_v = \begin{cases} vN_{CS} & v = 0,1,...,\lfloor N_{ZC}/N_{CS} \rfloor - 1, N_{CS} \neq 0 \quad \text{for unrestricted sets} \\ 0 & N_{CS} = 0 \quad \text{for unrestricted sets} \\ d_{start}\lfloor v/n_{shift}^{RA} \rfloor + (v \bmod n_{shift}^{RA})N_{CS} & v = 0,1,..., n_{shift}^{RA} n_{group}^{RA} + \bar{n}_{shift}^{RA} - 1 \quad \text{for restricted sets} \end{cases}$$

and N_{CS} is given by Tables 4.2.5.2-2 and 4.2.5.2-3 for preamble formats 0-3 and 4, respectively, where the parameter *zeroCorrelationZoneConfig* is provided by higher layers.

The parameter *High-speed-flag* provided by higher layers determines if unrestricted set or restricted set shall be used.

The variable d_u is the cyclic shift corresponding to a Doppler shift of magnitude $1/T_{SEQ}$ and is given by

$$d_u = \begin{cases} p & 0 \le p < N_{ZC}/2 \\ N_{ZC} - p & \text{otherwise} \end{cases}$$

where p is the smallest non-negative integer that fulfils $(pu) \bmod N_{ZC} = 1$. The parameters for restricted sets of cyclic shifts depend on d_u. For $N_{CS} \le d_u < N_{ZC}/3$, the parameters are given by

$$\begin{aligned} n_{shift}^{RA} &= \lfloor d_u / N_{CS} \rfloor \\ d_{start} &= 2d_u + n_{shift}^{RA} N_{CS} \\ n_{group}^{RA} &= \lfloor N_{ZC} / d_{start} \rfloor \\ \bar{n}_{shift}^{RA} &= \max\left(\left\lfloor (N_{ZC} - 2d_u - n_{group}^{RA} d_{start})/N_{CS} \right\rfloor, 0\right) \end{aligned}$$

For $N_{ZC}/3 \le d_u \le (N_{ZC} - N_{CS})/2$, the parameters are given by

$$\begin{aligned} n_{shift}^{RA} &= \lfloor (N_{ZC} - 2d_u)/N_{CS} \rfloor \\ d_{start} &= N_{ZC} - 2d_u + n_{shift}^{RA} N_{CS} \\ n_{group}^{RA} &= \lfloor d_u / d_{start} \rfloor \\ \bar{n}_{shift}^{RA} &= \min\left(\max\left(\left\lfloor (d_u - n_{group}^{RA} d_{start})/N_{CS} \right\rfloor, 0\right), n_{shift}^{RA}\right) \end{aligned}$$

For all other values of d_u, there are no cyclic shifts in the restricted set.

zeroCorrelationZoneConfig	N_{CS} value	
	Unrestricted set	Restricted set
0	0	15
1	13	18
2	15	22
3	18	26
4	22	32
5	26	38
6	32	46
7	38	55
8	46	68
9	59	82
10	76	100
11	93	128
12	119	158
13	167	202
14	279	237
15	419	-

Table 4.2.5.2-2: N_{CS} for preamble generation (preamble formats 0-3).

zeroCorrelationZoneConfig	N_{CS} value
0	2
1	4
2	6
3	8
4	10
5	12
6	15
7	N/A
8	N/A
9	N/A
10	N/A
11	N/A
12	N/A
13	N/A
14	N/A
15	N/A

Table 4.2.5.2-3: N_{CS} for preamble generation (preamble format 4).

4.2.5.3 Random access procedure

Prior to initiation of the non-synchronized physical random access procedure [3], Layer 1 shall receive the following information from the higher layers:

- Random access channel parameters (PRACH configuration and frequency position).
- Parameters for determining the root sequences and their cyclic shifts in the preamble sequence set for the cell: index to logical root sequence table, cyclic shift (N_{CS}), and set type (unrestricted or restricted set).

From the physical layer perspective, the L1 random access procedure encompasses the transmission of random access preamble and random access response. The remaining messages are scheduled for transmission by the higher layer on the shared data channel and are not considered part of the L1 random access procedure. A random access channel occupies 6 resource blocks in a subframe or set of consecutive subframes reserved for random access preamble transmissions. The eNodeB is not prohibited from scheduling data in the resource blocks reserved for random access channel preamble transmission.

The following steps are required for the L1 random access procedure:

- Layer 1 procedure is triggered upon request of a preamble transmission by higher layers.
- A preamble index, a target preamble received power (PREAMBLE_RECEIVED_TARGET_POWER), a corresponding RA-RNTI and a PRACH resource are indicated by higher layers as part of the request.
- A preamble transmission power P_{PRACH} is determined as $P_{PRACH} = \min\{P_{CMAX}, \text{PREAMBLE_RECEIVED_TARGET_POWER} + PL\}$_[dBm], where P_{CMAX} is the configured UE transmitted power and PL is the downlink pathloss estimate calculated in the UE.
- A preamble sequence is selected from the preamble sequence set using the preamble index.
- A single preamble is transmitted using the selected preamble sequence with transmission power P_{PRACH} on the indicated PRACH resource.
- Detection of a PDCCH with the indicated RA-RNTI is attempted during a window controlled by higher layers. If detected, the corresponding DL-SCH transport block is passed to higher layers. The higher layers parse the transport block and indicate the 20-bit uplink grant to the physical layer.

Random Access Response Grant

The higher layers indicate the 20-bit UL Grant to the physical layer, as defined in [3]. This is referred to the Random Access Response Grant in the physical layer. The content of these 20 bits starting with the MSB and ending with the LSB are as follows:

- Hopping flag – 1 bit
- Fixed size resource block assignment – 10 bits
- Truncated modulation and coding scheme – 4 bits
- TPC command for scheduled PUSCH – 3 bits
- UL delay – 1 bit
- CQI request – 1 bit

Timing

For the L1 random access procedure, UE's uplink transmission timing after a random access preamble transmission is as follows:

- If a PDCCH with associated RA-RNTI is detected in subframe *n*, and the corresponding DL-SCH transport block contains a response to the transmitted preamble sequence, the UE shall, according to the information in the response, transmit an UL-SCH transport block in the first subframe $n+k_1$, $k_1 \geq 6$, if the UL delay field in section 6.2 is set to zero where $n+k_1$ is the first available UL subframe for PUSCH transmission. The UE shall postpone the PUSCH transmission to the next available UL subframe after $n+k_1$ if the field is set to 1.
- If a random access response is received in subframe *n*, and the corresponding DL-SCH transport block does not contain a response to the transmitted preamble sequence, the UE shall, if requested by higher layers, be ready to transmit a new preamble sequence no later than in subframe $n+5$.
- If no random access response is received in subframe *n*, where subframe *n* is the last subframe of the random access response window, the UE shall, if requested by higher layers, be ready to transmit a new preamble sequence no later than in subframe $n+4$.

4.3 Reference signal

Two types of uplink reference signals are supported:

- Demodulation reference signal, associated with transmission of PUSCH or PUCCH
- Sounding reference signal, not associated with transmission of PUSCH or PUCCH

4.3.1 Reference signal sequence

Reference signal sequence $r_{u,v}^{(\alpha)}(n)$ is defined by a cyclic shift α of a base sequence $\bar{r}_{u,v}(n)$ according to

$$r_{u,v}^{(\alpha)}(n) = e^{j\alpha n}\bar{r}_{u,v}(n), \quad 0 \leq n < M_{\text{sc}}^{\text{RS}}$$

where $M_{\text{sc}}^{\text{RS}} = mN_{\text{sc}}^{\text{RB}}$ is the length of the reference signal sequence and $1 \leq m \leq N_{\text{RB}}^{\max,\text{UL}}$. Multiple reference signal sequences are defined from a single base sequence through different values of α.

Base sequences $\bar{r}_{u,v}(n)$ are divided into groups, where $u \in \{0,1,\ldots,29\}$ is the group number and v is the base sequence number within the group, such that each group contains one base sequence ($v=0$) of each length $M_{\text{sc}}^{\text{RS}} = mN_{\text{sc}}^{\text{RB}}$, $1 \leq m \leq 5$ and two base sequences ($v=0,1$) of each length $M_{\text{sc}}^{\text{RS}} = mN_{\text{sc}}^{\text{RB}}$, $6 \leq m \leq N_{\text{RB}}^{\max,\text{UL}}$. The sequence group number u and the number v within the group may vary in time as described in Sections 4.3.1.1 and 4.3.1.2, respectively.

4.3.1.3 Group hopping

The sequence-group number u in slot n_s is defined by a group hopping pattern $f_{gh}(n_s)$ and a sequence-shift pattern f_{ss} according to

$$u = \left(f_{gh}(n_s) + f_{ss}\right) \bmod 30$$

There are 17 different hopping patterns and 30 different sequence-shift patterns. Sequence-group hopping can be enabled or disabled by means of the parameter *Group-hopping-enabled* provided by higher layers. PUCCH and PUSCH have the same hopping pattern but may have different sequence-shift patterns.

The group-hopping pattern $f_{gh}(n_s)$ is the same for PUSCH and PUCCH and given by

$$f_{gh}(n_s) = \begin{cases} 0 & \text{if group hopping is disabled} \\ \left(\sum_{i=0}^{7} c(8n_s + i) \cdot 2^i\right) \bmod 30 & \text{if group hopping is enabled} \end{cases}$$

The pseudo-random sequence generator shall be initialized with $c_{init} = \left\lfloor \frac{N_{ID}^{cell}}{30} \right\rfloor$ at the beginning of each radio frame.

The sequence-shift pattern f_{ss} definition differs between PUCCH and PUSCH.

For PUCCH, the sequence-shift pattern f_{ss}^{PUCCH} is given by $f_{ss}^{PUCCH} = N_{ID}^{cell} \bmod 30$.

For PUSCH, the sequence-shift pattern f_{ss}^{PUSCH} is given by $f_{ss}^{PUSCH} = \left(f_{ss}^{PUCCH} + \Delta_{ss}\right) \bmod 30$, where $\Delta_{ss} \in \{0,1,\ldots,29\}$ is configured by higher layers.

4.3.1.2 Sequence hopping

Sequence hopping only applies for reference-signals of length $M_{sc}^{RS} \geq 6N_{sc}^{RB}$.

For reference-signals of length $M_{sc}^{RS} < 6N_{sc}^{RB}$, the base sequence number v within the base sequence group is given by $v = 0$.

For reference-signals of length $M_{sc}^{RS} \geq 6N_{sc}^{RB}$, the base sequence number v within the base sequence group in slot n_s is defined by

$$v = \begin{cases} c(n_s) & \text{if group hopping is disabled and sequence hopping is enabled} \\ 0 & \text{otherwise} \end{cases}$$

The parameter *Sequence-hopping-enabled* provided by higher layers determines if sequence hopping is enabled or not. The pseudo-random sequence generator shall be initialized with $c_{init} = \left\lfloor \frac{N_{ID}^{cell}}{30} \right\rfloor \cdot 2^5 + f_{ss}^{PUSCH}$ at the beginning of each radio frame

4.3.1.3 Mapping to physical resource

The sequence $r^{\mathrm{PUSCH}}(\cdot)$ shall be multiplied with the amplitude scaling factor β_{PUSCH} and mapped in sequence starting with $r^{\mathrm{PUSCH}}(0)$ to the same set of physical resource blocks used for the corresponding PUSCH transmission.

The mapping to resource elements (k,l), with $l=3$ for normal cyclic prefix and $l=2$ for extended cyclic prefix, in the subframe shall be in increasing order of first k, then the slot number.

4.3.2 Sounding reference signal

4.3.2.1 Definition

The sounding reference signal sequence $r^{\mathrm{SRS}}(n)=r_{u,v}^{(\alpha)}(n)$ where u is the PUCCH sequence-group number and v is the base sequence number. The cyclic shift α of the sounding reference signal is given as

$$\alpha = 2\pi \frac{n_{\mathrm{SRS}}^{\mathrm{cs}}}{8},$$

where $n_{\mathrm{SRS}}^{\mathrm{cs}}$ is configured for each UE by higher layers and $n_{\mathrm{SRS}}^{\mathrm{cs}}=0,1,2,3,4,5,6,7$.

For all subframes other than special subframes, the sounding reference signal shall be transmitted in the last symbol of the subframe.

4.3.2.2 Subframe configuration

The cell-specific subframe configuration period T_{SFC} and the cell-specific subframe offset Δ_{SFC} for the transmission of sounding reference signals are listed in Tables 4.3.2.2-1 and 4.3.2.2-2, for frame structures type 1 and 2 respectively, where the parameter *srs-SubframeConfig* is provided by higher layers. Sounding reference signal subframes are the subframes satisfying $\lfloor n_s/2 \rfloor \bmod T_{\mathrm{SFC}} \in \Delta_{\mathrm{SFC}}$. For frame structure type 2, sounding reference signal is transmitted only in configured upload subframes or UpPTS.

Srs-SubframeConfig	Binary	Configuration Period T_{SFC} (subframes)	Transmission offset Δ_{SFC} (subframes)
0	0000	1	{0}
1	0001	2	{0}
2	0010	2	{1}
3	0011	5	{0}
4	0100	5	{1}
5	0101	5	{2}
6	0110	5	{3}
7	0111	5	{0,1}
8	1000	5	{2,3}
9	1001	10	{0}
10	1010	10	{1}
11	1011	10	{2}
12	1100	10	{3}
13	1101	10	{0,1,2,3,4,6,8}
14	1110	10	{0,1,2,3,4,5,6,8}
15	1111	reserved	reserved

Table 4.3.2.2-1: Frame structure type 1 sounding reference signal subframe configuration.

Srs-SubframeConfig	Binary	Configuration Period T_{SFC} (subframes)	Transmission offset Δ_{SFC} (subframes)
0	0000	5	{1}
1	0001	5	{1, 2}
2	0010	5	{1, 3}
3	0011	5	{1, 4}
4	0100	5	{1, 2, 3}
5	0101	5	{1, 2, 4}
6	0110	5	{1, 3, 4}
7	0111	5	{1, 2, 3, 4}
8	1000	10	{1, 2, 6}
9	1001	10	{1, 3, 6}
10	1010	10	{1, 6, 7}
11	1011	10	{1, 2, 6, 8}
12	1100	10	{1, 3, 6, 9}
13	1101	10	{1, 4, 6, 7}
14	1110	reserved	reserved
15	1111	reserved	reserved

Table 4.3.2.2-2: Frame structure type 2 sounding reference signal subframe configuration.

4.4 SC-FDMA baseband signal generation

4.4.1 PUSCH and PUCCH

The time-continuous signal $s_l(t)$ in SC-FDMA symbol l in an uplink slot is defined by

$$s_l(t) = \sum_{k=-\lfloor N_{\mathrm{RB}}^{\mathrm{UL}} N_{\mathrm{sc}}^{\mathrm{RB}}/2 \rfloor}^{\lceil N_{\mathrm{RB}}^{\mathrm{UL}} N_{\mathrm{sc}}^{\mathrm{RB}}/2 \rceil - 1} a_{k^{(-)},l} \cdot e^{j2\pi(k+1/2)\Delta f(t - N_{\mathrm{CP},l} T_{\mathrm{s}})}$$

for $0 \le t < (N_{\mathrm{CP},l} + N) \times T_{\mathrm{s}}$ where $k^{(-)} = k + \lfloor N_{RB}^{UL} N_{sc}^{RB}/2 \rfloor$, $N = 2048$, $\Delta f = 15\,\mathrm{kHz}$ and $a_{k,l}$ is the content of resource element (k,l).

The SC-FDMA symbols in a slot shall be transmitted in increasing order of l, starting with $l = 0$, where SC-FDMA symbol $l > 0$ starts at time $\sum_{l'=0}^{l-1} (N_{\mathrm{CP},l'} + N) T_{\mathrm{s}}$ within the slot.

Table 4.4.1 lists the values of $N_{\mathrm{CP},l}$ that shall be used.

Configuration	Cyclic prefix length $N_{\mathrm{CP},l}$
Normal cyclic prefix	160 for $l = 0$ 144 for $l = 1,2,\ldots,6$
Extended cyclic prefix	512 for $l = 0,1,\ldots,5$

Table 4.4.1: SC-FDMA parameters.

4.4.2 PRACH

The time-continuous random access signal $s(t)$ is defined by

$$s(t) = \beta_{\mathrm{PRACH}} \sum_{k=0}^{N_{\mathrm{ZC}}-1} \sum_{n=0}^{N_{\mathrm{ZC}}-1} x_{u,v}(n) \cdot e^{-j\frac{2\pi nk}{N_{\mathrm{ZC}}}} \cdot e^{j2\pi(k+\varphi+K(k_0+1/2))\Delta f_{\mathrm{RA}}(t - T_{\mathrm{CP}})}$$

where $0 \le t < T_{\mathrm{SEQ}} + T_{\mathrm{CP}}$, β_{PRACH} is an amplitude scaling factor in order to conform to the transmit power P_{PRACH} and $k_0 = n_{\mathrm{PRB}}^{\mathrm{RA}} N_{\mathrm{sc}}^{\mathrm{RB}} - N_{\mathrm{RB}}^{\mathrm{UL}} N_{\mathrm{sc}}^{\mathrm{RB}}/2$. The location in the frequency domain is controlled by the parameter $n_{\mathrm{PRB}}^{\mathrm{RA}}$ is derived from section 4.7.1. The factor $K = \Delta f / \Delta f_{\mathrm{RA}}$ accounts for the difference in subcarrier spacing between the random access preamble and uplink data transmission. The variable Δf_{RA}, the subcarrier spacing for the random access preamble, and the variable φ, a fixed offset determining the frequency-domain location of the random access preamble within the physical resource blocks, are both given by Table 4.4.2.

Preamble format	Δf_{RA}	φ
0 – 3	1250 Hz	7
4	7500 Hz	2

Table 4.4.2: Random access baseband parameters.

Chapter 5

CHANNEL CODING

5.1 Downlink transport channels and control information

A schematic overview of the encoding process for the reference measurement channels is provided in Figure 5.1.

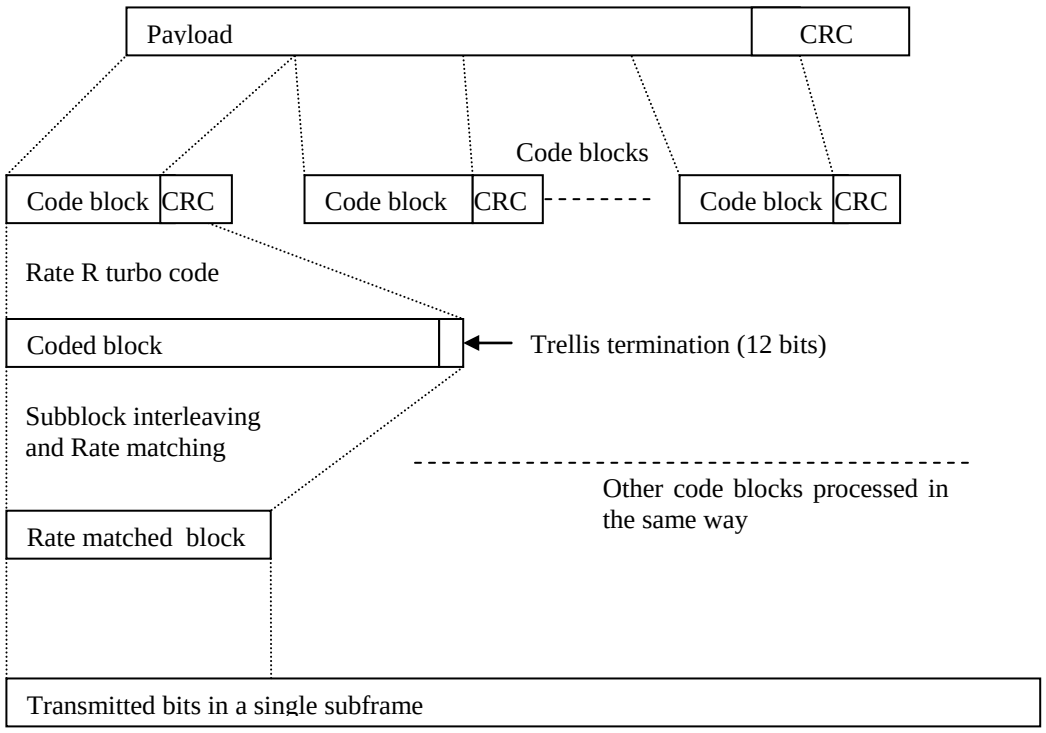

Figure 5.1: Schematic overview of the encoding process.

5.1.1 Broadcast channel

Figure 5.1.1 shows the processing structure for the BCH transport channel [2]. Data arrives to the coding unit in the form of a maximum of one transport block every transmission time interval (TTI) of 40ms. The following coding steps can be identified:

- Add CRC to the transport block
- Channel coding
- Rate matching

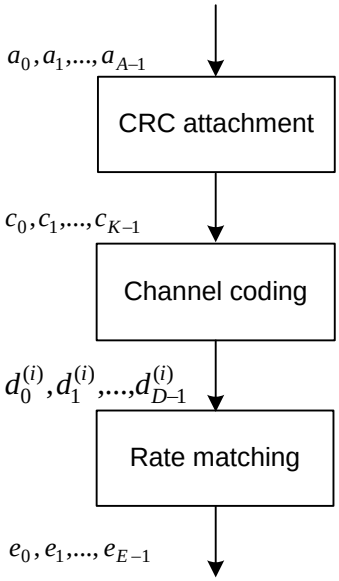

Figure 5.1.1: Transport channel processing for BCH.

5.1.1.1 Transport block CRC attachment

Error detection is provided on BCH transport blocks through a Cyclic Redundancy Check (CRC).

The entire transport block is used to calculate the CRC parity bits. Denote the bits in a transport block delivered to layer 1 by $a_0, a_1, a_2, a_3, ..., a_{A-1}$, and the parity bits by $p_0, p_1, p_2, p_3, ..., p_{L-1}$. A is the size of the transport block and set to 24 bits and L is the number of parity bits.

The parity bits are computed with setting L to 16 bits. After the attachment, the CRC bits are scrambled according to the eNodeB transmit antenna configuration with the sequence $x_{ant,0}, x_{ant,1}, ..., x_{ant,15}$ as indicated in Table 5.1.1.1 to form the sequence of bits $c_0, c_1, c_2, c_3, ..., c_{K-1}$ where

$$c_k = a_k \qquad \text{for } k = 0, 1, 2, ..., A\text{-}1$$

$$c_k = (p_{k-A} + x_{ant,k-A}) \bmod 2 \qquad \text{for } k = A, A\text{+}1, A\text{+}2, ..., A\text{+}15$$

Number of transmit antenna ports at eNodeB	PBCH CRC mask $< x_{ant,0}, x_{ant,1}, ..., x_{ant,15} >$
1	<0, 0, 0, 0, 0, 0, 0, 0, 0, 0, 0, 0, 0, 0, 0, 0>
2	<1, 1, 1, 1, 1, 1, 1, 1, 1, 1, 1, 1, 1, 1, 1, 1>
4	<0, 1, 0, 1, 0, 1, 0, 1, 0, 1, 0, 1, 0, 1, 0, 1>

Table 5.1.1.1: CRC mask for PBCH.

5.1.1.2 Channel coding

Information bits are delivered to the channel coding block. They are denoted by $c_0, c_1, c_2, c_3, \ldots, c_{K-1}$, where *K* is the number of bits, and they are tail biting convolutionally encoded.

After encoding the bits are denoted by $d_0^{(i)}, d_1^{(i)}, d_2^{(i)}, d_3^{(i)}, \ldots, d_{D-1}^{(i)}$, with $i = 0,1, \text{and } 2$, and where *D* is the number of bits on the *i*-th coded stream, i.e., $D = K$.

5.1.1.3 Rate matching

A tail biting convolutionally coded block is delivered to the rate matching block. This block of coded bits is denoted by $d_0^{(i)}, d_1^{(i)}, d_2^{(i)}, d_3^{(i)}, \ldots, d_{D-1}^{(i)}$, with $i = 0,1, \text{and } 2$, and where *i* is the coded stream index and *D* is the number of bits in each coded stream.

After rate matching, the bits are denoted by $e_0, e_1, e_2, e_3, \ldots, e_{E-1}$, where *E* is the number of rate matched bits.

5.1.2 Downlink shared channel, Paging channel and Multicast channel

Figure 5.1.2 shows the processing structure for each transport block for the DL-SCH, PCH and MCH transport channels. Data arrives to the coding unit in the form of a maximum of two transport blocks every TTI.

The following coding steps can be identified for each transport block:

- Add CRC to the transport block
- Code block segmentation and code block CRC attachment
- Channel coding
- Rate matching
- Code block concatenation

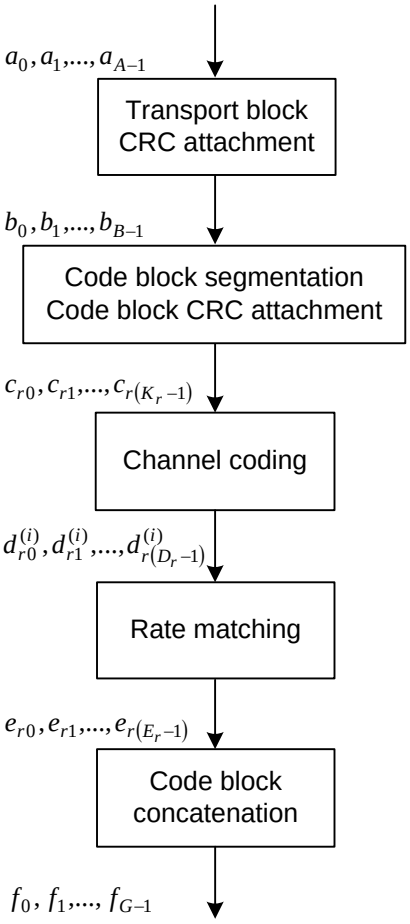

Figure 5.1.2: Transport channel processing for DL-SCH, PCH and MCH.

5.1.2.1 Transport block CRC attachment

Error detection is provided on transport blocks through a Cyclic Redundancy Check.

The entire transport block is used to calculate the CRC parity bits. Denote the bits in a transport block delivered to layer 1 by $a_0, a_1, a_2, a_3, ..., a_{A-1}$, and the parity bits by $p_0, p_1, p_2, p_3, ..., p_{L-1}$. A is the size of the transport block and L is the number of parity bits.

The parity bits are computed and attached to the transport block according to section 5.1.1 setting L to 24 bits and using the generator polynomial $g_{CRC24A}(D)$.

5.1.2.2 Code block segmentation and code block CRC attachment

The bits input to the code block segmentation are denoted by $b_0, b_1, b_2, b_3, ..., b_{B-1}$ where B is the number of bits in the transport block (including CRC).

The bits after code block segmentation are denoted by $c_{r0}, c_{r1}, c_{r2}, c_{r3}, ..., c_{r(K_r-1)}$, where r is the code block number and K_r is the number of bits for code block number r.

5.1.2.3 Channel coding

Code blocks are delivered to the channel coding block. They are denoted by $c_{r0}, c_{r1}, c_{r2}, c_{r3}, \ldots, c_{r(K_r-1)}$, where r is the code block number, and K_r is the number of bits in code block number r. The total number of code blocks is denoted by C and each code block is individually turbo encoded.

After encoding the bits are denoted by $d_{r0}^{(i)}, d_{r1}^{(i)}, d_{r2}^{(i)}, d_{r3}^{(i)}, \ldots, d_{r(D_r-1)}^{(i)}$, with $i = 0,1,\text{ and } 2$, and where D_r is the number of bits on the i-th coded stream for code block number r, i.e. $D_r = K_r + 4$.

5.1.2.4 Rate matching

Turbo coded blocks are delivered to the rate matching block. They are denoted by $d_{r0}^{(i)}, d_{r1}^{(i)}, d_{r2}^{(i)}, d_{r3}^{(i)}, \ldots, d_{r(D_r-1)}^{(i)}$, with $i = 0,1,\text{ and } 2$, and where r is the code block number, i is the coded stream index, and D_r is the number of bits in each coded stream of code block number r. The total number of code blocks is denoted by C and each coded block is individually rate matched.

After rate matching, the bits are denoted by $e_{r0}, e_{r1}, e_{r2}, e_{r3}, \ldots, e_{r(E_r-1)}$, where r is the coded block number, and where E_r is the number of rate matched bits for code block number r.

5.1.2.5 Code block concatenation

The bits input to the code block concatenation block are denoted by $e_{r0}, e_{r1}, e_{r2}, e_{r3}, \ldots, e_{r(E_r-1)}$ for $r = 0, \ldots, C-1$ and where E_r is the number of rate matched bits for the r-th code block.

The bits after code block concatenation are denoted by $f_0, f_1, f_2, f_3, \ldots, f_{G-1}$, where G is the total number of coded bits for transmission.

5.1.3 Downlink control information

A DCI transports downlink or uplink scheduling information, requests for aperiodic CQI reports, or uplink power control commands for one RNTI. The RNTI is implicitly encoded in the CRC.

Figure 5.1.3 shows the processing structure for the DCI. The following coding steps can be identified:

- Information element multiplexing
- CRC attachment
- Channel coding
- Rate matching

Are defined several format for DCI (0, 1, 1A, 1B, 1C, 1D, 2, 2A, 2B, 3, 3A) see [2] for further read.

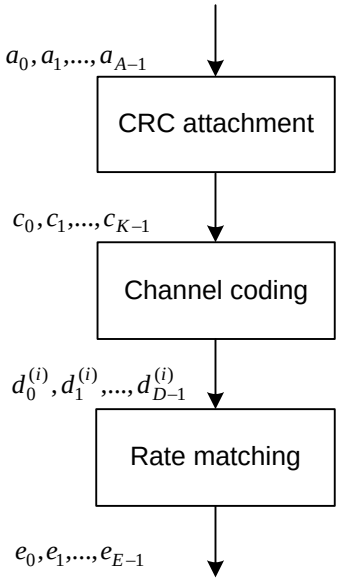

Figure 5.1.3: Processing for DCI.

5.1.3.1 CRC attachment

Error detection is provided on DCI transmissions through a Cyclic Redundancy Check.

The entire PDCCH payload is used to calculate the CRC parity bits. Denote the bits of the PDCCH payload by $a_0, a_1, a_2, a_3, ..., a_{A-1}$, and the parity bits by $p_0, p_1, p_2, p_3, ..., p_{L-1}$. A is the PDCCH payload size and L is the number of parity bits.

The parity bits are computed with setting L to 16 bits, resulting in the sequence $b_0, b_1, b_2, b_3, ..., b_{B-1}$, where

$B = A+L$.

In the case where UE transmit antenna selection is not configured or applicable, after attachment, the CRC parity bits are scrambled with the corresponding RNTI $x_{rnti,0}, x_{rnti,1}, ..., x_{rnti,15}$, where $x_{rnti,0}$ corresponds to the MSB of the RNTI, to form the sequence of bits $c_0, c_1, c_2, c_3, ..., c_{B-1}$. The relation between c_k and b_k is:

$$c_k = b_k \qquad \text{for } k = 0, 1, 2, ..., A\text{-}1$$

$$c_k = (b_k + x_{rnti,k-A}) \bmod 2 \qquad \text{for } k = A, A+1, A+2, ..., A+15.$$

5.1.3.2 Channel coding

Information bits are delivered to the channel coding block. They are denoted by $c_0, c_1, c_2, c_3, ..., c_{K-1}$, where K is the number of bits, and they are tail biting convolutionally encoded.

After encoding the bits are denoted by $d_0^{(i)}, d_1^{(i)}, d_2^{(i)}, d_3^{(i)}, ..., d_{D-1}^{(i)}$, with $i = 0, 1, \text{and } 2$, and where D is the number of bits on the i-th coded stream, i.e., $D = K$.

5.1.3.3 Rate matching

A tail biting convolutionally coded block is delivered to the rate matching block. This block of coded bits is denoted by $d_0^{(i)}, d_1^{(i)}, d_2^{(i)}, d_3^{(i)}, \ldots, d_{D-1}^{(i)}$, with $i = 0,1,\text{and } 2$, and where *i* is the coded stream index and *D* is the number of bits in each coded stream.

After rate matching, the bits are denoted by $e_0, e_1, e_2, e_3, \ldots, e_{E-1}$, where *E* is the number of rate matched bits.

5.1.4 Control format indicator (CFI)

Data arrives each subframe to the coding unit in the form of an indicator for the time span, in units of OFDM symbols, of the DCI in that subframe. The CFI takes values CFI = 1, 2 or 3. For system bandwidths $N_{\text{RB}}^{\text{DL}} > 10$, the span of the DCI in units of OFDM symbols, 1, 2 or 3, is given by the CFI. For system bandwidths $N_{\text{RB}}^{\text{DL}} \leq 10$, the span of the DCI in units of OFDM symbols, 2, 3 or 4, is given by CFI+1.

The coding flow is shown in Figure 5.1.4.

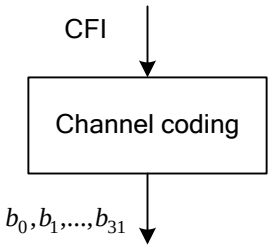

Figure 5.1.4 Coding for CFI.

Channel coding

The control format indicator is coded according to Table 5.1.4.

CFI	CFI code word < b_0, b_1, ..., b_{31} >
1	<0,1,1,0,1,1,0,1,1,0,1,1,0,1,1,0,1,1,0,1,1,0,1,1,0,1,1,0,1,1,0,1>
2	<1,0,1,1,0,1,1,0,1,1,0,1,1,0,1,1,0,1,1,0,1,1,0,1,1,0,1,1,0,1,1,0>
3	<1,1,0,1,1,0,1,1,0,1,1,0,1,1,0,1,1,0,1,1,0,1,1,0,1,1,0,1,1,0,1,1>
4	<0,0,0,0,0,0,0,0,0,0,0,0,0,0,0,0,0,0,0,0,0,0,0,0,0,0,0,0,0,0,0,0>

Table 5.1.4: CFI code words.

5.1.5 HARQ indicator (HI)

Data arrives to the coding unit in the form of indicators for HARQ acknowledgement.

The coding flow is shown in Figure 5.1.5.

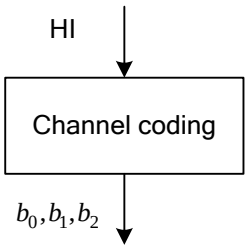

Figure 5.1.5 Coding for HI.

Channel coding

The HI is coded according to Table 5.1.5, where for a positive acknowledgement HI = 1 and for a negative acknowledgement HI = 0.

HI	HI code word < b_0, b_1, b_2 >
0	< 0,0,0 >
1	< 1,1,1 >

Table 5.1.5: HI code words.

5.2 Uplink transport channels and control information

5.2.1 Uplink shared channel

Figure 5.2.1 shows the processing structure for the UL-SCH transport channel.

Data arrives to the coding unit in the form of a maximum of one transport block every TTI.

The following coding steps can be identified:

- Add CRC to the transport block
- Code block segmentation and code block CRC attachment
- Channel coding of data and control information
- Rate matching
- Code block concatenation
- Multiplexing of data and control information
- Channel interleaver

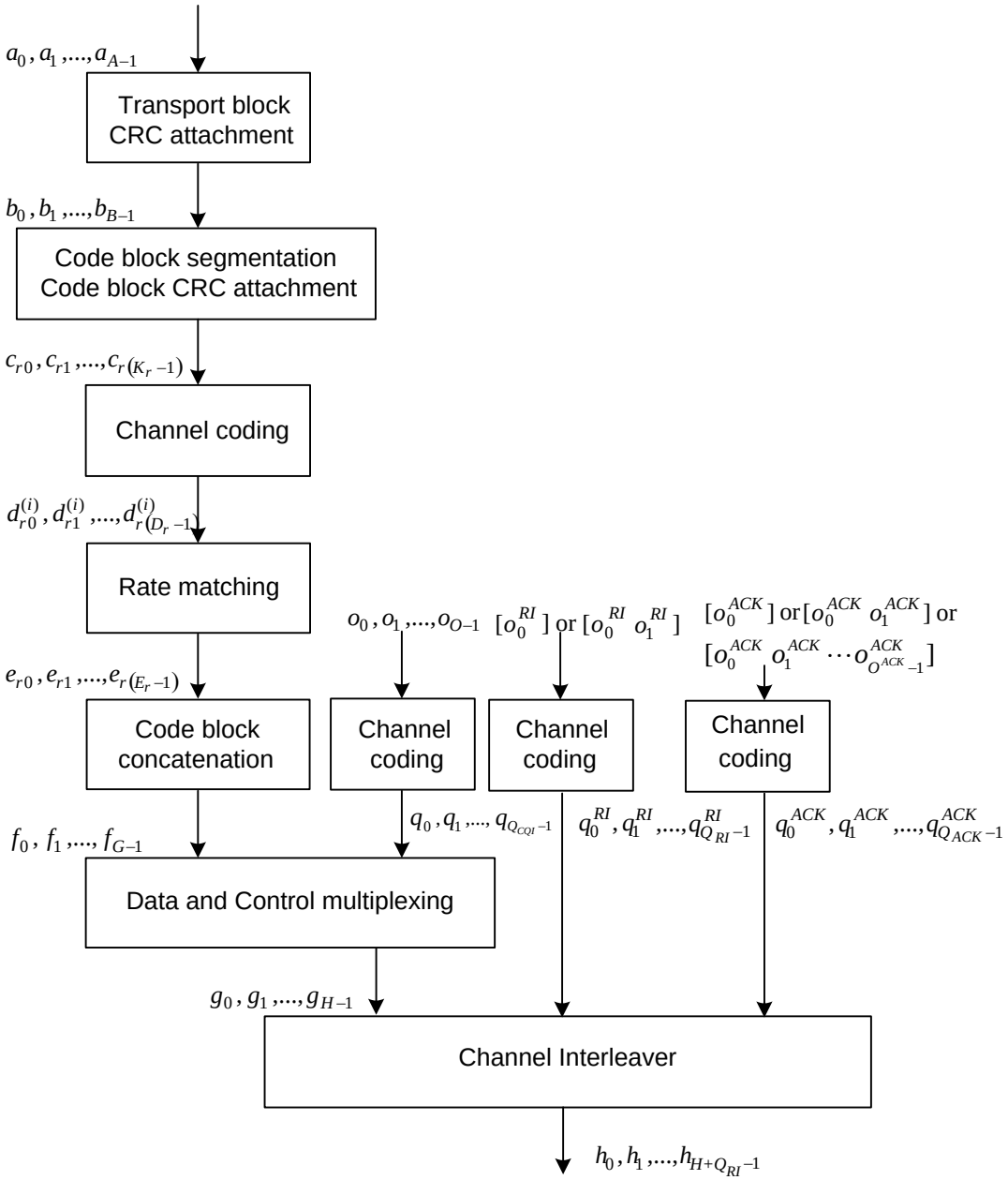

Figure 5.2.1: Transport channel processing for UL-SCH.

5.2.1.1 Transport block CRC attachment

Error detection is provided on UL-SCH transport blocks through a Cyclic Redundancy Check.

The entire transport block is used to calculate the CRC parity bits. Denote the bits in a transport block delivered to layer 1 by $a_0, a_1, a_2, a_3, ..., a_{A-1}$, and the parity bits by $p_0, p_1, p_2, p_3, ..., p_{L-1}$. A is the size of the transport block and L is the number of parity bits.

The parity bits are computed to the UL-SCH transport block setting L to 24 bits and using the generator polynomial $g_{CRC24A}(D)$.

5.2.1.2 Code block segmentation and code block CRC attachment

The bits input to the code block segmentation are denoted by $b_0, b_1, b_2, b_3, \ldots, b_{B-1}$ where B is the number of bits in the transport block (including CRC).

The bits after code block segmentation are denoted by $c_{r0}, c_{r1}, c_{r2}, c_{r3}, \ldots, c_{r(K_r-1)}$, where r is the code block number and K_r is the number of bits for code block number r.

5.2.1.3 Channel coding of UL-SCH

Code blocks are delivered to the channel coding block. The bits in a code block are denoted by $c_{r0}, c_{r1}, c_{r2}, c_{r3}, \ldots, c_{r(K_r-1)}$, where r is the code block number, and K_r is the number of bits in code block number r. The total number of code blocks is denoted by C and each code block is individually turbo encoded.

After encoding the bits are denoted by $d_{r0}^{(i)}, d_{r1}^{(i)}, d_{r2}^{(i)}, d_{r3}^{(i)}, \ldots, d_{r(D_r-1)}^{(i)}$, with $i = 0,1, \text{and } 2$ and where D_r is the number of bits on the i-th coded stream for code block number r, i.e. $D_r = K_r + 4$.

5.2.1.4 Rate matching

Turbo coded blocks are delivered to the rate matching block. They are denoted by $d_{r0}^{(i)}, d_{r1}^{(i)}, d_{r2}^{(i)}, d_{r3}^{(i)}, \ldots, d_{r(D_r-1)}^{(i)}$, with $i = 0,1, \text{and } 2$, and where r is the code block number, i is the coded stream index, and D_r is the number of bits in each coded stream of code block number r. The total number of code blocks is denoted by C and each coded block is individually rate matched.

After rate matching, the bits are denoted by $e_{r0}, e_{r1}, e_{r2}, e_{r3}, \ldots, e_{r(E_r-1)}$, where r is the coded block number, and where E_r is the number of rate matched bits for code block number r.

5.2.1.5 Code block concatenation

The bits input to the code block concatenation block are denoted by $e_{r0}, e_{r1}, e_{r2}, e_{r3}, \ldots, e_{r(E_r-1)}$ for $r = 0, \ldots, C-1$ and where E_r is the number of rate matched bits for the r-th code block.

The bits after code block concatenation are denoted by $f_0, f_1, f_2, f_3, \ldots, f_{G-1}$, where G is the total number of coded bits for transmission excluding the bits used for control transmission, when control information is multiplexed with the UL-SCH transmission.

5.2.1.6 Channel interleaver

The channel interleaver implements a time-first mapping of modulation symbols onto the transmit waveform while ensuring that the HARQ-ACK information is present on both slots in the subframe and is mapped to resources around the uplink demodulation reference signals.

Chapter 6

PERFORMANCE ANALYSIS

In this section we are going to do an analysis of the performance reached by the LTE.
First we see a real test conducted by Nokia Siemens Network that concentrates on the FDD duplex mode [6], after a simulation of the behavior of LTE conducted by the Public University of Navarre [7].

6.1 Real world outdoor test

6.1.1 Scenario

With this in mind, we selected three test cases/drive routes of our test program for this paper:

- A route on the Nokia Siemens Network campus in Munich within about 300 meters of the base station antenna.
- A wide area route on public streets within about 1000 meters of the Munich test site antenna.
- A long distance route up to about 4000 meters from the base station at the Berlin test site.

Test cases 1 and 3 were performed with a single mobile user terminal, test case 2 used four user terminals in parallel. Two terminals were real mobiles in a measurement van, while the others were stationary and placed in a building in order to measure the impact on system performance of indoor penetration.

Nokia Siemens Networks LTE development platform

All tests were performed using the Nokia Siemens Networks LTE development platform, which consists of an LTE base station, a specially developed LTE test terminal, GPS receivers and various laptops to act as local maintenance terminals, application servers and application clients (Figure 1).
The test terminals implement a modular structure combining boards of SW-upgradeable digital signal processors and field programmable gate arrays. The test mobile controller (LMT) allows engineers to select operating modes such as fixed MCS, link adaption, SIMO, MIMO.
The LTE development platform currently operates in the 2.6 GHz frequency band, which is expected to be the initial spectrum band for LTE deployment in Europe.
A measurement van was used to accommodate the mobile terminals for the drive tests. Two UEs (UE2, UE3) are mounted in the car and are connected to antennas on the roof (Figure 6.1.1-1). This provides variable SNR as channel conditions change along the drive route.

Figure 6.1.1-1: Measurement van with LTE UEs.

Table 6.1.1 show the Features of LTE development platform for FDD mode.

Carrier frequency	2.6 GHz (UMTS Extension band)
Duplex	FDD
Scalable bandwidth	20 MHz, 10 MHz, 5 MHz
Data rate @ 20 MHz	>150 Mbps (DL), >50 Mbps (UL)
Transmission Time Interval (TTI)	1 ms
Tx power DL	40 dBm
Tx power UL	23 dBm
Modulation schemes:	• Downlink OFDMA (64QAM, 16QAM, QPSK) • Uplink SC-FDMA (16QAM, QPSK)
Antenna techniques:	• Downlink 2x2 MIMO • Uplink SDMA, Rx-Diversity
CQI based link adaptation (DL)	Time, Frequency, Space
Setup	single Cell – multi user
Number eUE per Node B per Sector	4

Table 6.1.1: Features of LTE development platform for FDD mode.

A 20 MHz bandwidth at 2.6 GHz with a 2x2 MIMO antenna system was used in all the tests. Running in adaptive MIMO mode, the base transceiver station (BTS) switched automatically between single-stream transmission (transmit diversity) and multi-stream transmission (spatial multiplexing), depending on the reported SNR of the UE. In addition, adaptive modulation using QPSK, 16 QAM and 64 QAM was applied depending on the actual channel condition, in other words the reported SNR.

Munich test site

The test site in Munich is installed on the Nokia Siemens Networks campus.

The Nokia Siemens Networks campus in Munich consists of several buildings between 17 and 23 meters tall, with two rows of 5–8 meter trees along the road through the middle. The drive route on the campus is about 900 meters long, with a distance to the BTS of between 50 and 300 meters.

The LTE antenna is mounted on a pole on the roof of a building at a height of 30 meters above the ground (see the upper antenna in Figure 6.1.1-2), co-sited with an WCDMA antenna (middle antenna) and a Flash-OFDM antenna (lowest antenna) on the same pole. It is a commercial 3-sector cross-polarized wideband antenna with 45° directivity operating in a frequency range of 1800 to 2600 MHz.

The system can support MIMO implementing an antenna gain of about 18 dBi.

Figure 6.1.1-2: LTE antenna at Munich test site.

Berlin test site

The LTE test bed in Berlin is operated by Nokia Siemens Networks in cooperation with the Heinrich-Hertz-Institut and located on the city-center campus of the Technical University Berlin.

The environment along the drive route is typically urban, with a mixture of LOS and NLOS with some multipath propagation due to the buildings between the base station site and Tiergarten park. The buildings have heights ranging from 40–70 meters.

The park is about 1000 meters from the base station site and is mostly covered with trees. To the east, the park ends at the Brandenburger Tor that is approximately 67 meters high with a marble base and the radio signal suffers from strong shadowing.

As shown in Figure 6.1.1-3, the overall scenario consists of three base station sites, each of them with three sectors (30°, 150°, 270°).

The sector marked ① was used for the measurements outlined in this paper. It is served by an antenna on top of a tower at a height of 85 meters above ground, the downtilt of the antennas is typically set to cover a radius of 500 meters (optionally 0–10°), which corresponds to the typical setup of commercial UMTS antennas.

For the long distance measurements the northeast sector of the antenna set on the Telefunken building was used, and the antenna downtilt was modified to 1°.

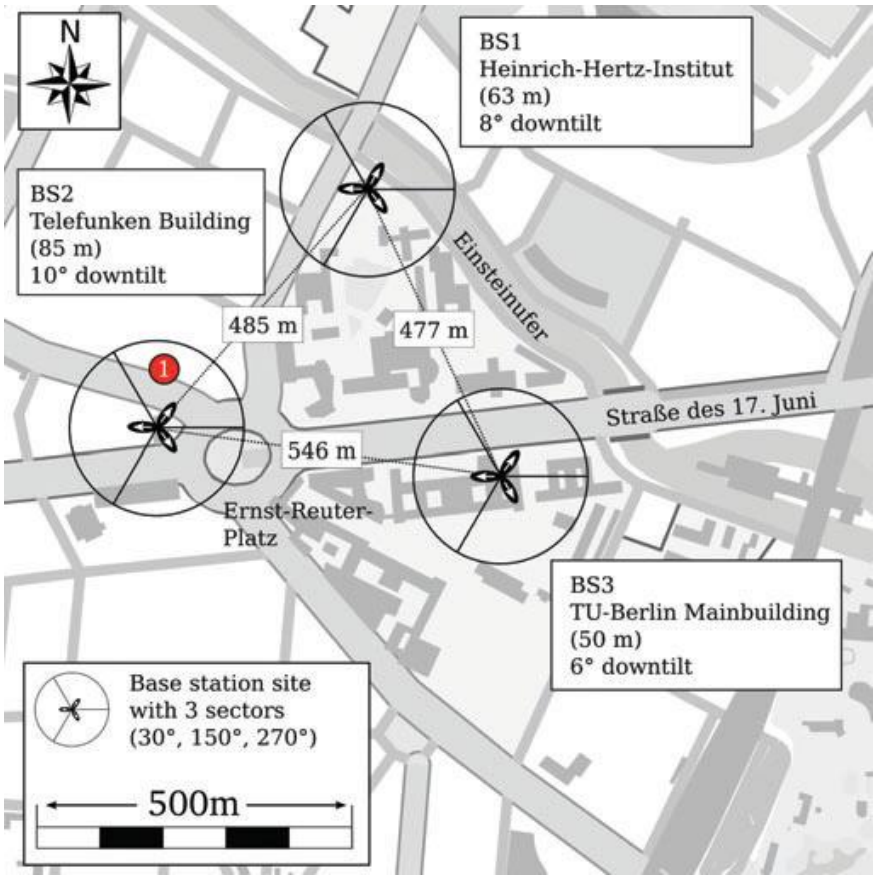

Figure 6.1.1-3: Test site Berlin.

6.1.2 Results

6.1.2.1 Campus route

Figure 6.1.2-2.1 shows the measured L1 throughput data rates for a single user, together with the speed of the measurement van when driving along the campus route in the direction shown by the arrows in Figure 6.1.2.1-1.

The narrow streets and nearby high buildings led to shadowing of the BTS antenna signal, resulting in average L1 throughput from 60 to 100 Mbps at relatively low speeds of about 10–20 km/h. In fact, almost no line of sight was available, except at a few street crossings where L1 throughput rates of about 140 Mbps could be measured. On the other hand, the achieved L1 throughput on the campus route was always above 50 Mbps.

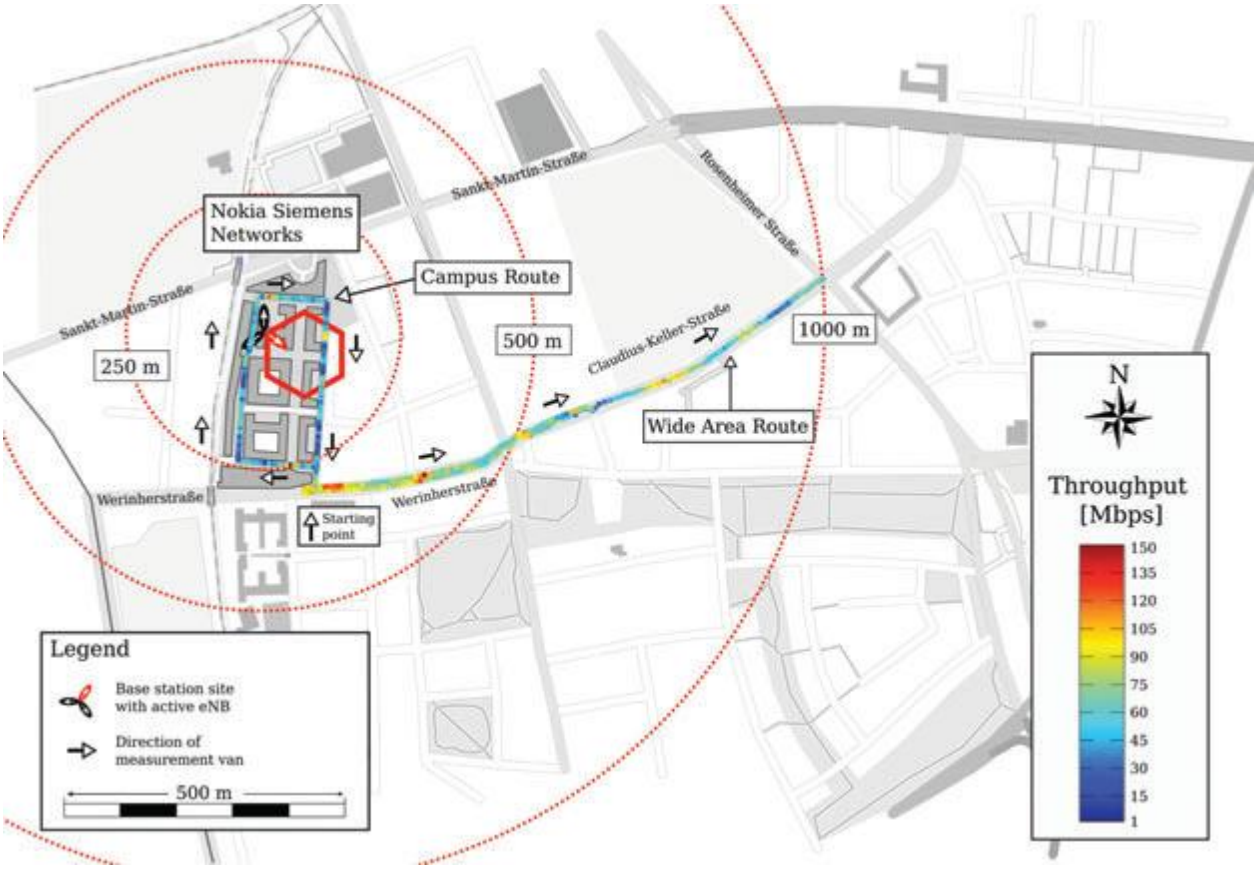

Figure 6.1.2.1-1: Road test in Munich and data rates achieved along campus and wide area routes.

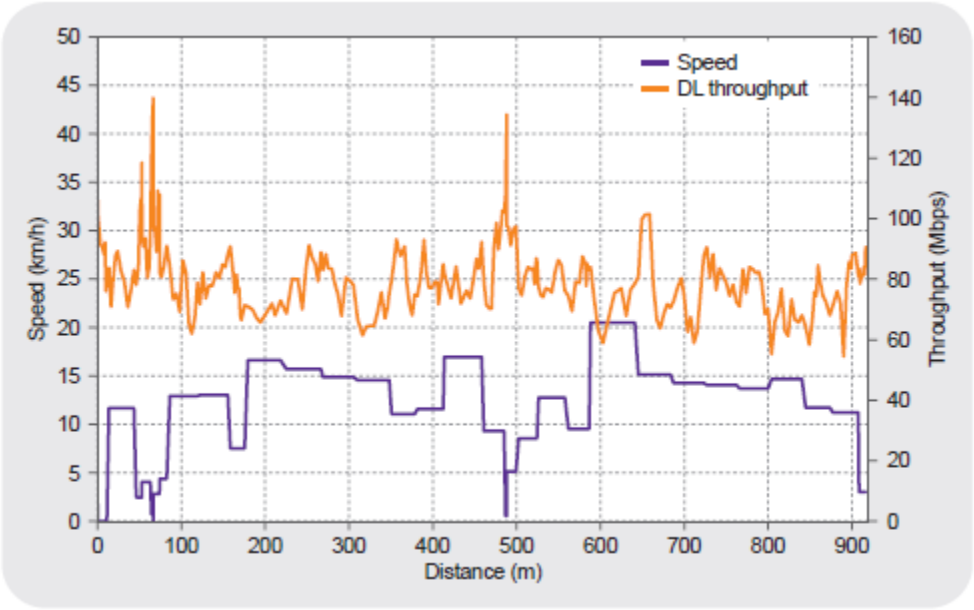

Figure 6.1.2.1-2: DL throughput on campus route.

6.1.2.2 Wide area route

The wide area route was on public roads near the Munich Nokia Siemens Networks campus, between 350 and 1000 meters away from the BTS (Figure 6.1.2.1-1). This area is characterized by medium building density along a main road, mainly apartment houses with a height of 10–20 meters.

These are typical suburban to urban deployment conditions.

Two different measurement scenarios were performed on the route:

- A single user scenario with only one UE active in the cell.
- A multi-user scenario with four users active in the cell, two of them mobile and located in the measurement van, the other two placed inside buildings on the campus.

Single user test

The purpose of the single user test was to measure the achievable DL throughput rate in typical urban/suburban cells with a cell diameter of approximately 1000 meters under highly varying channel conditions and typical urban speeds of up to 40 km/h.

The measurement was performed at a time with high traffic density thus the average speed was only 30–40 km/h.

The measured L1 throughput was in the range of 14–83 Mbps. It varied extensively depending on the shadowing conditions along the test route and decreased on average with the increasing distance from the site.

Even at a distance of about 1000 meters from the BTS the average L1 throughput reaches a level of 30 Mbps.

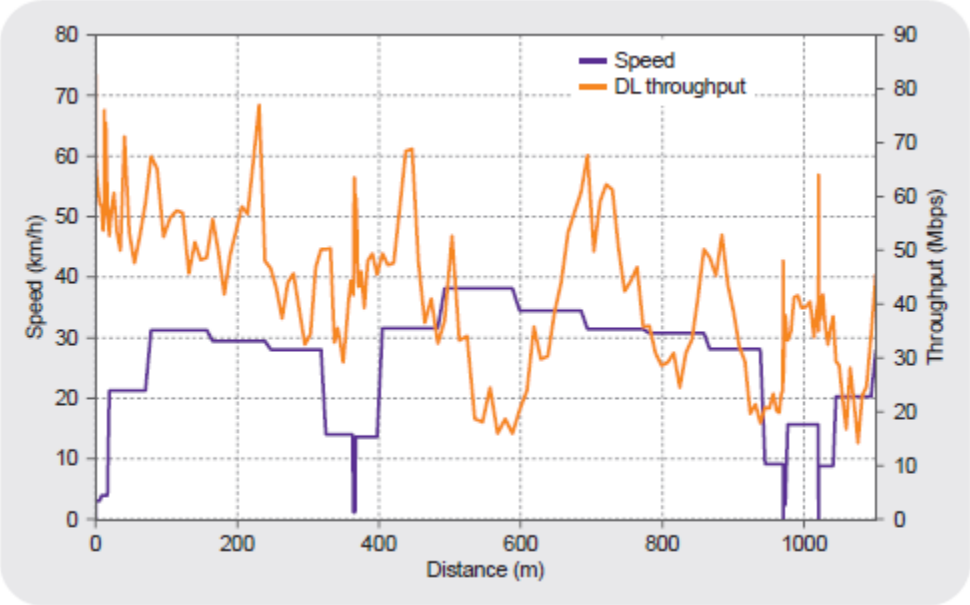

Figure 6.1.2.2-1: DL single user throughput along wide area route.

Multi-user measurement

The scope of the multi-user measurement was to evaluate the achievable DL data rates in a multiuser environment consisting of mobile and stationary users. The stationary users were mobile terminals placed inside an office. At least one of them experienced indoor penetration losses that are typical for urban and suburban LTE cells with a diameter of 1000 meters.

The measurements were performed on the same test route as the single user wide area tests. During these tests four UEs were active in the cell:

- Two UEs (UE2, UE3) were mounted in the car and connected to antennas on the roof. This provided variable SNR due to changing channel conditions along the drive route. A different orientation of the two antennas was selected for U2 and U3.
- One UE (UE4) was located in the lab with antennas very close to the window to get a good SNR. The distance between lab and BTS site is 282 meters.
- One UE (UE1) was located in the lab (same distance from the BTS site as above) with the antenna round about 4 meters away from the window, which provides only medium SNR.

Figure 6.1.2.2-2 shows the measured L1 throughput of each UE while moving along the drive route, together with the speed of the van, which was on average about 40 km/h. The figure shows that the stationary UE with the antenna close to the window (UE4) has the highest data rate (about 30–60 Mbps), followed by the second stationary UE in the middle in the room (UE1) (about 12–25 Mbps). The two fully mobile UEs (UE2 und UE3) achieved an L1 throughput in the range of 5–25 Mbps, depending on the channel conditions along the drive route.

In fact, all radio resources are shared between the terminals connected to one and the same radio cell depending on the channel condition and the decisions of the proportional fair scheduler.
The results also show slightly different throughput rates for UE2 and UE3, which are caused by the different antenna orientation as the van drives along the route towards the antenna at an almost constant angle.

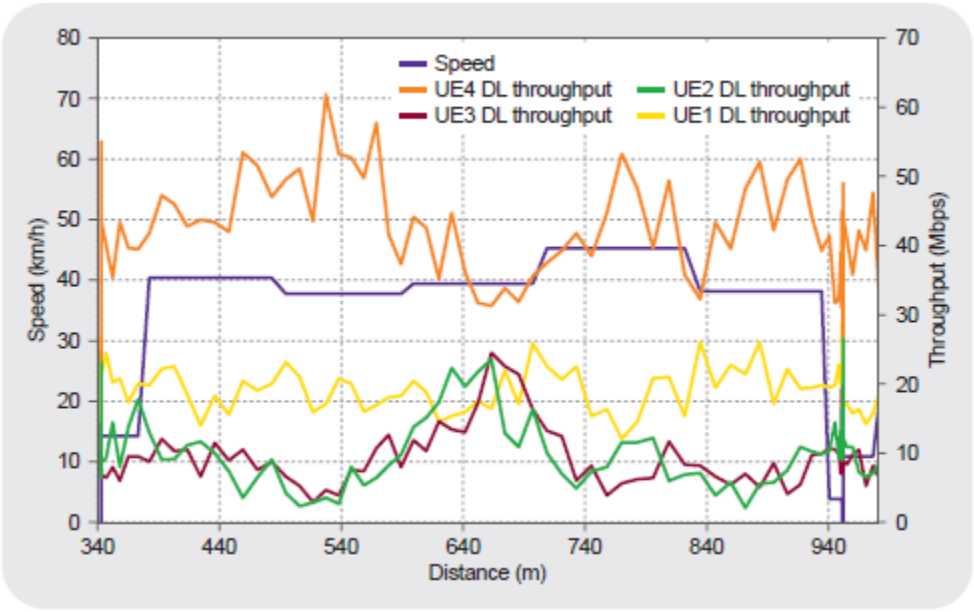

Figure 6.1.2.2-2: DL throughput for multi-user test on wide area route.

6.1.2.3 Long distance route

The arrows in Figure 6.1.2.3-1 indicate the driving direction of the measurement van and the achieved L1 throughput.

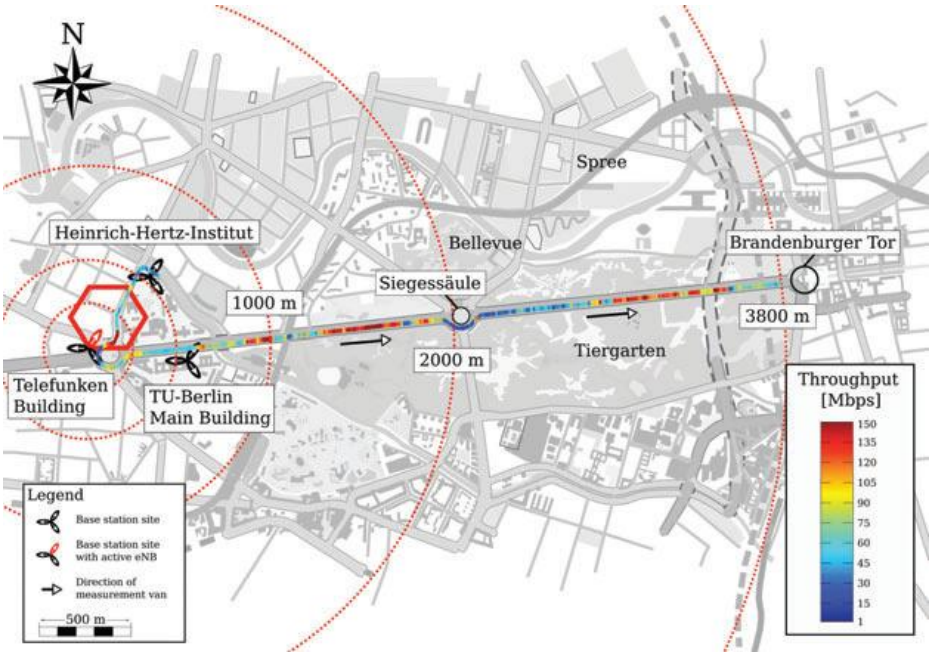

Figure 6.1.2.3-1: Long distance route.

The L1 throughput results for the long distance measurements are shown in Figure 6.1.2.3-2 with a maximum data rate of approximately 150 Mbps.

Synchronization with the base station was stable and the data rate never dropped below 1 Mbps throughout the measurements. These results show a robust system performance without signal loss and high throughputs for a distance of up to 4 km under LOS conditions in the 2.6 GHz spectrum band.

Furthermore, the total throughput rate as shown in Figure 6.1.2.3-2 is split to its two decoupled components related to the MIMO modes allocated by the scheduler. The scheduling algorithm supports adaptive MIMO mode switching to transmit a given physical resource block (PRB) either in single or multi-stream mode depending on the channel condition. The multistream is realized via 2x2 MIMO antenna configurations. The results show the following:

- The multi-stream mode is often chosen and the multi-stream rate never drops to zero, demonstrating that some PRBs are always transmitted in multi-stream mode. This shows that the second stream substantially contributes to the high overall system performance.
- Multi-stream transmission is the key to achieving high data rates that cannot be realized in a single-antenna/SISO system.
- When the channel conditions degrade, the adaptive scheduling algorithm increasingly utilizes single-stream transmission. This contributes to stable transmission along the whole measurement track.

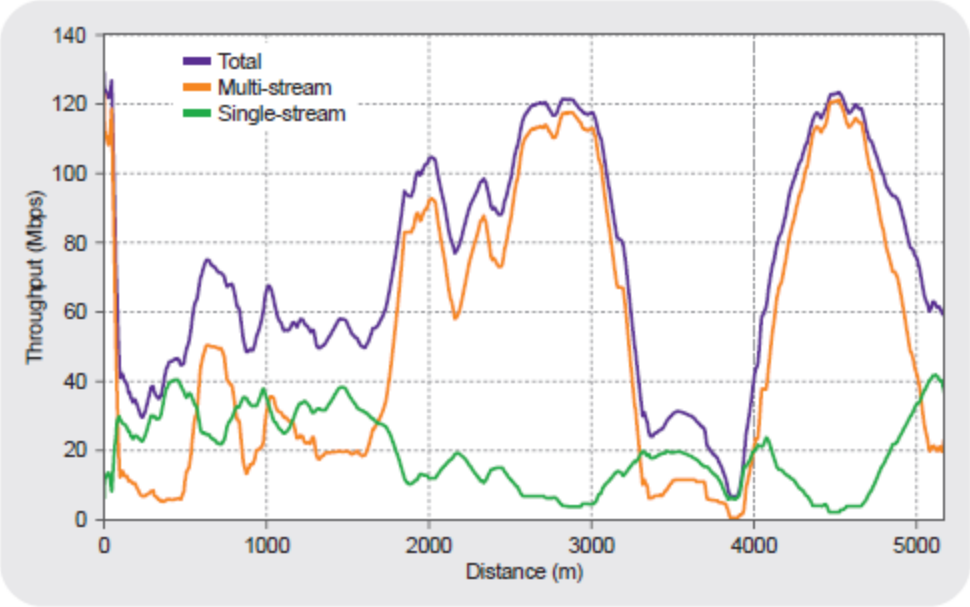

Figure6.1.2.3-2: DL throughput on long distance route for single-stream and multi-stream transmission.

6.2 Simulation of indoor environments

This simulation have the scope of evaluate the behavior in an indoor environment of the modulation schemes supported by LTE and show how a realistic indoor scenario can affect the performance.

To achieve this result a 3D ray tracing algorithm has been developed.

Ray tracing is used, due to the fact that it is a deterministic approach which reduces estimation errors.

The algorithm has been programmed in Matlab.

The indoor environment that has been chosen is depicted in Figure 6.2-1. All the material characteristics as well as 3D morphological aspects have been introduced in order to obtain realistic values.

Several antennas have been placed in the indoor scenario, simulating a conventional radio layout. The simulation results for each one of the antennas are shown in Figure 6.2-2.

As it can be seen from the 3D ray tracing simulation results, power is distributed considering not only the LOS prediction but also the placement of different objects (walls, indoor furniture, windows, etc.), which determines the received signal power and hence the grade of coverage.

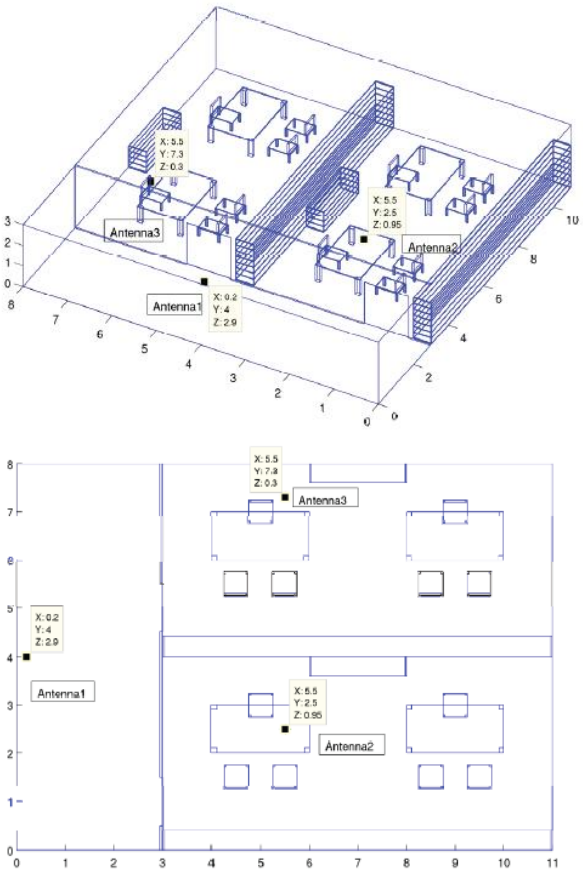

Figure 6.2-1. Left figure: 3D layout of simulation scenario. Right figure: cross section layout of the simulation scenario.

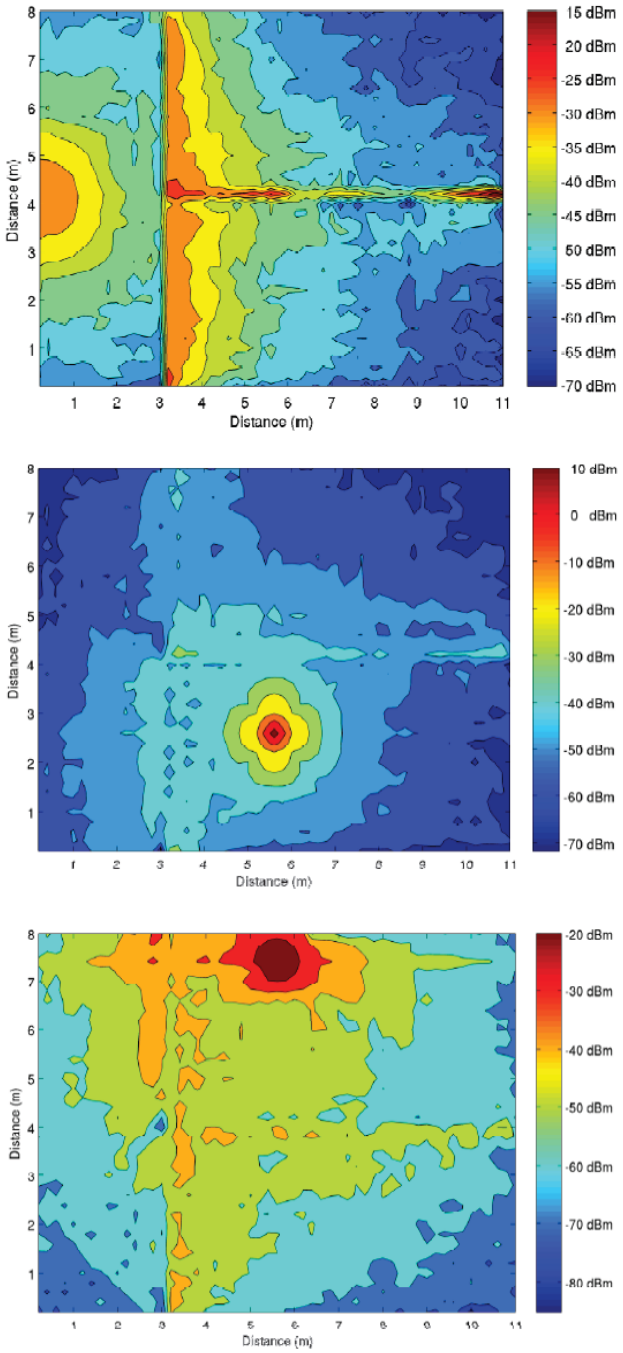

Figure 6.2-2: Received power regarding respectively antenna1, antenna 2 and antenna3, obtained by 3D raytracing at 2Ghz. Simulation height is 1.4m from ground level.

Figure 6.2-3 show how the constellations are degraded as SNR are lowered, due to higher interference scenarios. As the constellation increases the number of elements, the degradation of the symbols becomes more severe, due to higher packing of the modulation scheme. As a consequence, higher order modulation schemes require more power in order to adequately decode the information, which implies smaller coverage radius.

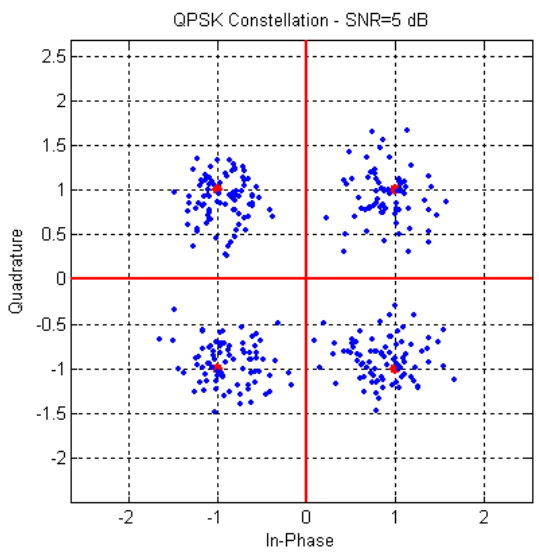
QPSK Constellation - SNR=5 dB
Quadrature
In-Phase

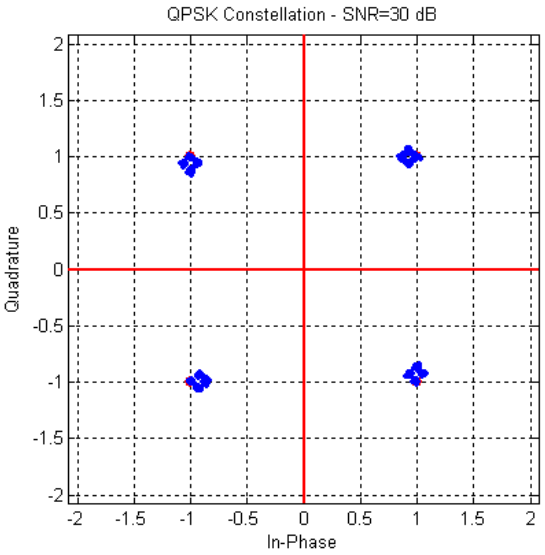
QPSK Constellation - SNR=30 dB
Quadrature
In-Phase

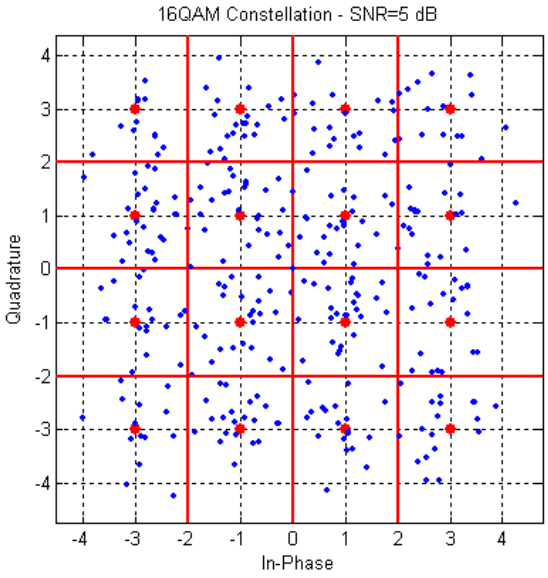
16QAM Constellation - SNR=5 dB
Quadrature
In-Phase

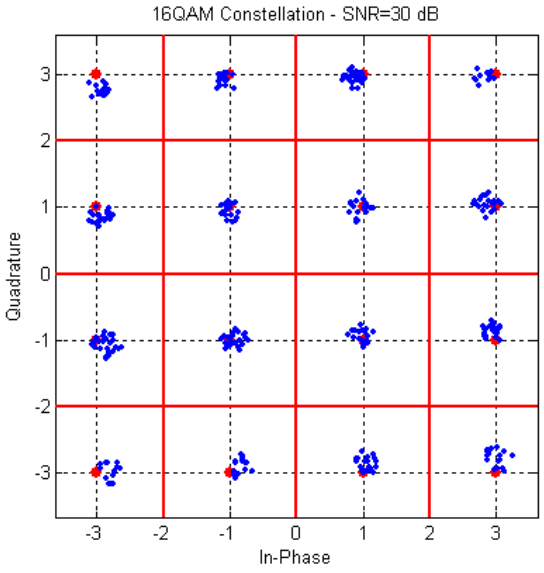
16QAM Constellation - SNR=30 dB
Quadrature
In-Phase

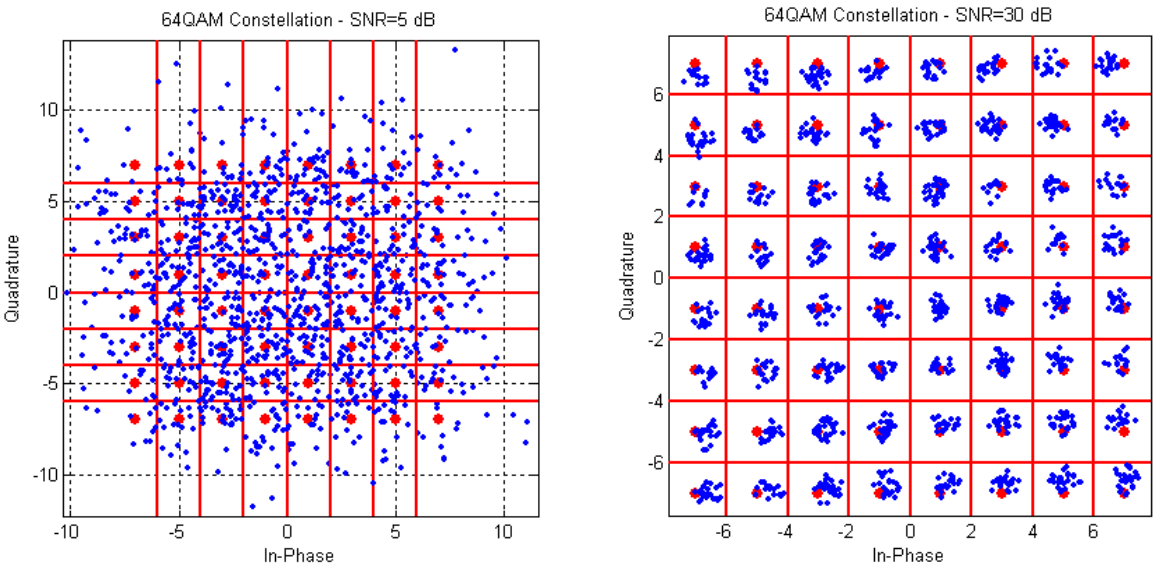

Figure 6.2-3: In Phase and Quadrature representation for QPSK, 16QAM and 64QAM constellation considering SNR of 5 and 30dB.

Another factor to analyze the performance of indoor coverage is the value of Error Vector Magnitude (EVM) related with the relative position of each symbol in the constellation. Due to the fact that outer symbols have in principle more immunity to noise and external interference, the performance of the total system will depend on the use that it can make of the complete constellation. Simulation results have been obtained for each one of the higher order modulation schemes considered (QPSK, 16-QAM and 64-QAM) and the results are depicted in figure 6.2-4.

As it can be seen, as the order of the modulation increases, so does degradation of EVM. Under different SNR ratios, as the interference increases, the value of EVM also increases, which leads to less efficient use of the modulation and in consequence to a reduction of the raw bit rate of the system. In order to gain insight in this behavior, figures 6.2-5 represent the evolution of EVM as a function of constellation type as well as different SNR ratios. As the bit rate is increased, so is the value of EVM, consistent with coverage capacity relations that govern LTE performance in general instance.

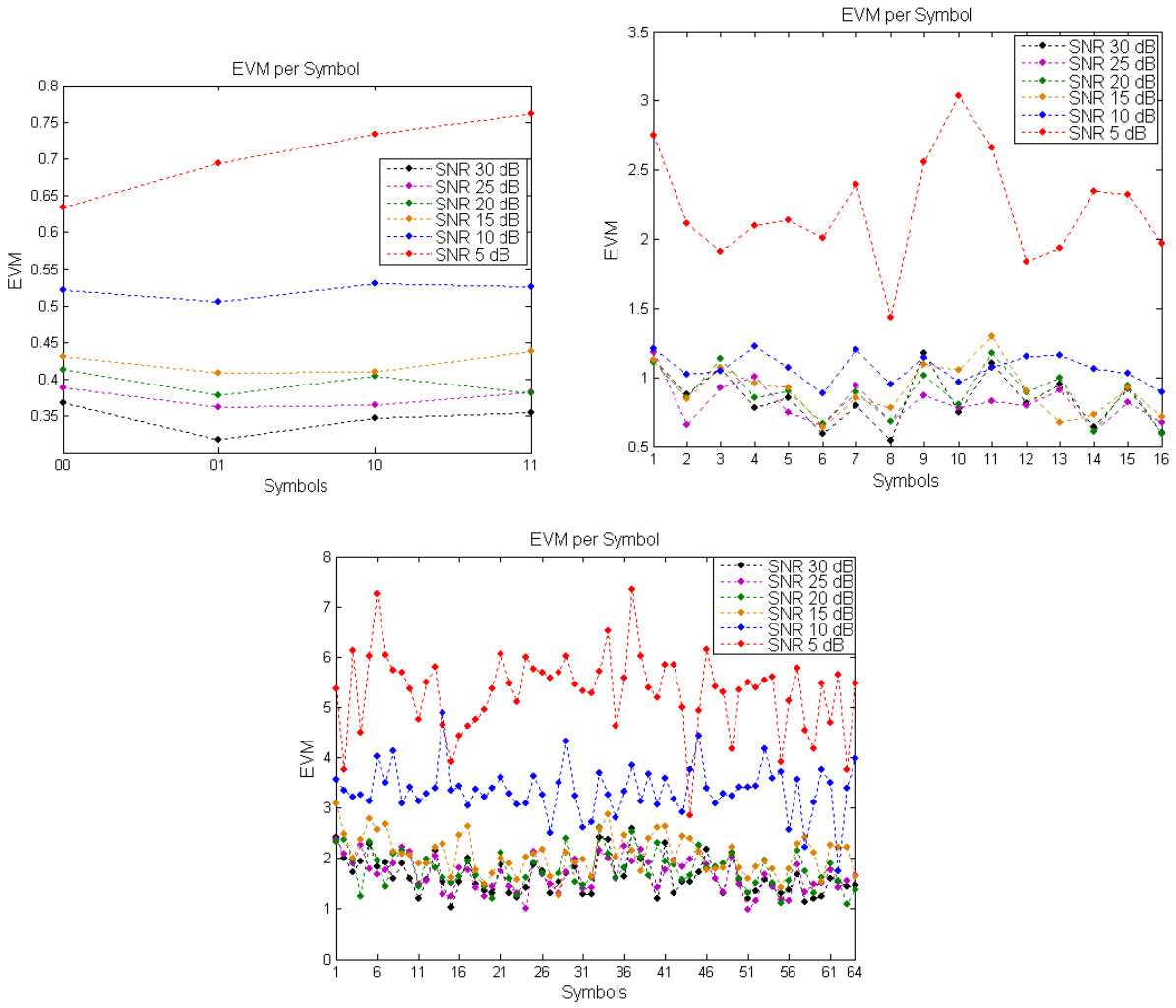

Figure 6.2-4: Values of EVM per symbol in the case of QPSK, 16QAM and 64QAM constellation for different SNR ratios.

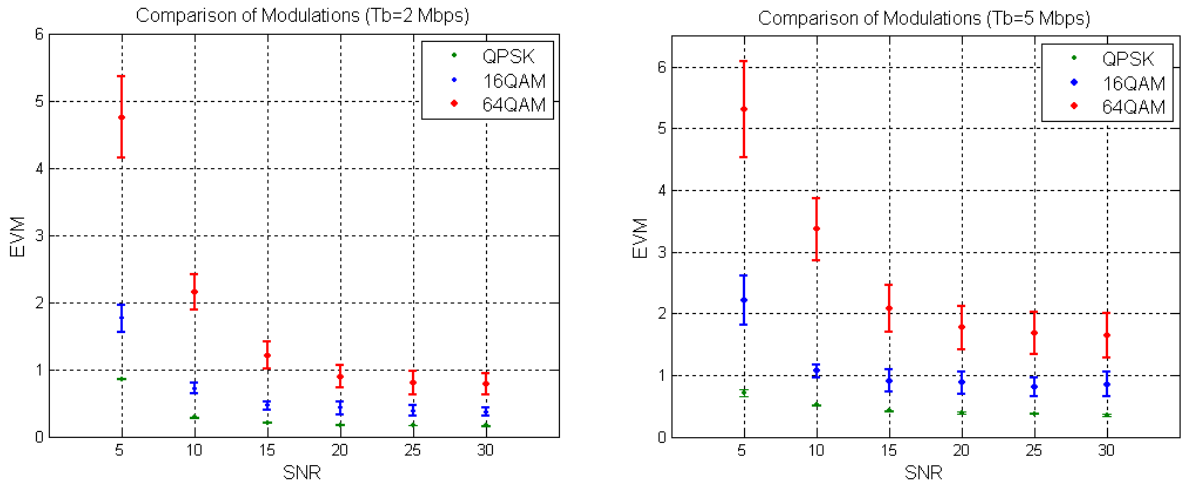

Figure 6.2-5: Comparison of EVM values for QPSK, 16-QAM and 64-QAM for a bit rate of 2 and 5 Mbps.

Finally, Table 6.2 show values for EVM for each one of the modulation schemes in LTE and different SNR ratios and bit rates. As the modulation order is increased, so is the value of EVM and the same is valid for an increase in bit rate.

Therefore, as transmission speed is increased, so is the sensitivity of the receiver and hence the coverage region is decreased.

		SNR (dB)		
		30	15	5
Modulation	Speed (Mbps)	EVM		
QPSK	1	0,0852	0,1339	0,3584
	2	0,1622	0,2080	0,8553
	5	0,3472	0,4219	0,7057
	10	0,5716	0,6060	0,8848
16QAM	1	0,1811	0,2879	0,7924
	2	0,3666	0,4572	1,7555
	5	0,8488	0,9108	2,2207
	10	1,2909	1,3625	1,7331
64QAM	1	0,4048	0,9567	2,9147
	2	0,7767	1,2104	4,7499
	5	1,6406	2,0841	5,3093
	10	2,6370	2,9056	7,1312

Table 6.2: Value of EVM for QPSK, 16QAM and 64QAM at different SNR ratios and bit rates.

APPENDIX

A.1 Modulation schemes

A.1.1 BPSK

In case of BPSK modulation, a single bit, $b(i)$, is mapped to a complex-valued modulation symbol $x=I+jQ$ according to Table A.1.1.

$b(i)$	I	Q
0	$1/\sqrt{2}$	$1/\sqrt{2}$
1	$-1/\sqrt{2}$	$-1/\sqrt{2}$

Table A.1.1: BPSK modulation mapping.

A.1.2 QPSK

In case of QPSK modulation, pairs of bits, $b(i), b(i+1)$, are mapped to complex-valued modulation symbols $x=I+jQ$ according to Table A.1.2.

$b(i), b(i+1)$	I	Q
00	$1/\sqrt{2}$	$1/\sqrt{2}$
01	$1/\sqrt{2}$	$-1/\sqrt{2}$
10	$-1/\sqrt{2}$	$1/\sqrt{2}$
11	$-1/\sqrt{2}$	$-1/\sqrt{2}$

Table A.1.2: QPSK modulation mapping.

A.1.3 16QAM

In case of 16QAM modulation, quadruplets of bits, $b(i), b(i+1), b(i+2), b(i+3)$, are mapped to complex-valued modulation symbols $x=I+jQ$ according to Table A.1.3.

$b(i), b(i+1), b(i+2), b(i+3)$	I	Q
0000	$1/\sqrt{10}$	$1/\sqrt{10}$
0001	$1/\sqrt{10}$	$3/\sqrt{10}$
0010	$3/\sqrt{10}$	$1/\sqrt{10}$
0011	$3/\sqrt{10}$	$3/\sqrt{10}$
0100	$1/\sqrt{10}$	$-1/\sqrt{10}$
0101	$1/\sqrt{10}$	$-3/\sqrt{10}$
0110	$3/\sqrt{10}$	$-1/\sqrt{10}$
0111	$3/\sqrt{10}$	$-3/\sqrt{10}$
1000	$-1/\sqrt{10}$	$1/\sqrt{10}$
1001	$-1/\sqrt{10}$	$3/\sqrt{10}$
1010	$-3/\sqrt{10}$	$1/\sqrt{10}$
1011	$-3/\sqrt{10}$	$3/\sqrt{10}$
1100	$-1/\sqrt{10}$	$-1/\sqrt{10}$
1101	$-1/\sqrt{10}$	$-3/\sqrt{10}$
1110	$-3/\sqrt{10}$	$-1/\sqrt{10}$
1111	$-3/\sqrt{10}$	$-3/\sqrt{10}$

Table A.1.3: 16QAM modulation mapping.

A.1.4 64QAM

In case of 64QAM modulation, hextuplets of bits, $b(i), b(i+1), b(i+2), b(i+3), b(i+4), b(i+5)$, are mapped to complex-valued modulation symbols $x=I+jQ$ according to Table A.1.4.

$b(i), b(i+1), b(i+2), b(i+3), b(i+4), b(i+5)$	I	Q	$b(i), b(i+1), b(i+2), b(i+3), b(i+4), b(i+5)$	I	Q
000000	$3/\sqrt{42}$	$3/\sqrt{42}$	100000	$-3/\sqrt{42}$	$3/\sqrt{42}$
000001	$3/\sqrt{42}$	$1/\sqrt{42}$	100001	$-3/\sqrt{42}$	$1/\sqrt{42}$
000010	$1/\sqrt{42}$	$3/\sqrt{42}$	100010	$-1/\sqrt{42}$	$3/\sqrt{42}$
000011	$1/\sqrt{42}$	$1/\sqrt{42}$	100011	$-1/\sqrt{42}$	$1/\sqrt{42}$
000100	$3/\sqrt{42}$	$5/\sqrt{42}$	100100	$-3/\sqrt{42}$	$5/\sqrt{42}$
000101	$3/\sqrt{42}$	$7/\sqrt{42}$	100101	$-3/\sqrt{42}$	$7/\sqrt{42}$
000110	$1/\sqrt{42}$	$5/\sqrt{42}$	100110	$-1/\sqrt{42}$	$5/\sqrt{42}$
000111	$1/\sqrt{42}$	$7/\sqrt{42}$	100111	$-1/\sqrt{42}$	$7/\sqrt{42}$
001000	$5/\sqrt{42}$	$3/\sqrt{42}$	101000	$-5/\sqrt{42}$	$3/\sqrt{42}$
001001	$5/\sqrt{42}$	$1/\sqrt{42}$	101001	$-5/\sqrt{42}$	$1/\sqrt{42}$
001010	$7/\sqrt{42}$	$3/\sqrt{42}$	101010	$-7/\sqrt{42}$	$3/\sqrt{42}$
001011	$7/\sqrt{42}$	$1/\sqrt{42}$	101011	$-7/\sqrt{42}$	$1/\sqrt{42}$
001100	$5/\sqrt{42}$	$5/\sqrt{42}$	101100	$-5/\sqrt{42}$	$5/\sqrt{42}$
001101	$5/\sqrt{42}$	$7/\sqrt{42}$	101101	$-5/\sqrt{42}$	$7/\sqrt{42}$
001110	$7/\sqrt{42}$	$5/\sqrt{42}$	101110	$-7/\sqrt{42}$	$5/\sqrt{42}$
001111	$7/\sqrt{42}$	$7/\sqrt{42}$	101111	$-7/\sqrt{42}$	$7/\sqrt{42}$
010000	$3/\sqrt{42}$	$-3/\sqrt{42}$	110000	$-3/\sqrt{42}$	$-3/\sqrt{42}$
010001	$3/\sqrt{42}$	$-1/\sqrt{42}$	110001	$-3/\sqrt{42}$	$-1/\sqrt{42}$
010010	$1/\sqrt{42}$	$-3/\sqrt{42}$	110010	$-1/\sqrt{42}$	$-3/\sqrt{42}$
010011	$1/\sqrt{42}$	$-1/\sqrt{42}$	110011	$-1/\sqrt{42}$	$-1/\sqrt{42}$
010100	$3/\sqrt{42}$	$-5/\sqrt{42}$	110100	$-3/\sqrt{42}$	$-5/\sqrt{42}$
010101	$3/\sqrt{42}$	$-7/\sqrt{42}$	110101	$-3/\sqrt{42}$	$-7/\sqrt{42}$
010110	$1/\sqrt{42}$	$-5/\sqrt{42}$	110110	$-1/\sqrt{42}$	$-5/\sqrt{42}$
010111	$1/\sqrt{42}$	$-7/\sqrt{42}$	110111	$-1/\sqrt{42}$	$-7/\sqrt{42}$
011000	$5/\sqrt{42}$	$-3/\sqrt{42}$	111000	$-5/\sqrt{42}$	$-3/\sqrt{42}$
011001	$5/\sqrt{42}$	$-1/\sqrt{42}$	111001	$-5/\sqrt{42}$	$-1/\sqrt{42}$
011010	$7/\sqrt{42}$	$-3/\sqrt{42}$	111010	$-7/\sqrt{42}$	$-3/\sqrt{42}$
011011	$7/\sqrt{42}$	$-1/\sqrt{42}$	111011	$-7/\sqrt{42}$	$-1/\sqrt{42}$
011100	$5/\sqrt{42}$	$-5/\sqrt{42}$	111100	$-5/\sqrt{42}$	$-5/\sqrt{42}$
011101	$5/\sqrt{42}$	$-7/\sqrt{42}$	111101	$-5/\sqrt{42}$	$-7/\sqrt{42}$
011110	$7/\sqrt{42}$	$-5/\sqrt{42}$	111110	$-7/\sqrt{42}$	$-5/\sqrt{42}$
011111	$7/\sqrt{42}$	$-7/\sqrt{42}$	111111	$-7/\sqrt{42}$	$-7/\sqrt{42}$

Table A.1.4: 64QAM modulation mapping.

A.2 Pseudo-random sequence generation

Pseudo-random sequences are defined by a length-31 Gold sequence. The output sequence $c(n)$ of length M_{PN}, where $n = 0,1,\ldots,M_{\mathrm{PN}}-1$, is defined by

$$c(n) = \left(x_1(n+N_C) + x_2(n+N_C)\right) \bmod 2$$
$$x_1(n+31) = \left(x_1(n+3) + x_1(n)\right) \bmod 2$$
$$x_2(n+31) = \left(x_2(n+3) + x_2(n+2) + x_2(n+1) + x_2(n)\right) \bmod 2$$

where $N_C = 1600$ and the first m-sequence shall be initialized with $x_1(0) = 1, x_1(n) = 0, n = 1,2,\ldots,30$. The initialization of the second m-sequence is denoted by $c_{\mathrm{init}} = \sum_{i=0}^{30} x_2(i) \cdot 2^i$ with the value depending on the application of the sequence.

A.3 CRC calculation

Denote the input bits to the CRC computation by $a_0, a_1, a_2, a_3, \ldots, a_{A-1}$, and the parity bits by $p_0, p_1, p_2, p_3, \ldots, p_{L-1}$. A is the size of the input sequence and L is the number of parity bits. The parity bits are generated by one of the following cyclic generator polynomials:

- $g_{\mathrm{CRC24A}}(D) = [D^{24} + D^{23} + D^{18} + D^{17} + D^{14} + D^{11} + D^{10} + D^7 + D^6 + D^5 + D^4 + D^3 + D + 1]$ for a CRC length $L = 24$
- $g_{\mathrm{CRC24B}}(D) = [D^{24} + D^{23} + D^6 + D^5 + D + 1]$ for a CRC length $L = 24$
- $g_{\mathrm{CRC16}}(D) = [D^{16} + D^{12} + D^5 + 1]$ for a CRC length $L = 16$
- $g_{\mathrm{CRC8}}(D) = [D^8 + D^7 + D^4 + D^3 + D + 1]$ for a CRC length of $L = 8$

The bits after CRC attachment are denoted by $b_0, b_1, b_2, b_3, \ldots, b_{B-1}$, where $B = A + L$. The relation between a_k and b_k is:

$b_k = a_k$ for $k = 0, 1, 2, \ldots, A-1$

$b_k = a_{k-A}$ for $k = A, A+1, A+2, \ldots, A+L-1$

A.4 Code block segmentation and code block CRC attachment

The input bit sequence to the code block segmentation is denoted by $b_0, b_1, b_2, b_3, \ldots, b_{B-1}$, where $B > 0$. If B is larger than the maximum code block size Z, segmentation of the input bit sequence is performed and an additional CRC sequence of $L = 24$ bits is attached to each code block. The maximum code block size is $Z = 6144$.

If the number of filler bits F calculated below is not 0, filler bits are added to the beginning of the first block. Note that if $B < 40$, filler bits are added to the beginning of the code block.

The filler bits shall be set to <*NULL*> at the input to the encoder.

Total number of code blocks C is determined by:

if $B \le Z$

$L = 0$

Number of code blocks: $C = 1$

$B' = B$

else

$L = 24$

Number of code blocks: $C = \left\lceil \frac{B}{Z - L} \right\rceil$

$B' = B + C \cdot L$

end if

The bits output from code block segmentation, for $C \neq 0$, are denoted by $c_{r0}, c_{r1}, c_{r2}, c_{r3}, \ldots, c_{r(K_r-1)}$, where r is the code block number, and K_r is the number of bits for the code block number r.

Number of bits in each code block (applicable for $C \neq 0$ only):

The sequence $c_{r0}, c_{r1}, c_{r2}, c_{r3}, \ldots, c_{r(K_r-L-1)}$ is used to calculate the CRC parity bits $p_{r0}, p_{r1}, p_{r2}, \ldots, p_{r(L-1)}$ according to section 5.1.1 with the generator polynomial $g_{CRC24B}(D)$. For CRC calculation it is assumed that filler bits, if present, have the value 0.

A.5 Tail biting convolutional coding

A tail biting convolutional code with constraint length 7 and coding rate 1/3 is defined.

The configuration of the convolutional encoder is presented in figure A.5.

The initial value of the shift register of the encoder shall be set to the values corresponding to the last 6 information bits in the input stream so that the initial and final states of the shift register are the same. Therefore, denoting the shift register of the encoder by $s_0, s_1, s_2, \ldots, s_5$, then the initial value of the shift register shall be set to $s_i = c_{(K-1-i)}$

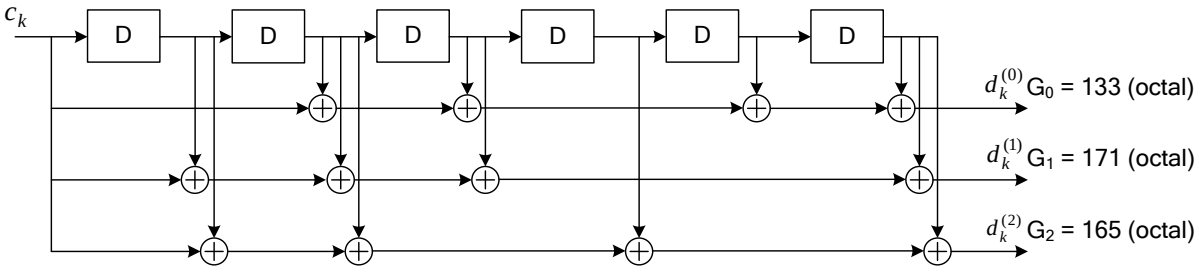

Figure A.5: Rate 1/3 tail biting convolutional encoder.

The encoder output streams $d_k^{(0)}$, $d_k^{(1)}$ and $d_k^{(2)}$ correspond to the first, second and third parity streams, respectively as shown in Figure A.5.

A.6 Turbo coding

A.6.1 Turbo encoder

The scheme of turbo encoder is a Parallel Concatenated Convolutional Code (PCCC) with two 8-state constituent encoders and one turbo code internal interleaver. The coding rate of turbo encoder is 1/3. The structure of turbo encoder is illustrated in Figure A.6.1.

The transfer function of the 8-state constituent code for the PCCC is:

$$G(D) = \left[1, \frac{g_1(D)}{g_0(D)}\right], \text{ where } g_0(D) = 1 + D^2 + D^3, g_1(D) = 1 + D + D^3.$$

The initial value of the shift registers of the 8-state constituent encoders shall be all zeros when starting to encode the input bits.

The output from the turbo encoder is

$$d_k^{(0)} = x_k, \quad d_k^{(1)} = z_k, \quad d_k^{(2)} = z'_k \quad \text{for } k = 0,1,2,\ldots,K-1$$

If the code block to be encoded is the 0-th code block and the number of filler bits is greater than zero, i.e., $F > 0$, then the encoder shall set $c_k = 0$, $k = 0,\ldots,(F-1)$ at its input and shall set $d_k^{(0)} = < NULL >$, $k = 0,\ldots,(F-1)$ and $d_k^{(1)} = < NULL >$, $k = 0,\ldots,(F-1)$ at its output.

The bits input to the turbo encoder are denoted by $c_0, c_1, c_2, c_3, \ldots, c_{K-1}$, and the bits output from the first and second 8-state constituent encoders are denoted by $z_0, z_1, z_2, z_3, \ldots, z_{K-1}$ and $z'_0, z'_1, z'_2, z'_3, \ldots, z'_{K-1}$, respectively. The bits output from the turbo code internal interleaver are denoted by $c'_0, c'_1, \ldots, c'_{K-1}$, and these bits are to be the input to the second 8-state constituent encoder.

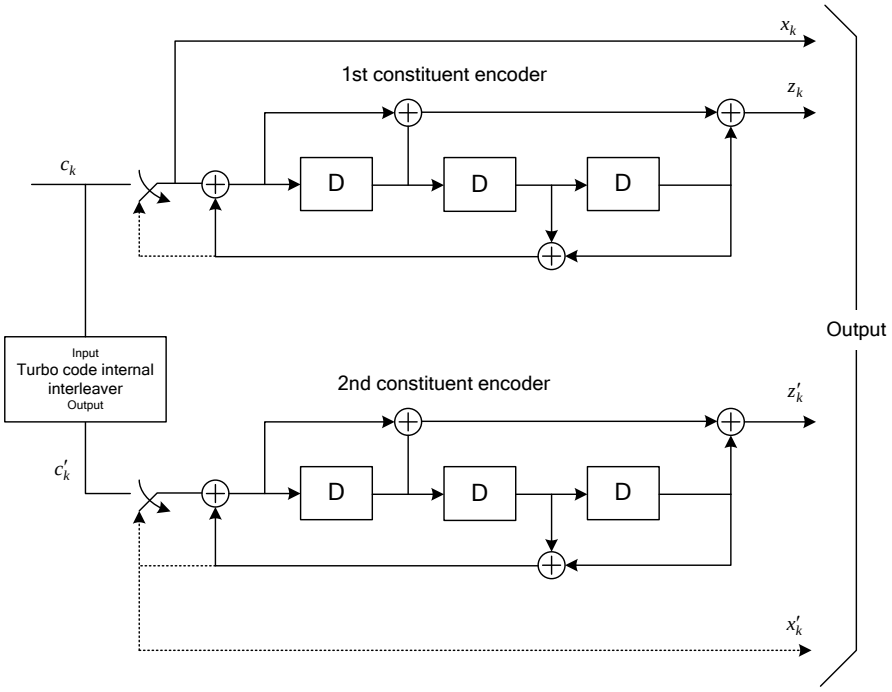

Figure A.6.1: Structure of rate 1/3 turbo encoder (dotted lines for trellis termination only).

A.6.2 Trellis termination for turbo encoder

Trellis termination is performed by taking the tail bits from the shift register feedback after all information bits are encoded. Tail bits are padded after the encoding of information bits.

The first three tail bits shall be used to terminate the first constituent encoder (upper switch of Figure A.6.1 in lower position) while the second constituent encoder is disabled. The last three tail bits shall be used to terminate the second constituent encoder (lower switch of Figure A.6.1 in lower position) while the first constituent encoder is disabled.

The transmitted bits for trellis termination shall then be:

$$d_K^{(0)} = x_K,\ d_{K+1}^{(0)} = z_{K+1},\ d_{K+2}^{(0)} = x'_K,\ d_{K+3}^{(0)} = z'_{K+1}$$

$$d_K^{(1)} = z_K,\ d_{K+1}^{(1)} = x_{K+2},\ d_{K+2}^{(1)} = z'_K,\ d_{K+3}^{(1)} = x'_{K+2}$$

$$d_K^{(2)} = x_{K+1},\ d_{K+1}^{(2)} = z_{K+2},\ d_{K+2}^{(2)} = x'_{K+1},\ d_{K+3}^{(2)} = z'_{K+2}$$

A.6.3 Turbo code internal interleaver

The bits input to the turbo code internal interleaver are denoted by $c_0, c_1, \ldots, c_{K-1}$, where K is the number of input bits. The bits output from the turbo code internal interleaver are denoted by $c'_0, c'_1, \ldots, c'_{K-1}$.

The relationship between the input and output bits is as follows $c'_i = c_{\Pi(i)}$, i=0, 1,..., (K-1)

where the relationship between the output index i and the input index $\Pi(i)$ satisfies the following quadratic form $\Pi(i) = \left(f_1 \cdot i + f_2 \cdot i^2\right) \bmod K$

The parameters f_1 and f_2 depend on the block size K and are summarized in Table A.6.3.

i	*K*	f_1	f_2	*i*	*K*	f_1	f_2	*i*	*K*	f_1	f_2	*i*	*K*	f_1	f_2
1	40	3	10	48	416	25	52	95	1120	67	140	142	3200	111	240
2	48	7	12	49	424	51	106	96	1152	35	72	143	3264	443	204
3	56	19	42	50	432	47	72	97	1184	19	74	144	3328	51	104
4	64	7	16	51	440	91	110	98	1216	39	76	145	3392	51	212
5	72	7	18	52	448	29	168	99	1248	19	78	146	3456	451	192
6	80	11	20	53	456	29	114	100	1280	199	240	147	3520	257	220
7	88	5	22	54	464	247	58	101	1312	21	82	148	3584	57	336
8	96	11	24	55	472	29	118	102	1344	211	252	149	3648	313	228
9	104	7	26	56	480	89	180	103	1376	21	86	150	3712	271	232
10	112	41	84	57	488	91	122	104	1408	43	88	151	3776	179	236
11	120	103	90	58	496	157	62	105	1440	149	60	152	3840	331	120
12	128	15	32	59	504	55	84	106	1472	45	92	153	3904	363	244
13	136	9	34	60	512	31	64	107	1504	49	846	154	3968	375	248
14	144	17	108	61	528	17	66	108	1536	71	48	155	4032	127	168
15	152	9	38	62	544	35	68	109	1568	13	28	156	4096	31	64
16	160	21	120	63	560	227	420	110	1600	17	80	157	4160	33	130
17	168	101	84	64	576	65	96	111	1632	25	102	158	4224	43	264
18	176	21	44	65	592	19	74	112	1664	183	104	159	4288	33	134
19	184	57	46	66	608	37	76	113	1696	55	954	160	4352	477	408
20	192	23	48	67	624	41	234	114	1728	127	96	161	4416	35	138
21	200	13	50	68	640	39	80	115	1760	27	110	162	4480	233	280
22	208	27	52	69	656	185	82	116	1792	29	112	163	4544	357	142
23	216	11	36	70	672	43	252	117	1824	29	114	164	4608	337	480
24	224	27	56	71	688	21	86	118	1856	57	116	165	4672	37	146
25	232	85	58	72	704	155	44	119	1888	45	354	166	4736	71	444
26	240	29	60	73	720	79	120	120	1920	31	120	167	4800	71	120
27	248	33	62	74	736	139	92	121	1952	59	610	168	4864	37	152
28	256	15	32	75	752	23	94	122	1984	185	124	169	4928	39	462
29	264	17	198	76	768	217	48	123	2016	113	420	170	4992	127	234
30	272	33	68	77	784	25	98	124	2048	31	64	171	5056	39	158
31	280	103	210	78	800	17	80	125	2112	17	66	172	5120	39	80
32	288	19	36	79	816	127	102	126	2176	171	136	173	5184	31	96
33	296	19	74	80	832	25	52	127	2240	209	420	174	5248	113	902
34	304	37	76	81	848	239	106	128	2304	253	216	175	5312	41	166
35	312	19	78	82	864	17	48	129	2368	367	444	176	5376	251	336
36	320	21	120	83	880	137	110	130	2432	265	456	177	5440	43	170
37	328	21	82	84	896	215	112	131	2496	181	468	178	5504	21	86
38	336	115	84	85	912	29	114	132	2560	39	80	179	5568	43	174
39	344	193	86	86	928	15	58	133	2624	27	164	180	5632	45	176
40	352	21	44	87	944	147	118	134	2688	127	504	181	5696	45	178
41	360	133	90	88	960	29	60	135	2752	143	172	182	5760	161	120
42	368	81	46	89	976	59	122	136	2816	43	88	183	5824	89	182
43	376	45	94	90	992	65	124	137	2880	29	300	184	5888	323	184
44	384	23	48	91	1008	55	84	138	2944	45	92	185	5952	47	186
45	392	243	98	92	1024	31	64	139	3008	157	188	186	6016	23	94
46	400	151	40	93	1056	17	66	140	3072	47	96	187	6080	47	190
47	408	155	102	94	1088	171	204	141	3136	13	28	188	6144	263	480

Table A.6.3: Turbo code internal interleaver parameters.

REFERENCES

[1] 3GPP *Evolved Universal Terrestrial Radio Access (E-UTRA): Physical channels and modulation, specification paper,*
http://www.3gpp.org/ftp/Specs/html-info/36211.htm

[2] 3GPP Evolved Universal Terrestrial Radio Access (E-UTRA): Multiplexing and channel coding, specification paper,
http://www.3gpp.org/ftp/Specs/html-info/36212.htm

[3] 3GPP *Evolved Universal Terrestrial Radio Access (E-UTRA): Physical layer procedures,*
specification paper,
http://www.3gpp.org/ftp/Specs/html-info/36213.htm

[4] Anders Furuskar, Tomas Jonsson, and Magnus Lundevall,
The LTE Radio Interface – Key Characteristics and Performance,
IEEE 19th International Symposium on Personal, Indoor and Mobile Radio Communications - PIMRC 2008.

[5] Mamoru Sawahashi, Yoshihisa Kishiyama, Hidekazu Taoka, Motohiro Tanno, and Takehiro Nakamura,
Broadband Radio Access: LTE and LTE-Advanced
International Symposium on Intelligent Signal Processing and Communication Systems -ISPACS 2009, December 7-9, 2009

[6] Nokia Siemens Network,
LTE performance for initial deployments,
http://www.nokiasiemensnetworks.com/sites/default/files/document/LTE_measurement_A4_1302_0.pdf

[7] Victor Torres, Fermin Esparza, Francisco Falcone,
Simulation and Analysis of Performance of LTE in indoor environments,
Mediterrannean Microwave Symposium (MMS),
November 15-17, 2009